

UNIVERSIDAD DE INVESTIGACIÓN DE TECNOLOGÍA EXPERIMENTAL YACHAY

Escuela de Ciencias Químicas e Ingeniería

PREPARATION AND EVALUATION OF CHITOSAN/HYDROXYETHYLCELLULOSE BASED HYDROGEL FILMS LOADED WITH MANGOSTEEN AND POMEGRANATE EXTRACTS

Trabajo de titulación presentado como requisito para la obtención del título de
Magister en Ciencias Químicas con mención en Ciencia e Ingeniería de
los Materiales.

Autor:

Luis Alberto Calderón Salas

Tutor:

Lola De Lima Eljuri, MSc.

Co-Tutor:

Manuel Caetano Sousa, PhD.

Urququí, Septiembre 2024

AUTORÍA

Yo, **LUIS ALBERTO CALDERÓN SALAS**, con cédula de identidad 1003742525, declaro que las ideas, juicios, valoraciones, interpretaciones, consultas bibliográficas, definiciones y conceptualizaciones expuestas en el presente trabajo; así como, los procedimientos y herramientas utilizadas en la investigación, son de absoluta responsabilidad del autor del trabajo de titulación.

Así mismo, me acojo a la normativa interna de la Universidad de Investigación de Tecnología Experimental Yachay.

San Miguel de Urququí, Septiembre 2024

Luis Alberto Calderón Salas

CI:1003741525

AUTORIZACIÓN DE PUBLICACIÓN

Yo, **LUIS ALBERTO CALDERÓN SALAS**, con cédula de identidad 1003741525, cedo a la Universidad de Tecnología Experimental Yachay, los derechos de publicación de la presente obra, sin que deba haber un reconocimiento económico por este concepto. Declaro además que el texto del presente trabajo de titulación no podrá ser cedido a ninguna empresa editorial para su publicación u otros fines, sin contar previamente con la autorización escrita de la Universidad.

Asimismo, autorizo a la Universidad que realice la digitalización y publicación de este trabajo de titulación en el repositorio virtual, de conformidad a lo que dispone la Ley Orgánica de Educación Superior

San Miguel de Urququí, Septiembre 2024

Luis Alberto Calderón Salas

CI:1003741525

Dedicatoria

Dedico este trabajo de investigación a mis padres, mi tía y, sobre todo, a Dios, quienes me han brindado su apoyo incondicional en cada etapa de mi formación y en la realización de este sueño de obtener el título de Máster en Ciencias Químicas con mención en Ciencia e Ingeniería de Materiales.

Agradezco también a todas las personas que, con su colaboración, han contribuido al éxito de este proyecto, especialmente a quienes nos ofrecieron su tiempo y compartieron sus conocimientos en las áreas de química y biología.

Luis Alberto Calderón Salas

Agradecimientos

Expreso mi más sincero agradecimiento a los miembros de la Escuela de Ciencias Químicas e Ingeniería y de la Escuela de Ciencias Biológicas e Ingeniería de la Universidad Yachay Tech, quienes han compartido generosamente sus ideas, conocimientos y experiencias a lo largo de mi formación profesional y de investigación, así como durante mis estudios de cuarto nivel. De manera especial, agradezco a mis tutores, MSc. Lola De Lima Eljuri y Ph.D. Caetano Sousa Manuel, por su inestimable guía y motivación en el desarrollo de nuestro proyecto de investigación, contribuyendo de manera significativa a mi crecimiento personal, profesional y académico. Asimismo, extiendo mi gratitud a los profesionales dedicados a la investigación en campos multidisciplinarios, cuyo apoyo e inspiración fueron fundamentales para el progreso de esta investigación, brindándome el impulso necesario para continuar explorando las áreas de estudio abordadas en este trabajo.

Luis Alberto Calderón Salas

RESUMEN

El estudio de materiales a base de quitosano e hidroxietilcelulosa que incorporan extractos naturales para apósitos antimicrobianos de próxima generación está atrayendo cada vez más interés debido a su eficacia para mejorar la cicatrización de heridas. Esta investigación presenta la síntesis y evaluación de una película de hidrogel compuesta de quitosano e hidroxietilcelulosa, cargada con extractos de mangostino y granada. Los principales compuestos biológicos se identificaron mediante espectroscopia infrarroja y cromatografía líquida de alta resolución. Las pruebas antimicrobianas indicaron efectos positivos para *S. aureus* y *E. coli*. En particular, el extracto de mangostán mejoró significativamente el cierre de la herida con fibroblastos adherentes (NIH3T3) dentro de las 24 horas posteriores a la prueba. Estos extractos, ricos en antioxidantes, podrían ayudar a regular las especies reactivas de oxígeno en las heridas. Las películas de hidrogel, analizadas por reflectancia total atenuada-espectroscopía de infrarrojo con transformada de Fourier ATR-FTIR, revelaron reticulación tanto química como física. La inclusión de los extractos redujo el grado de hinchazón y transparencia de las películas de hidrogel. El análisis termogravimétrico mostró ligeros cambios en las propiedades térmicas de las películas debido a los extractos. El aumento de las concentraciones del extracto de mangostino redujo la elongación a la rotura, mientras que el extracto de granada la mejoró. Las micrografías por microscopía de barrido electrónico revelaron estructuras lisas que podrían impedir la adhesión celular. Las pruebas antimicrobianas realizadas en las películas demostraron su eficacia contra *S. Aureus*, lo que indica su posible aplicación como apósitos para heridas. Las propiedades químicas, físicas y biológicas de los extractos y las películas de polímero sugieren un futuro prometedor para estos materiales en aplicaciones médicas, en particular en la creación de apósitos avanzados para heridas con propiedades antimicrobianas y cicatrizantes mejoradas.

Palabras clave: Mangostino, hidrogel, hidroxietilcelulosa, Granada y quitosano.

ABSTRACT

The study of chitosan and hydroxyethylcellulose-based materials incorporating natural extracts for next-generation antimicrobial dressings is attracting increasing interest due to their efficacy in improving wound healing. This research presents the synthesis and evaluation of a hydrogel film composed of chitosan and hydroxyethylcellulose loaded with mangosteen and pomegranate extracts. The main biological compounds were identified by infrared spectroscopy and high-performance liquid chromatography. Antimicrobial testing indicated positive effects against *S. aureus* and *E. coli*. In particular, mangosteen extract significantly enhanced wound closure with adherent fibroblasts (NIH3T3) within 24 hours of testing. These extracts, rich in antioxidants, could help regulate reactive oxygen species in wounds. The hydrogel films, analyzed by attenuated total reflectance-Fourier transform infrared spectroscopy (ATR-FTIR), revealed both chemical and physical cross-linking. Including the extracts reduced the degree of swelling and transparency of the hydrogel films. Thermogravimetric analysis showed slight changes in the thermal properties of the films due to the extracts. Increasing concentrations of the mangosteen extract reduced the elongation at break, while the pomegranate extract improved it. Scanning electron microscopy micrographs revealed smooth structures that could prevent cell adhesion. Antimicrobial tests on the films demonstrated their efficacy against *S. Aureus*, indicating their potential application as wound dressings. The extracts and polymer films' chemical, physical, and biological properties suggest a promising future for these materials in medical applications, particularly in creating advanced wound dressings with enhanced antimicrobial and wound-healing properties.

Key Words: Mangosteen, hydrogel, hydroxyethylcellulose, Pomegranate, and chitosan.

ABBREVIATIONS AND ACRONYMS

CA	Citric Acid
CH	Chitosan
CHHEC	Films Chitosan- Hydroxyethylcellulose
GL	Glycerol
GM	Mangosteen
GME	Mangosteen ethanolic extract
GME1	Film with low concentration of Mangosteen extract
GME2	Film with high concentration of Mangosteen extract
HEC	Hydroxyethylcellulose
PG	Pomegranate
PGE	Pomegranate ethanolic extract
PGE1	Film with low concentration of Pomegranate extract
PGE2	Film with high concentration of Pomegranate extract
FTIR	Transform Infrared Spectroscopy
SEM	Scanning Electron Microscopy
TGA	Thermogravimetric analysis
UTM	Universal Testing Machine

TABLE OF CONTENTS

ABSTRACT.....	7
1 INTRODUCTION	1
2 PROBLEM STATEMENT.....	4
3 GENERAL AND SPECIFIC OBJECTIVES	5
3.1 General objective	5
3.2 Specific objectives	5
4 THEORETICAL BACKGROUND.....	6
4.1 Overview of Wound Healing Process.....	7
4.2 Hydrogels in wound healing	8
4.3 The Role of Plant Extracts in the Wound Healing Process	11
5 MATERIALS AND METHODS.....	14
5.1 Reagents and solutions.....	14
5.2 Preparation of mangosteen and pomegranate peel extract.....	17
5.3 Phytochemical screening of mangosteen and pomegranate extracts	17
5.3.1 Detection of flavonoids.....	17
5.3.1.1 Acid Test.....	17
5.3.1.2 Shinoda Test	19
5.3.2 Phenol compounds test	19
5.3.2.1 Iodine test	19
5.3.2.2 Ferric chloride.....	19
5.3.3 Tannins compounds	19
5.3.3.1 10% NaOH test.....	19
5.3.3.2 Braymer's test	19

5.3.4	Coumarins test	19
5.3.4.1	10% NaOH test.....	19
	Two milliliters of each extract were added to each test tube, followed by one milliliter of sodium hydroxide and one milliliter of chloroform. The yellow color of the sample confirms the presence of coumarins.....	19
5.3.5	Alkaloids test	20
5.3.5.1	Dragendroff's Test	20
5.3.5.2	Wagner's Test	20
5.3.6	Phytosterols test	20
5.3.6.1	Acetic Anhydride test	20
5.3.6.2	Hesse's response	20
5.3.7	Saponins test	20
5.3.7.1	Sodium bicarbonate Test	20
5.3.8	Proteins and amino acid test	21
5.3.8.1	Ninhydrin Test.....	21
5.3.8.2	Xanthoproteic tests	21
5.4	Chemical Characterization of Extracts	21
5.5	Determination of Total Polyphenol content of GME and PGE	21
5.6	Determination of Antioxidant Activity by the Radical Scavenging DPPH Method	22
5.6.1	Reaction Mechanism.....	22
5.7	Pomegranate and mangosteen peel extracts antimicrobial studies	23
5.8	Wound healing test	24
5.9	Preparation of hydrogel films	24
5.10	Preparation of Hydrogel film with extracts	25
5.11	Thickness, Weight Variation	26
5.12	Chemical Characterization of hydrogel films	26

5.13	Swelling ratio	28
5.13.1	Preparation of Phosphate Buffered Saline (PBS)	28
5.13.2	Preparation of Simulated Body Fluid (SBF).....	28
5.14	Transparency/Opacity	29
5.15	Thermogravimetric analysis TGA	29
5.16	Mechanical Strength of Films	30
5.17	Scanning electron microscope	30
5.18	Antimicrobial study of hydrogel films with GME and PGE	30
5.19	Cell culture.....	31
6	RESULTS AND DISCUSSION	32
6.1	GME and PGE Extracts	32
6.1.1	Qualitative phytochemical analysis	32
6.1.2	Analysis of extracts using FTIR Spectrophotometer	33
6.1.3	HPLC Profiling of Mangosteen and Pomegranate.....	36
6.1.4	Total phenol content of Pomegranate and Mangosteen Peel	39
6.1.5	Antioxidant DPPH assay protocol	41
6.1.6	Extracts of mangosteen and pomegranate peel antimicrobial studies	43
6.1.7	Wound healing assay	47
6.2	Characterization of Composite Hydrogel CHHEC.....	49
6.2.1	Fourier transform infrared FT-IR.....	49
6.2.2	Swelling ratio	52
6.2.3	Mechanical Properties.....	53
6.3	Hydrogel films loaded with and without GME and PGE extracts.....	55
6.3.1	Thickness and Weight Variation.....	55
6.3.2	Swelling ratio of Hydrogel films with GME and PGE.....	56

6.3.3	Transparency/Opacity	60
6.3.4	Fourier transform infrared FT-IR.....	62
6.3.5	Thermogravimetric analysis TGA of Hydrogel films with GME and PGE	64
6.3.6	Mechanical Strength of Hydrogel films with GME and PGE	66
6.3.7	Scanning electron microscope	71
6.3.8	Disc diffusion of hydrogel films loaded with extracts.....	74
6.3.9	Cell culture on hydrogel films	77
7	CONCLUSIONS.....	79
8	RECOMMENDATIONS	79
9	References.....	80

LIST OF FIGURES

Figure 1 Wound healing process taken from Akhtari [37] et al.	7
Figure 2 Main polysaccharides and applications in wound dressings from Ribeiro [61] et al.	10
Figure 3 Molecules of biological interest present in the pericarp of Mangosteen from Karim [78] et al.....	12
Figure 4 Molecules of biological interest present in the pericarp of Pomegranate from Gullón[85] et al.....	13
Figure 5 Preparation of ethanolic extracts of Mangosteen and Pomegranate.....	18
Figure 6 Reaction mechanism DPPH radical reduce to 2,2-diphenyl-1-hydrazine (DPPH-H).....	22
Figure 7 Preparation scheme of hydrogel films loaded in situ with extracts.....	27
Figure 8 Dimensions of specimens for mechanical tests.....	30
Figure 9 Reactions of screening of major phytochemical compounds in the peel a) Mangosteen and b) pomegranate.....	33
Figure 10 FTIR extracts GME and PGE.....	34
Figure 11 HPLC chromatogram of <i>P. Granatum</i> ethanolic extract.....	37
Figure 12 UV-Vis spectra from <i>P. Granatum</i> extract ethanolic.....	37
Figure 13 HPLC chromatogram of <i>G. Mangostana</i> ethanolic extract.....	38
Figure 14 UV-Vis spectra from <i>G. Mangostana</i> extract ethanolic.....	39
Figure 15 Gallic acid standard calibration curve for the quantification of total phenolic compound.....	40
Figure 16 Calibration standards before and after 2 hours for measurements for the calibration standard curve.....	41
Figure 17 Graph of ethanolic extracts concentration versus % DPPH inhibition.....	42
Figure 18 Mangosteen assay DPPH.....	43
Figure 19 Diffusion disk of GME and PGE extracts against <i>S. Aureus</i> and <i>E. Coli</i> and inverted microscope.....	46
Figure 20 Representative images Scratch assay 10x for control and GME 50 ug/mL in the following time intervals 0h, 24h y 48h.....	48
Figure 21 FTIR CH Film and CHHEC.....	50
Figure 22 Second derivative of FTIR CH Film and CHHEC.....	50
Figure 23 Reaction equation for the formation of the hydrogel film.....	51

Figure 24 Swelling ratios of the different polymer compositions of the hydrogel films.....	53
Figure 25 Tensile strength (a), Elongation (b), and Young's Modulus (c) of dried samples CHL45HEC30CA5GL1 and CHH45HEC30CA5GL1.....	54
Figure 26 Photography of the synthesized films without extract and with extracts	56
Figure 27 Swelling behavior of hydrogel films in different fluids: a) Deionized water (DI), b) phosphate buffered saline (PBS), c) simulation of blood plasma (SBF) and d) Appearance of the films 24 hours after immersion in each fluid	59
Figure 28 Effect of GME and PGE on the a) transparency, b) opacity in the films and c) appearance of the films.CH-HEC, GME-1 and PGE-1	61
Figure 29 FTIR film compositions a) CH-HEC Film, b) CH-HEC-GM-1-PG-1 Film, c) CH-HEC-GM-1 Film and d) CH-HEC-PG-1 F	63
Figure 30 Thermal gravimetric analysis of films CH-HEC, CH-HEC-GM-2, CH-HEC-PG-2 and CH-HEC-GM-1-PG-1 a) Weight (%) vs Temperature, b) Deriv. Weight (%/min) vs Temperature and c) representative image of TGA 5500.....	65
Figure 31 Tensile mechanical properties a) Tensile Strength b) Elongation at break c) Young's Modulus (MPa) and d) Representative Sample. Different films with and without extract content were evaluated in dry and wet conditions. Error bars indicate standard deviations.....	70
Figure 32SEM micrographs a) CHHEC bright side 1000x; b) CHHEC opaque side 1000x ; c) GME1 bright side 1000x; d) GME1 opaque side 1000x ; e) PGE1 bright side 1000x; and f) PGE1 opaque side 1000x.....	73
Figure 33 Hydrogel films. with extracts and without extracts against S. Aureus and E. Coli; CH-HEC-PG-1 (4); CH-HEC-PG-1 (5); CH-HEC(F); and Ampicilim (A)	76
Figure 34 NIH/3T3 fibroblast cell culture on films after 24 h incubation images. Micrographs obtained with inversion microscope a) control t=0, b) control t=24h, c) CH-HEC t=0, d) CH-HEC t=24h, e) CH-HEC-PG-1 t=0 , f) CH-HEC-PG-1 t=24h, g) CH-HEC-GM-1 t=0, and h) CH-HEC-GM-1 t=24h.	78

1 INTRODUCTION

Healing wounds stands as a paramount clinical challenge globally, with an escalating number of cases annually spanning from acute to chronic injuries. The wound or tissue regeneration is intricate, involving phases such as inflammation, proliferation, maturation, and remodeling to restore the tissue to its original state[1]. Conventional methods employing gauze and cotton for wound coverage pose challenges regarding biocompatibility, biodegradability, costs, pain, and allergic problems[2]. However, emerging materials like hydrogels, films, colloids, and sponges show promising properties that could effectively expedite the wound healing process [3], [4].

Traditional treatments for injured tissues often face challenges related to infection control, flexibility, pain management, transparency, and hemostasis, leading to potential secondary injuries[5]. The design of materials for wound healing must meet several criteria, including wound protection, good mechanical properties, antimicrobial properties, compounds with biological activity, biocompatibility, capacity to absorb exudate, and costs[6]. Hydrogels, categorized as new-generation materials, are promising alternatives capable of addressing many drawbacks associated with conventional materials. Their 3D chemical structure, facilitated by crosslinking, enables the controlled release of various pharmaceutical or biological compounds, promoting a more efficient wound-healing process[7].

Extracts derived from plant or fruit waste have significant potential in wound healing[8]. Polymeric films incorporating plant extracts for wound healing in bandages have garnered clinical and economic interest [9]. Notably, the pericarp of the Mangosteen (*Garcinia Mangostana*) fruit, commonly known as mangosteen, constitutes approximately half its weight and is typically discarded as waste [10]. However, mangosteen's composition counts with xanthenes, anthocyanins, cinnamic acid, syringaldehyde, and flavonoids [11] [12]. These constituents exhibit diverse biological activities, including their ability to treat cancer cells, reduce inflammation, act as antioxidants, and provide antidiabetic properties[13]. Notably, flavonoids enhance the anti-inflammatory efficacy of patches utilized in treating burns in experimental models [14]. Patches made from bacterial cellulose with mangosteen peel extract have effectively closed wounds in diabetic mice[15]. Boonmak and collaborators[16] synthesized a spray based on PVA and 1 to 3% mangosteen extract, demonstrating no toxicity

for L929 cells. Pugar et al.[17] investigated the effect of alginate and garcinia mangosteen ethanolic extract in diabetic mice, promoting the formation of collagen and fibroblasts attributed to exudate absorption and the anti-inflammatory and antioxidant properties of xanthenes.

The pomegranate (*Punica Granatum*) peel represents forty to fifty percent of the total fruit weight[18]. Utilizing pomegranate waste helps mitigate pollution and enhances the value of waste-derived products. The peel contains active compounds such as phenolic acids, polyphenols, and flavonoids [19], known for their physiological functions and anti-inflammatory properties, including antibacterial, anticancer, and antioxidant[20]. Ethanolic pomegranate extract has increased collagen production and fibronectin gene expression, promoting wound healing [21]. Films loaded with pomegranate extract have demonstrated in vitro efficiency in reducing scratch areas and achieving closure within forty-eight hours[22]. Hashemi et al.[23] found that an ethanolic extract of pomegranate peel at 25 $\mu\text{g}/\text{mL}$ improves the migration and proliferation of human dermal fibroblasts.

Garcinia mangostana and *Punica granatum* extracts, which contain antibacterial, anti-inflammatory, and antioxidant compounds, are suitable for developing wound dressings as they can reduce bacterial load and improve wound confluence[24]. Additionally, the antioxidants present in the extracts help decrease reactive oxygen species in wound processes, improving wound healing. The presence of α -mangostin and γ -mangostin regulates the production of nitric oxide species and prostaglandins[25]. Meanwhile, gallic acid, ellagic acid, and punicalagin present in *Punica granatum* can regulate free radical levels, protect cells from oxidative stress, and reduce damaged cellular[26]. Both extracts have been tested on different strains of fibroblasts and in vivo test, demonstrating efficacy under conditions that suggest their viability for incorporation into wound dressing materials [16] [17] [21] [22] [23].

Chitosan is a widely abundant polysaccharide known for its amino group content[27]. Derived from the deacetylation of chitin, chitosan is sourced primarily from crustaceans, algae, and mollusks. The presence of amino groups attributes several beneficial properties to chitosan, including biocompatibility, non-toxicity, antimicrobial activity, moisture retention, tissue regeneration promotion, and release of biologically active compounds, making it an ideal candidate for biomaterial design [28]. Its antimicrobial action operates through mechanisms such

as electrostatic interactions, DNA replication inhibition, formation of soluble complexes, and membrane perturbation[29]. Hydrogels that use chitosan in their composition create a favorable microenvironment that promotes granulation and epithelialization, thereby enhancing the collagen generation process[30]. However, studies utilizing crosslinking agents with chitosan have yet to yield optimal results, highlighting the need to effectively identify agents that address this issue.

Hydroxyethylcellulose, derived from cellulose, is extensively utilized at a commercial scale. Its structure is distinguished by including the hydroxyethyl functional group, which enhances its solubility. This compound finds wide application in the formulation of cosmetics, pharmaceuticals, emulsions, stabilizers, and water retainers[31]. When incorporated into hydrogel formulations, hydroxyethylcellulose can reduce irritation and create a moist environment conducive to wound healing[32]. The production of hydrogels utilizing hydroxyethylcellulose combined with polymers sourced from synthetic or natural origins has demonstrated favorable physicochemical and thermal properties alongside controlled drug release capabilities—suitable conditions for producing materials in the form of dressings for wound regeneration[33].

This study aimed to prepare and evaluate chitosan/hydroxyethylcellulose-based hydrogel films loaded with extracts from Mangosteen and Pomegranate. The study focused on achieving suitable swelling behavior, flexibility, wound contact, and release of biological compounds from the hydrogel films. Physical-chemical studies, antimicrobial tests, and scratch tests were conducted to evaluate their potential for wound treatment. This research introduces the novel use of mangosteen and pomegranate extracts in developing a biopolymeric hydrogel film. Moreover, the hydrogels were produced using an environmentally friendly technique, emphasizing their swelling properties, bio-adhesive nature, antibacterial efficacy, and antioxidant potential, all of which are crucial for the development of advanced wound healing materials

2 PROBLEM STATEMENT

The demand for wound dressings is growing worldwide to meet needs such as low toxicity, easy removal, decreased wound healing time, physical performance, and affordable costs. Traditional wound dressings often lack the environment for optimal healing, such as maintaining appropriate moisture levels, delivering antimicrobial agents, and ensuring biocompatibility, highlighting the need for innovative materials to meet these critical demands. Hydrogels have emerged as promising materials for wound dressings precisely due to their excellent moisture retention, biocompatibility, and ability to incorporate bioactive compounds.

HEC, CH, GME, and PGE extract have been extensively studied for their bioactive compounds and biological properties, making them ideal candidates for producing bio-films and hydrogels for biomedical applications. Despite the potential benefits, the development of hydrogels from HEC and chitosan incorporating Mangosteen or Pomegranate extracts for wound dressing applications has yet to be extensively studied. This gap in the current research presents a unique opportunity to explore and develop these materials for a crucial application. The optimal preparation methods, properties, and efficacy of such hydrogels in promoting wound healing and preventing infection still need to be determined. This thesis addresses this gap by developing and characterizing hydroxyethyl cellulose and chitosan hydrogels, incorporating extracts from Mangosteen or Pomegranate. The research will focus on optimizing the preparation methods, evaluating the physicochemical properties, and assessing the hydrogels' biological performance in wound healing applications. Additionally, the study will investigate the synergistic effects of biopolymers and natural extracts in enhancing wound healing and antimicrobial efficacy.

By advancing the preparation and application of these hydrogels, this research seeks to contribute to developing effective, biocompatible, and multifunctional wound dressings, ultimately improving patient outcomes in wound care management.

3 GENERAL AND SPECIFIC OBJECTIVES

3.1 General objective

- The main objective of this research is to develop and evaluate chitosan/hydroxyethylcellulose-based hydrogel films loaded with Mangosteen and Pomegranate extracts for biomedical applications in wound healing.

3.2 Specific objectives

- Develop and characterize chitosan/hydroxyethylcellulose-based hydrogel films incorporating Mangosteen and Pomegranate extracts, following sustainable synthesis using green chemistry principles.
- Evaluate the antioxidant potential of the extracts and evaluate their effectiveness in enhancing wound healing through in vitro studies
- Evaluate the hydrogel films' bioactive properties, including antibacterial sensitivity against gram-positive and gram-negative bacteria.
- Investigate the physicochemical, morphological, thermal, and mechanical properties of the hydrogel films, focusing on swelling behavior in distilled water and simulated biological fluids and mechanical strength and elasticity for wound dressing applications.

4 THEORETICAL BACKGROUND

In the evolving landscape of biomedical materials and wound healing technologies, developing advanced materials that promote efficient healing processes remains a critical area of research. The following sections provide a comprehensive review of theoretical concepts and background that underpin the study of the design, synthesis, and application of hydrogel films loaded with extracts from Mangosteen (*Garcinia Mangostana*) and Pomegranate (*Punica Granatum*) for wound healing. These materials hold promise for addressing challenges in wound care, such as infection control, tissue regeneration, and biocompatibility.

This chapter begins by outlining the current knowledge of wound healing processes, emphasizing the physiological stages involved and the key factors influencing healing outcomes. It reviews existing literature on the significant role of biomaterials in wound care, highlighting their importance in creating conducive environments for tissue regeneration and minimizing infection risks.

Following this, the chapter discusses the properties of hydrogels that are particularly relevant to wound care applications. These properties, including biocompatibility, swelling behavior, and mechanical strength, are crucial in understanding the efficacy of hydrogel-based wound dressings. The various fabrication methods employed, such as solvent casting and crosslinking techniques, will also be explored, and how they contribute to the properties of hydrogels will be examined.

The exploration then extends to natural extracts, specifically mangosteen, and pomegranate, known for their potential benefits in wound healing. The chapter explores the mechanisms of action underlying their antioxidant, antimicrobial, anti-inflammatory, and tissue regeneration properties. This includes a critical review of recent studies and findings that support their therapeutic potential in biomedical applications.

4.1 Overview of Wound Healing Process

The wound healing process comprises four stages[34], [35]. The first stage is hemostasis, where bleeding stops as blood vessels constrict and platelets change shape to facilitate clot formation[36]. The second stage, inflammation, involves neutrophils and macrophages destroying bacteria and clearing debris to prepare the area for new tissue growth. These cells also secrete growth factors and proteins that attract other immune system cells[37]. In the third stage, new cells, and tissues are formed in proliferation. Fibroblasts produce collagen and develop blood vessels, while new epithelial cells are generated at the surface[38]. Finally, in the remodeling stage, the collagen matrix is reorganized, forming a scar that gradually resembles the original tissue in appearance and function[39]. Figure 1 illustrates the phases of wound healing, from the beginning of the wound to the modeling phase.

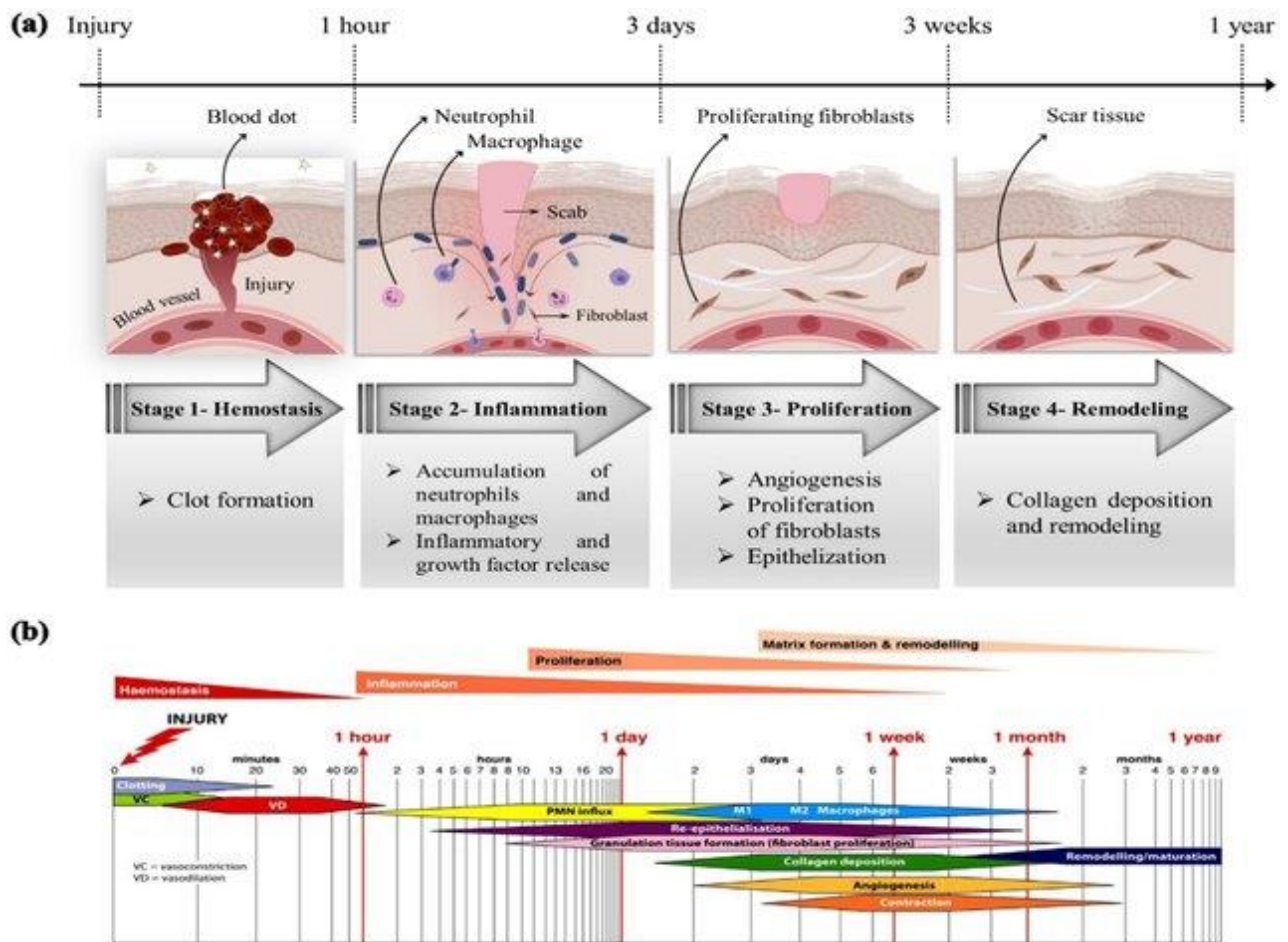


Figure 1. Wound healing process taken from Akhtari [40] et al.

Wounds can face various limitations that impact their healing trajectory and duration. For instance, autoimmune conditions like diabetes can impair healing by damaging blood vessels and reducing blood flow due to elevated sugar levels[41]. Disorders affecting collagen production can also disrupt tissue formation. Infections introduce additional complexities as bacteria release toxins that degrade tissues[42]. Furthermore, the location of a wound may expose it to mechanical stress during joint movement, potentially hindering recovery. Other factors such as nutritional status, age, humidity, maceration, and medication use further influence tissue regeneration processes[43].

4.2 Hydrogels in wound healing

Hydrogels play a crucial role in wound treatment within biomedicine due to their biocompatibility with epithelial tissues and their ability to provide a moist environment to accelerate wound healing [44]. They facilitate the absorption of exudates, alleviate pain, reduce scarring, and expedite the healing process, making them suitable for a broad spectrum of wounds from minor to chronic[45]. For instance, hydrogels can be customized to enhance moisture levels in dry wounds like burns and aid in diabetic wound care.

The fabrication of hydrogels typically involves polymer dissolution followed by gelation or polymerization[46]. Gelation methods utilize chemical reagents or rely on physical changes such as pH, temperature variations, or exposure to ultraviolet light. Chemical or physical cross-linking agents create desired three-dimensional networks within the polymeric matrices[47]. Furthermore, the incorporation of antimicrobial agents, anti-inflammatory factors, drug delivery, and growth factors enhances the hydrogel's ability to promote cell migration and proliferation[48], [49], [50].

Hydrogels are formulated in various formats, such as films, gels, or foams, all requiring sterilization before application[51]. The efficacy of these materials is not left to chance. It involves rigorous testing in both in vitro and in vivo settings, followed by preclinical and clinical trials to establish their feasibility and safety for widespread biomedical use. This thorough process instills confidence in their safety and effectiveness.

Wound dressings play a crucial role in promoting efficient wound healing. The materials used are selected based on their ability to absorb exudate and the dimensions and depth of the wounds they are intended to treat. The latest generation of wound dressing materials includes foams, alginates, hydrocolloids, hydrogels, and films[52]. Films, thin and transparent materials, can protect

damaged tissues and monitor wound progress. The films have some advantages, such as non-adhesion, air permeation, water vapor permeability, impermeable to water, and mechanical properties resembling skin [53]. The films allow medical personnel to inspect wounds by being transparent[54]. They also help prevent infections with bacteria or external germs by acting as a barrier. The films can create a moist environment that can help regenerate damaged tissues. In addition, the films allow perspiration and prevent high humidity. These flexible materials do not adhere to the skin like gauze, causing pain and tissue removal. The mechanical design of the films allows proper movement of the films with the patient. Hydrogels can regulate the amount of water and improve the wound microenvironment, reducing healing time. The films can also be loaded with several medications for controlled release to relieve pain symptoms and as healing promoters[55]. The films can be used for superficial wounds, burns, infected wounds, and ulcers[56].

Hydrogels have been used and studied extensively in the area of bioengineering. Hydrogels are made up of polymers of natural and synthetic origin, which retain moisture[57]. Hydrogel-based dressings can be used on both dry and moist wounds. Hydrogels promote cell autolysis and, therefore, help in the debridement process. Eliminating necrotic tissues favors cell movement, promoting healing and possible new infections[58]. The advantages of these materials are based on promoting a moist environment and facilitating healing. These materials can reduce pain and give a cooling sensation. Hydrogels do not adhere to the skin, reducing the risk of scar tissue removal. Hydrogels also promote the formation of connective tissue, accelerating wound healing. These materials can also be loaded with several medications for controlled release to reduce pain symptoms and as healing promoters[59]. Hydrogels are used in wounds with a low level of infection and low exudate. Depending on the type of hydrogel and its swelling capacity, they can be applied to wounds with exudate in the moderate to high range. Hydrogels can be used in applications such as burns, diabetic ulcers, and painful wounds[60].

Polysaccharides, whether of natural or synthetic origin, can be applied in treating wounds due to their biological and physicochemical properties that promote healing[61]. Naturally occurring polymers include gelatin, collagen, chitosan, alginate, and cellulose, as well as synthetic polymers such as polyethylene glycol, polyglycolide, polyurethane, polyvinylpyrrolidone, polycaprolactone, polyvinyl, have been widely used in wound regeneration[62], [63]. These polymers enable

cultivation in three-dimensional matrices, controlled drug release, development of biosensors, and intrinsically promote wound healing[61]. Depicts polysaccharides from natural and synthetic origins, which have been thoroughly researched for their utilization in wound dressings, highlighting the essential criteria they must fulfill in Figure 2.

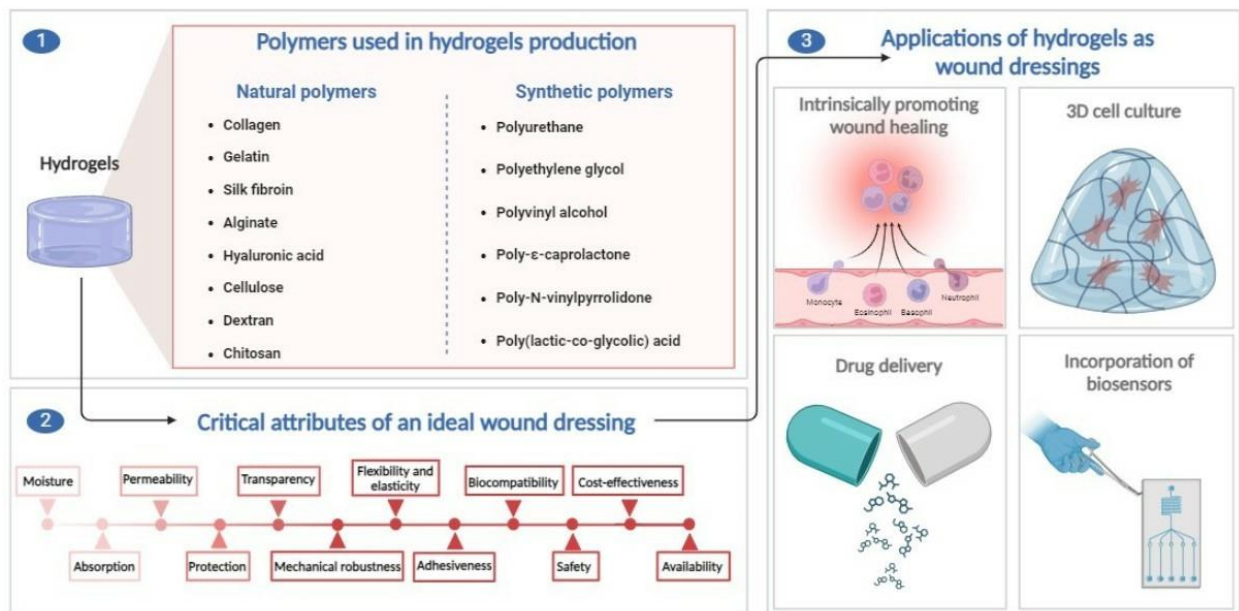


Figure 2. Main polysaccharides and applications in wound dressings taken from Ribeiro [64] et al.

CH-HEC-based films incorporating titanium oxide nanoparticles have been reported for food packing to extend the life of lychee fruit[65]. Materials based on CH-HEC were studied in the adhesion of elastic films on oral mucosa in pigs, focusing on formulations containing a more significant amount of hydroxyethylcellulose to chitosan[66]Balcik reported that incorporating nano clays into this type of mixture crosslinking with citric acid favors the production of packaging that replaces those produced by petrochemical companies. [67]In biomedicine, carboxymethylcellulose has been included as a third component in the mixture, introducing growth factors into the polymeric matrix to accelerate the regeneration of dermal tissues.[68]. Other studies on materials incorporate cerium nanoparticles into the chitosan hydroxyethylcellulose mixture to achieve antibacterial and mechanical properties suitable for the design of packaging materials[69]

4.3 The Role of Plant Extracts in the Wound Healing Process

The presence of active components in plants has been extensively researched and used widely within the fields of wound-healing medicine[70]. Research on extracts for the development of new drugs is of high medical and economic interest. The factors found in regeneration are the following: cell growth, antioxidant, anti-inflammatory, anticarcinogenic, and antimicrobial properties[71], [72]. In more detail, the components of the extracts facilitate the proliferation of epithelial cells and blood coagulation, as well as better anchoring of collagen to damaged tissues and barrier against infections.[73]. Extracts like aloe vera, curcumin, chamomile, and lavender are obtained through methods such as distillation and maceration [74]. These extracts contain active ingredients that enhance healing in vitro, in vivo, and animal models [75] Clinical studies are expanding wound care applications for these extracts.

The pericarps of mangosteen are rich in various compounds, including xanthenes, tannins, triterpenoids, benzophenones, flavonoids, anthocyanins, and phenolic compounds[76]. Xanthenes, in particular, are the primary active molecules with demonstrated antimicrobial, antiviral, anticancer, and antimutagenic properties[77]. Figure 3 illustrates the main molecules of biological interest found in the peel of the mangosteen fruit. Harvesting approximately 2 grams of xanthenes from every 1000 mangosteen fruit significantly elevates its commercial value by 15 times. Notably, the pericarp specifically yields alpha mangostin and omega mangostin, ranging from 145 to 382 mg per gram on a dry basis[78]. Extracts from mangosteen pericarp contain both non-polar and polar compounds. The non-polar compounds include prenylated benzophenones and xanthenes, while the polar compounds consist of anthocyanins, procyanidins, and catechins[78]. Mangosteen peel extracts can be obtained using different solvents, such as maceration or Soxhlet, to improve the yield of xanthenes[79].

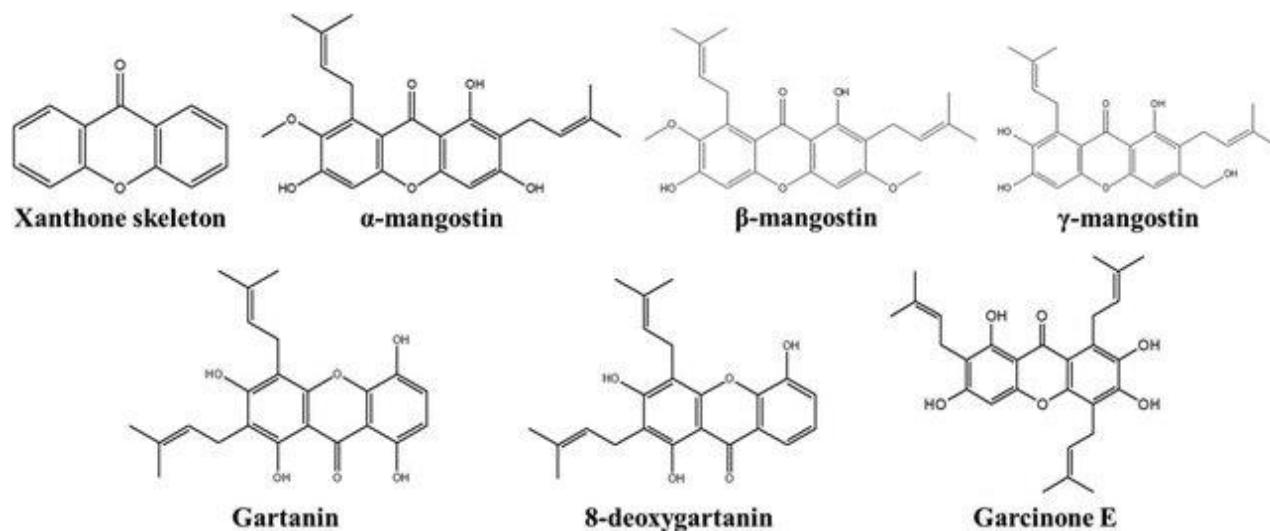


Figure 3. Molecules of biological interest present in the pericarp of Mangosteen taken from Karim [80] et al.

The following materials, incorporating mangosteen extracts, were investigated for biomedical applications. The ethanol extract of Mangosteen (GME) was immersed into a bacterial nanocellulose film. Research suggests that these materials have antibacterial anticancer, properties and are suitable for developing dressings for skin cancer and anti-acne [81]. The research on bacterial cellulose, gelatin, and mangosteen extract yielded promising results. The absence of toxicity towards human keratinocytes was demonstrated, suggesting a favorable safety profile.

Furthermore, significant anticancer properties were observed against oral cancer, representing a substantial advance in oral oncology. These findings suggest that this combination could be suitable for treating problems such as periodontitis and skin wounds, which could be necessary for dentistry and wound healing treatments. An analogous study used bacterial cellulose and incorporated ethanolic mangosteen extract and found significant inhibition of breast cancer cells and melanoma cells[82]

Pomegranate peel contains various components with relevant biological activity, including flavonoids, tannins, fibers, and phenolic acids[83]. Figure 4 depicts the main bioactive compounds found in pomegranate peel. The peel represents approximately 26- 30 percent of the total weight of the fruit[84]. These active compounds have been recognized for their antibacterial, anticancer, anti-inflammatory, and cardiovascular properties [83]. Punicalagin and ellagic acid are the main antioxidants in the peel [85]. Various extraction methods and solvents have been used to obtain

these molecules of interest. Bacterial cellulose films were soaked in aqueous pomegranate extract solutions, which exhibited antibacterial activity against *P. acnes*, *S. aureus*, and *S. epidermidis*. These films also showed good mechanical properties, making them suitable for acne treatment. [86]

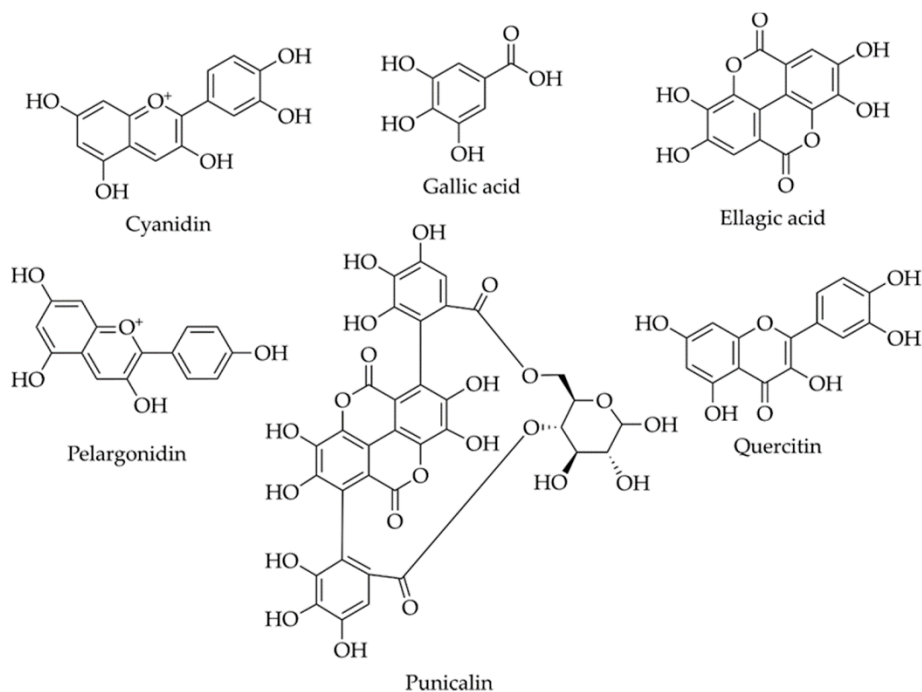


Figure 4 Molecules of biological interest present in the pericarp of Pomegranate from Gullón[87] et al.

Natural plant and fruit extracts have remarkable wound-healing properties[88]. Traditionally used in medicine for their therapeutic benefits, these extracts are rich in biologically active molecules such as vitamins, phenolic compounds, flavonoids, saponins, amino acids, and xanthenes[89], [90]. These constituents endow the extracts with antioxidant, anti-inflammatory, astringent, antibacterial, and antifungal properties[91]. The potential of these natural resources is increasing in biomedicine, particularly for their incorporation into dressings for skin regeneration. Additionally, current scientific research is focused on optimizing the extraction and purification processes to enhance the effectiveness of these compounds. Recent studies have demonstrated that these extracts can significantly accelerate healing by promoting cell regeneration and reducing inflammation[92]. Thus, applying natural extracts in biomedical products offers a promising alternative to conventional treatments.

5 MATERIALS AND METHODS

The following reagents were used directly to prepare extracts and films. The preparation media for the cells used in the biological tests needed to be purified.

5.1 Reagents and solutions

- **Reagents hydrogel film**

Chitosan 448869 (Low molecular weight, 50,000–190,000 Da, 75.0% Deacetylated), Hydroxyethylcellulose 09368 (viscosity ~145 mPa.s, 1 % in H₂O (20 °C)), Citric acid C0759, and Glycerol G5516 (molecular biology ≥99.0%), were acquired from Sigma Aldrich, USA.

- **Reagents Phytochemical screening**

Sulfuric acid CAS 7664-93-9 (ACS Plus, 96%) was acquired from Fischer chemical, Canada. Magnesium ribbon. Resublimed iodine from Químicos e Importaciones, Ecuador. Ferric chloride (ACS reagent, ≥ 99.7%) was acquired from ISOLAB, Germany. Hydroxide Sodium 106498 (pro analysis) was acquired from MERCK, Germany. Chloroform 67-66-3(ACS reagent, ≥ 99%) was acquired from ISOLAB, Germany. Dragendroff's reagent spray solution was acquired from Merck, Germany. Acetic anhydride CAS 7664-93-9 (ACS,98%) was acquired from Avantor-JTBaker, Mexico. Sodium hydrogen carbonate CAS 144-55-8 (ACS) was acquired from Merck, Germany. Nitric Acid CAS 7697-37-2 (ACS Plus) was acquired from Fischer Chemical, USA.

- **Reagents DPPH**

DPPH (2,2-Diphenyl-1-picrylhydrazyl) is a stable free radical (ACS, 97%) was acquired from Tokyo Chemical Industry, Japan.

- **Reagents PBS y SBF**

Sodium chloride (Merck, 99.99%), Sodium Bicarbonate (ACS reagent, ≥ 99.7%), Potassium chloride (Fisher, 99.0% USP), di-Potassium hydrogen phosphate anhydrous (SCHARLAU reagent, ≥ 99.8%), Magnesium chloride anhydrous (ACS, ≥ 98%) from SIGMA-ALDRICH, USA. Hydrochloric acid (ACS reagent, 1M), Calcium dichloride (ACS reagent, ≥ 99%, 0.2897 g) from Merck, Germany. Sodium sulfate anhydrous (ACS reagent, ≥ 99%), and tris(hydroxymethyl)aminomethane (ACS reagent, ≥ 99.99%), Sodium Phosphate Dibasic

AR(Dihydrate) CAS 10028-24-7(ACS, $\geq 99.5\%$) was acquired from LOBAChemie, India. Potassium Phosphate Monobasic CAS 7778-77-0(ACS, $\geq 99.6\%$) was acquired from Fischer Scientific, USA.

- **Biological reagents**

Phosphate buffered Saline p2272(pH 7.2, suitable for cell culture) was acquired from Sigma Aldrich, Germany. Dulbecco's Modified Eagle Medium (high glucose, cell culture, L-glutamine, pyridoxine hydrochloride, 110 mg/mL sodium pyruvate, sodium bicarbonate) was acquired from Thermo Fisher, USA. Ampiciline from GenAmerica, Ecuador. MUELLER-HINTON Agar (pH: 7.4 ± 0.2) from Merck, Germany. NIH-3T3(Embryonic fibroblast adherent, -196 C) from Sigma Aldrich, Germany

- **Solutions for preparing hydrogel films**

The hydrogel films were prepared from the following solutions: Chitosan low molecular weight 2% (w/v) dissolved in 2% (v/v) acetic acid reached a (pH 5-6), hydroxyethylcellulose 2% (w/v), citric acid 2% and glycerol 1% (v/v). All solutions were shaken at 500 rpm for 24 hours and were placed in an ultrasound bath and finally stored in bottles.

- **Laboratory equipment**

		Model	Serie	Brand	Country
ATR-FTIR	Fourier transform infrared spectrometer	L1600401 Spectrum two	1226	PerkinElmer	UK
UHPLC	Ultra high-performance liquid chromatography Systems	Ultimate 3000	UltiMate™ 3000	Thermo SCIENTIFIC	
TGA	Thermogravimetric analyzer	TGA 55	Discovery 0550-1517	Waters TM TA Instruments	Newcastle United
UV-Vis/DAD	Ultraviolet visible spectrophotometer	SPECORD S 600	VS AJ-824- 06001-2	Analytikjena	Germany
UTM	Universal testing machine	SSTM-10KN	1119547	UNITEDTESTINF SYSTEMS	USA
SEM	Scanning electron microscope	Quanta 400	Quanta	FEI	USA
ES	Encoded stereoscopic software LAZ EZ	LEICA M205 C	M205 C	LEICA	Germany
TM	Trinocular microscope	AE31E	AE31E	Motic™	China
UB	Ultrasonic bath	SELECTA P	3000866	P Selecta	España
RE	Rotary evaporator	R-210		BUCHY SWITZERLAND	Swiss
FD	Freeze dryer	Freeze Dryer - 55C		OPERON	South Korea
HSEGG	High-speed electric grain grinder industrial mill	Homend High-Speed Electric Grain Grinder		Homend	Turkey
AB	Analytical balance	HR-150A	HR	COBOS precision	Argentina

Table 1 Equipment used for the manufacture of hydrogel films and extracts

5.2 Preparation of mangosteen and pomegranate peel extract

Fresh mangosteens and pomegranates were purchased from a local store. The fruits underwent prior washing with distilled water. The pericarps were extracted and cut into small fragments. These pericarps were dried in an oven set at 50°C. Once completely dry, the peels were ground into a fine powder using an industrial mill. Previously, extracts were prepared using different solvents, including deionized water, a 1:1 mixture of water and ethanol, and 96% ethanol. The extract obtained using deionized water exhibited low antibacterial activity. The extract prepared with the water-ethanol mixture demonstrated moderate antibacterial activity. Notably, a significant enhancement in antimicrobial activity was observed in the extracts prepared using 96% ethanol. Subsequently, a maceration process was conducted using 40 g of the powder and 200 mL of 96% ethanol for 72 hours at room temperature. The resultant macerate was filtered through a Whatman® filter with 8 µm pore size. The liquid was then subjected to a rotary evaporator at 38 C for one hour until an extract with a viscous consistency was achieved, as shown in Figure 5. From 40 g of mangosteen powder, 1.1707 g of extract was obtained. In contrast to the pomegranate extract, 40 g was obtained per 5.55 g of pomegranate peel powder.

5.3 Phytochemical screening of mangosteen and pomegranate extracts

Mangosteen (GM) and Pomegranate (PG) peel ethanolic extracts were analyzed to determine their phytochemical compounds such as flavonoids (acid test and Shinoda Test), phenolic compounds (iodine test, Lugol test, and ferric chloride), tannins (10% NaOH test and Braymer's test), coumarins(10% NaOH test), alkaloids (Dragendroff's Test and Wagner's Test), Phytosterols (Acetic Anhydride test, Hesse's response), saponins (NaHCO₃), proteins and amino acids test (Ninhydrin Test and xanthoproteic tests) according to procedures previously reported[93], [94]

5.3.1 Detection of flavonoids

Acid Test

One milliliter mL of GME and PGE extracts were added to half milliliter of sulfuric acid individually, if the solution presents an orange color it is related with the presence of secondary metabolites.

Wash the peels and cut into small pieces



Garcinia Mangostana Peel



Punica Granatum Peel

Dry in oven at 50 °C



Grinding process until reaching a fine powder



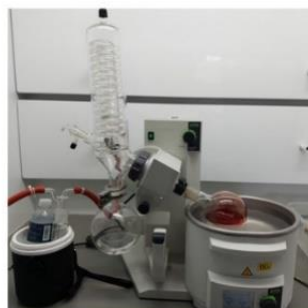
Maceration 3 days



Appearance of extracts diluted



Lyophilization



Rotavaporation



Filtration

Figure 5 Preparation of ethanolic extracts of Mangosteen and Pomegranate

Shinoda Test

Five milliliters of each ethanolic extract were placed with small pieces of magnesium. Half milliliter of hydrochloric acid was added slowly to each test tube. If the resulting solution has a crimson to pink appearance, the presence of flavonoids is confirmed.

5.3.2 Phenol compounds test

Iodine test

Two milliliters of each ethanolic extract were placed with six drops of iodine solution. If the sample shows a red color change, the presence of the phenol compounds is confirmed.

Ferric chloride

Two milliliters of each extract were placed in each test tube, and eight drops of 5% ferric chloride were slowly added. The presence of phenols is confirmed if the sample changes to dark green or bluish-black.

5.3.3 Tannins compounds

10% NaOH test

One milliliter of the extracts was placed with four milliliters of sodium hydroxide and gently shaken. If an emulsion is formed through this process, the presence of tannins is confirmed.

Braymer's test

One milliliter of PGE and GME were placed with three milliliters of distilled water in a ratio of 1 to 3, additionally, six drops of ferric chloride were added. If the sample has a blue or green color, the presence of tannins is confirmed.

5.3.4 Coumarins test

10% NaOH test

Two milliliters of each extract were added to each test tube, followed by one milliliter of sodium hydroxide and one milliliter of chloroform. The yellow color of the sample confirms the presence of coumarins.

5.3.5 Alkaloids test

Dragendorff's Test

To confirm the presence of alkaloids, two milliliters of each extract were combined with two milliliters of Dragendorff's reagent. The solution's color change to reddish-brown tones indicated a positive reaction for alkaloids.

Wagner's Test

One milliliter of each extract of GME and PGE in each assay tube reacted with two drops of Wagner's reagent. The color change to reddish-brown tones confirms the presence of alkaloids.

5.3.6 Phytosterols test

Acetic Anhydride test

A quart of milliliter of each ethanolic extract was combined with one milliliter of the acetic anhydride reagent, followed by the slow addition of one milliliter of concentrated sulfuric acid. The confirmation of phytosterols' presence is indicated by a color change to violet, green, or blue in the sample.

Hesse's response

Four milliliters of mangosteen and pomegranate extracts were placed in separate test tubes with two milliliters of chloroform. Furthermore, 30 drops of sulfuric acid were introduced into each test tube. This resulted in the formation of two distinct layers, with a red ring forming at the interface of the chloroform layer in the lower portion. This observation indicates the existence of phytosterols in the extracts.

5.3.7 Saponins test

Sodium bicarbonate Test

Two milliliters of each extract were combined with one milliliter of sodium bicarbonate solution and one milliliter of distilled water, followed by gentle agitation. The formation of foam indicates the presence of saponins in the sample.

5.3.8 Proteins and amino acid test

Ninhydrin Test

A 2% (w/v) ninhydrin solution in acetone was prepared. One drop of this solution was added for every 1 milliliter of each extract. A purple color change signifies the presence of these compounds.

Xanthoproteic tests

Two milliliters of each extract were combined with eight drops of concentrated nitric acid. The changes in the color of the solutions to yellow confirm the presence of xanthoproteic compounds.

5.4 Chemical Characterization of Extracts

For the chemical characterization of GME and PGE, attenuated total reflection-Fourier transform infrared spectroscopy (ATR-FTIR) and high-performance liquid chromatography (HPLC) were used.

The FTIR spectra were performed from wavenumber 650–4000 cm^{-1} with a resolution of 4 cm^{-1} and four scans. The data were analyzed with Spectrum 10 software.

An isocratic elution method was used for the chromatographic analysis; the mobile phases comprised acetonitrile (phase A) and 0.1% H_3PO_4 in water (phase B) using 95% phase A and 5% phase B for 10 minutes. The column temperature was maintained at 30°C, with a flow rate set at 1 mL/min and an injection volume of 20 μl . Chromeleon software was used for data acquisition.

5.5 Determination of Total Polyphenol content of GME and PGE

Initially, a stock solution of 1000 ppm of gallic acid was prepared. Standards were prepared in concentrations ranging from 20 to 160 ppm, along with the control. A solution of 20% sodium carbonate (w/v) was also prepared. The procedure began by adding fifty milliliters of distilled water and 1 milliliter of Folin-C phenol reagent into each test tube. Subsequently, 1 milliliter of each gallic acid standard was added. After six minutes, 3 milliliters of sodium carbonate were added under low-light conditions. After 2 hours, the absorbances were measured in triplicate at 765 nm to establish the standard curve for gallic acid. Following this calibration, extracts were prepared, and the phenol content was quantified[95].

5.6 Determination of Antioxidant Activity by the Radical Scavenging DPPH Method

The calibration curve was generated utilizing a 1mM solution of 2,2-Diphenyl-1-Picrylhydrazyl (DPPH) and a 1000ppm solution of gallic acid. Gallic acid standards ranging from 1 to 50 ppm were prepared, followed by the addition of DPPH until reaching a final volume of 5 mL. The samples were placed in a dark place shielded from light for 30 minutes. Subsequently, the samples were transferred into cuvettes, and their absorbance was measured at 515 nm. This procedure was repeated for both GME and PGE samples, and each experiment was conducted in duplicate. The percentage of DPPH inhibition was determined using the following equation:

$$\% \text{ DPPH inhibition} = \left[\frac{A_c - A_s}{A_c} \right] 100 \quad (1)$$

Where: A_c —Control reaction absorbance; A_s —sample absorbance.

5.6.1 Reaction Mechanism

The DPPH radical is a methanol-soluble molecule that exhibits a violet color. Antioxidants can interact with this molecule by donating an electron or a hydrogen atom, thereby reducing it to 2,2-diphenyl-1-hydrazine (DPPH-H)[96], which shows a yellow color, as indicated in Figure 6. This assay can be easily monitored using a spectrophotometer at 515 nm.

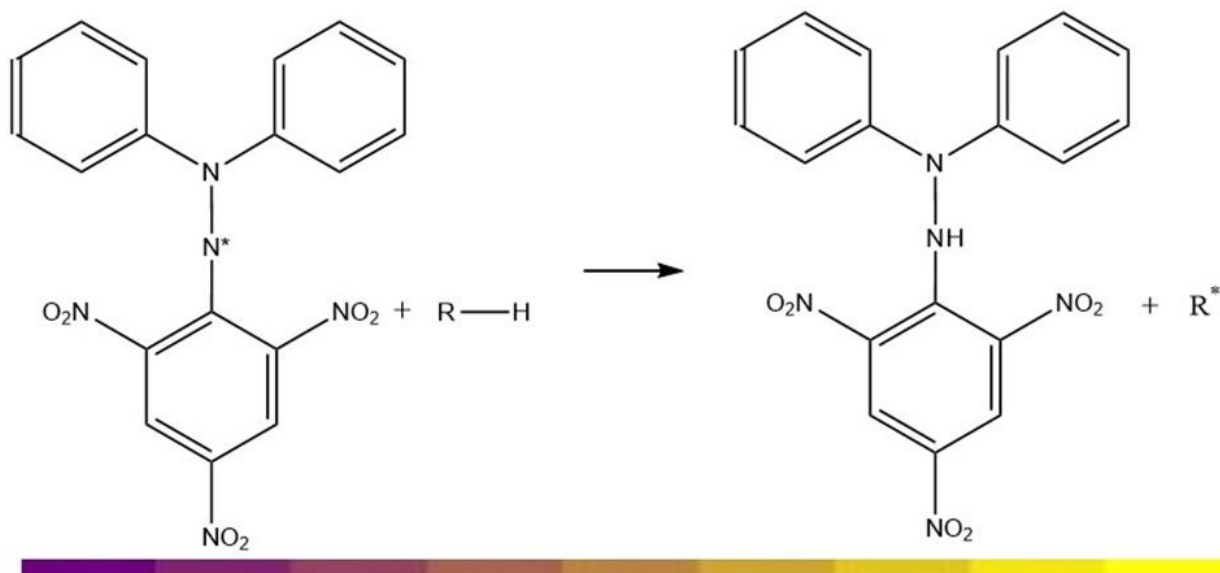


Figure 6 Reaction mechanism DPPH radical reduce to 2,2-diphenyl-1-hydrazine (DPPH-H)

The information on the antioxidant activity of the chemical acid and the PGE and GME extracts was analyzed using the Origin software. The logarithmic equations provided the best fit for the data in this research, allowing the determination of IC₅₀ values. To find the IC₅₀ for each extract, the corresponding 50 percent inhibition was substituted into the equation relative to the DPPH value, enabling the calculation of the specific concentration required.

It is adjusted using the logarithmic calculations based on the following equation:

$$y = a \log(x) + b \quad (2)$$

The EC₅₀ was calculated using the equation obtained for each graph with y=50.

Extracts exhibiting higher antioxidant activity, as indicated by lower IC₅₀ values, are more effective in neutralizing free radicals and mitigating oxidative stress within the wound area. This enhanced antioxidant capacity can potentially lead to improved wound healing outcomes. Specifically, lower IC₅₀ values signify that a minor extract concentration is required to achieve 50% inhibition of radical activity. Conversely, higher IC₅₀ values imply that a greater concentration is necessary to reach the same level of inhibition. Extracts with elevated IC₅₀ values may demonstrate reduced antioxidant efficacy, which could adversely affect their effectiveness in promoting wound healing.

5.7 Pomegranate and mangosteen peel extracts antimicrobial studies

Disk diffusion susceptibility tests were performed following recent CLSI guidelines. The test was carried out for each of the extracts GME and PGE. The study was conducted following the standardized single-disk method for research on antibiotic susceptibility [97]. The strains used in this study were *S. aureus* (ATCC 25923) and *E. coli* (ATCC 25922), respectively, were diluted to a turbidity of 0.5 McFarland standard and inoculated in three different orientations on Mueller-Hinton agar plates with the help of a cotton swab. Paper filter disks (Whatman™) with a diameter of 6mm were then applied onto the surface of the plates, and 10 µl of each plant extract was placed onto the disks. As positive controls, the following concentrations were used: ampicillin (Genamerica SA, Ecuador), 100 µg/mL for *E. coli* and 5 µg/mL for *S. aureus*, respectively. Plates were incubated for 16 hours at 37°C in an atmosphere of CO₂. The GME and PGE inhibition zones were measured to determine their antibacterial efficacy. The test was carried out in triplicate

to ensure the reliability of the data. The inhibition halos were also observed under a stereoscope to confirm the antimicrobial effect of the extracts.

5.8 Wound healing test

Mouse embryonic fibroblast cells (NIH-3T3, SIGMA-ALDRICH) were cultured in Dulbecco's Modified Eagle Medium (DMEM) containing high glucose, supplemented with 100 U/mL penicillin, 100 µg/mL streptomycin, and 10% bovine calf serum in culture flasks until achieve 80% of confluency. A 0.5 mL cell suspension volume was seeded in a 24-well plate equivalent to 250000 cells/well. After 24 hours, the medium was replaced with fresh medium. Standards of GME and PGE were prepared in DMSO and PBS, respectively. GME concentrations ranged from 1 to 30 µg/mL, while PGE concentrations ranged from 5 to 100 µg/mL. After adding fresh medium to the cell culture, the specified treatments were applied, and wounds were induced in the monolayer, creating a scratch that mimicked a wound. Throughout the experiment, wound healing progression was monitored using an inverted microscope at 0, 24, and 48 hours, enabling measurement of wound healing progress and evaluation of cellular activities such as migration. It was monitored using the trinocular Microscope in 10x magnification. The plates were incubated in a controlled humidity with 5% CO₂. The study involved a comparison between the control and the extract samples. Welch's t-test was employed for statistical analysis to assess the significance of differences between these two groups. Measurements of the wound area were obtained in pixels using ImageJ software. Five measurements were taken for wound opening and multiplied by a height, and the area was calculated. The following equation was then utilized to determine the wound confluence:

$$\% \text{ wound confluence} = \left[\frac{A_o - A_f}{A_o} \right] 100 \quad (3)$$

Where: A_o —Initial area; A_f —final area.

5.9 Preparation of hydrogel films

Hydrogel films were synthesized utilizing the solvent casting technique. Initially, stock solutions were prepared: 2% (w/v) chitosan in 2% (v/v) acetic acid and 2% (w/v) hydroxyethylcellulose under stirring at 400 rpm for two days, followed by degassing using an ultrasound bath. A Solution of 2% (w/v) citric acid was used as a cross-linking agent and 1% (w/v) glycerol as a plasticizer.

Chitosan was added using a homogenizer operating at 7000 rpm for 15-minute intervals between each solution addition to ensure homogeneity. Subsequently, hydroxyethylcellulose was incorporated until a faint yellow color was attained. Next, a crosslinking agent and glycerol were added. The samples were heated in an oven at 90°C for one hour. Afterward, they were taken out and allowed to cool to room temperature. Finally, each mixture was transferred into Petri dishes and dried at room temperature for three days. The CH: HEC polysaccharides were evaluated in ratios of 3:1 and 1:1. Additionally, the effect of increasing the concentration of the cross-linking agent and plasticizer on the final properties of the material as depicted in Table 2.

Formulation Code	Composition films			
	CH-LMW 2% (mL)	HEC 2% (mL)	CA 2% (mL)	Gl 1% (mL)
CHL3-HEC1-CA5-GL 1	45	15	5	1
CHL1-HEC1-CA5-GL 1	30	30	5	1
CHL3-HEC1-CA10-GL 1	45	15	10	1
CHL1-HEC1-CA10-GL 1	30	30	10	1
CHL3-HEC1-CA5-GL 5	45	15	5	5
CHL1-HEC1-CA5-GL 5	30	30	5	5

Table 2 Composition of the different initial films

5.10 Preparation of Hydrogel film with extracts

The final hydrogel films were prepared using the composition of CHL3-HEC1-CA5-GL 1, selected for its chemical structure, swelling, adhesiveness, and mechanical properties suitable for the inclusion of the extracts of GME and PGE. The preparation followed the previously described methodology for hydrogel films, with slight modifications. Ethanolic extracts of GME and PGE were incorporated inside the mix in situ. Previously, the extracts were dissolved with ethanol as the solvent and slowly added by drip. After adding extracts, the stirring continued for half an hour until it presented a homogeneous appearance. The mixtures were then subjected to an oven at 70°C

to prevent the decomposition of active compounds. After, the samples were transported in an ultrasound bath for 30 minutes at 40 °C. The samples were then cooled to room temperature. The resulting blends were transferred into Petri dishes and dried in an extraction hood for three days. Figure 7 details the manufacturing process of hydrogel films with extracts in Table 3. Below is the composition of the different film variations and the different amounts of extracts of GME and PGE included in hydrogel films. In our previous antibacterial studies, we investigated various concentrations of each extract. We calculated the quantity of each extract required based on the dimensions of the diffusion disks used in the assays, specifically the low concentrations of inhibitions, and the value increased tenfold. These values were then extrapolated to determine the amounts needed to cover the entire surface area of the Petri dishes.

Formulation Code	Hydrogel final composition					
	CH(2% w/v)	HEC (2% w/v)	CA(2% w/v)	GI(1% v/v)	GME	PGE
	% v/v				% w/v	% w/v
CH-HEC	63.4	21.12	14.08	1.40	-	-
GME1	63.4	21.12	14.08	1.40	0.20	-
GME2	63.4	21.12	14.08	1.40	2.0	-
PGE1	63.4	21.12	14.08	1.40	-	1.05
PGE2	63.4	21.12	14.08	1.40	-	2.11
GME1-PGE1	63.4	21.12	14.08	1.40	0.20	1.05

Table 3 Proportion of hydrogel films with and without content of ethanolic extracts of Mangosteen and Pomegranate

5.11 Thickness, Weight Variation

The thickness of the synthesized materials was measured using a digital micrometer REXBETI. Thickness measurements were randomly taken at different positions on the film, with five repetitions for each sample. [98]. Samples with petri dish dimensions were weighed, and weight fluctuations were assessed [99].

5.12 Chemical Characterization of hydrogel films

ATR-FTIR spectroscopy was used to characterize hydrogel films chemically. The FTIR spectra were performed from wavenumber 650–4000 cm⁻¹ with a resolution of 4 cm⁻¹ and four scans.

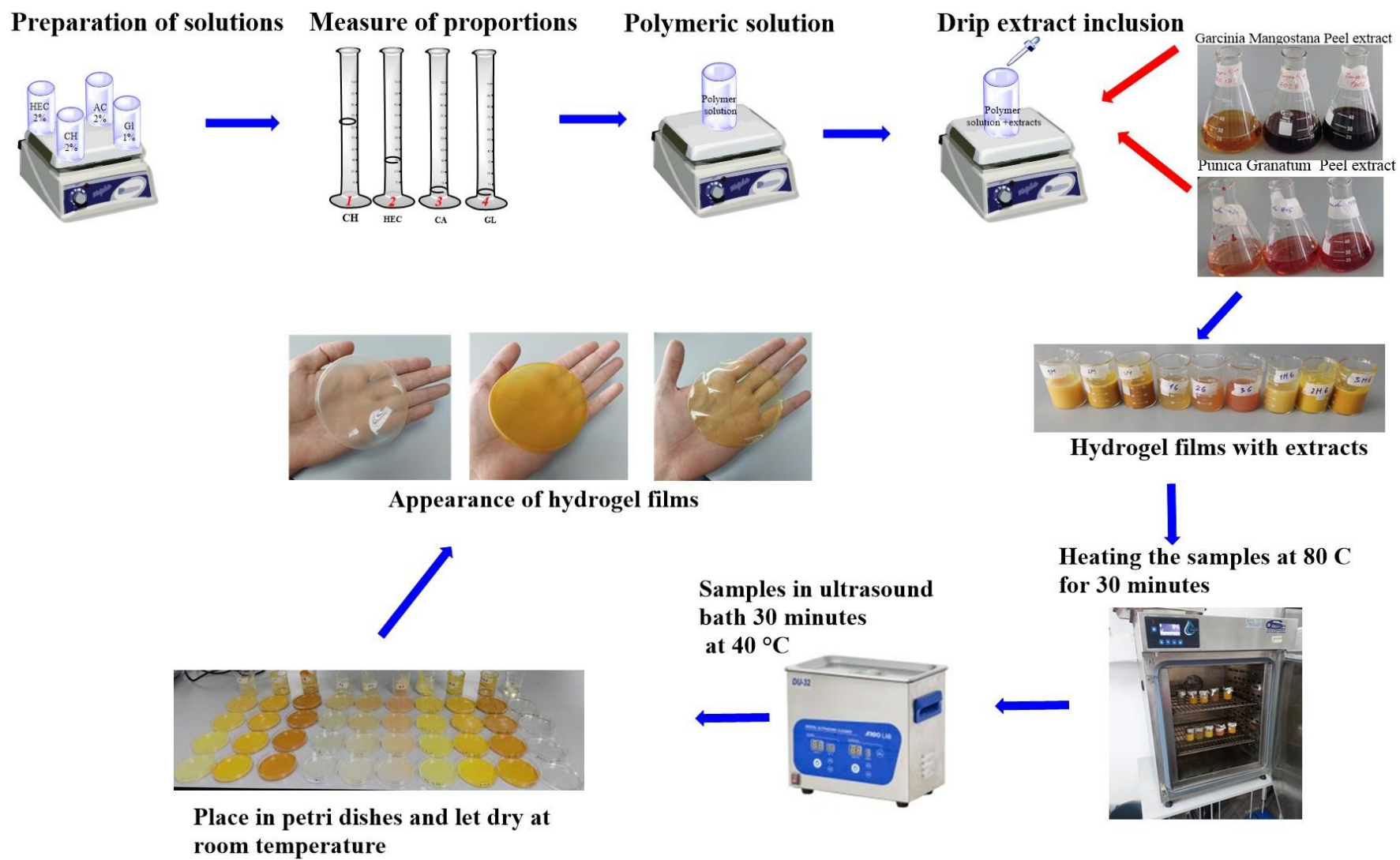


Figure 7 Preparation scheme of hydrogel films loaded in situ with extracts

5.13 Swelling ratio

The hydrogel films were initially cut into dimensions of 1x1 cm². Before immersion, the samples were weighed using a Cobus precision analytical balance. The samples were then submerged in three different liquid mediums. The first swelling study was conducted in deionized water. The second swelling study used phosphate buffer solution (PBS), a commonly used buffer in biological research. The third swelling study used simulated body fluid (SBF), a solution closely mimicking the ion concentrations found in human blood plasma. The swelling study was carried out in 10-minute intervals. The immersed samples were removed from the liquid medium and weighed, and the excess liquid was removed using filter paper to eliminate residual moisture. The samples were then re-immersed, which was repeated until it reached 3 hours. The swelling ratio was determined by correlating the weight of the dry film (*W_d*) with the weight of the swollen film (*W_s*) using the following equation.

$$\% \text{ Swelling ratio} = \left[\frac{W_s - W_d}{W_s} \right] 100 \quad (4)$$

Where: W_d—weight of the dry film; *W_s*— weight of the swollen films.

5.13.1 Preparation of Phosphate Buffered Saline (PBS)

All materials undergo a thorough cleaning with a neutral detergent. Subsequently, they were immersed in a 0.1M HCl solution for two hours and thoroughly rinsed with distilled water multiple times. Afterward, the materials were wrapped in aluminum foil until ready for use. If any materials were damp, they were dried at 50°C [100]. 700 mL of deionized water was added into a beaker and magnetic stirred at 36.5°. Each reagent was added in the following order: 8g of NaCl, 0.2g of KCl, 1.44g of Na₂HPO₄, and 0.24g of KH₂PO₄. The pH variation followed the process; after adding all solvents, the pH was adjusted to 7.4 using a diluted HCl solution. Finally, the volume was adjusted to 1L using a volumetric flask and transferred into a plastic bottle to store it at room temperature [101].

5.13.2 Preparation of Simulated Body Fluid (SBF)

The same principle of cleaning materials for PBS was followed before preparing the SBF solution. Once the materials were cleaned. The Simulated Body Fluid (SBF) solution was meticulously

prepared in a dust-free environment. In a 2000 mL beaker, 700 mL of deionized water was stirred at 37°C. Sequentially, the following amounts of each reagent were added in the following order: 7.956 g of NaCl, 0.353 g of NaHCO₃, 0.224 g of KCl, 0.176 g of K₂HPO₄, 0.143 of MgCl₂, 40 mL of 1M HCl, 0.2897 g of CaCl₂, and 0.071 g of Na₂SO₄, ensuring complete dissolution of each one before the next addition. The pH was carefully monitored and adjusted by slow addition of (CH₂OH)₃CNH₂ (tris(hydroxymethyl)aminomethane until reaching 7.4 at 36.5-37°C. After transferring the solution to a 1000 mL volumetric flask and adjusting the volume with distilled water, the SBF solution was stored in a sterile bottle at 4 °C for swelling tests[100].

5.14 Transparency/Opacity

The transparency and opacity of hydrogel films containing mangosteen and pomegranate extracts were examined using the methodology outlined in [102], [103], [104]. The films were prepared in rectangular shapes and positioned within the cells. Measurements were taken at a wavelength of 600 nm, with air serving as the reference blank. The transparency and opacity values were calculated and reported as percentages using the following equation.

$$\text{Transparency \%} = \frac{A}{L} \quad (5)$$

$$\text{Opacity} = A * L \quad (6)$$

Where: *A*-Absorbance at 600 nm e; *L* film thickness in mm.

5.15 Thermogravimetric analysis TGA

The thermal stability of hydrogel films composed of hydroxyethylcellulose and chitosan, with and without extract content of GME and PGE, was evaluated using thermogravimetric analysis. The analysis was performed from room temperature up to 800°C under a controlled atmosphere, with a heating rate of 10°C/min. The sample weight was continuously monitored and recorded throughout the analysis as a function of temperature increase.

5.16 Mechanical Strength of Films

Dry and hydrated films were analyzed for tensile strength, elongation at break percentage, and Young's modulus, adhering to the ASTM D638 standard. The testing was conducted at a speed of 10 mm/min. The measurements for tensile strength, elongation at break, and Young's modulus were obtained through five repetitions with each sample. The specimens were cut to the dimensions detailed in Figure 8 and clamped in the machine's jaws.

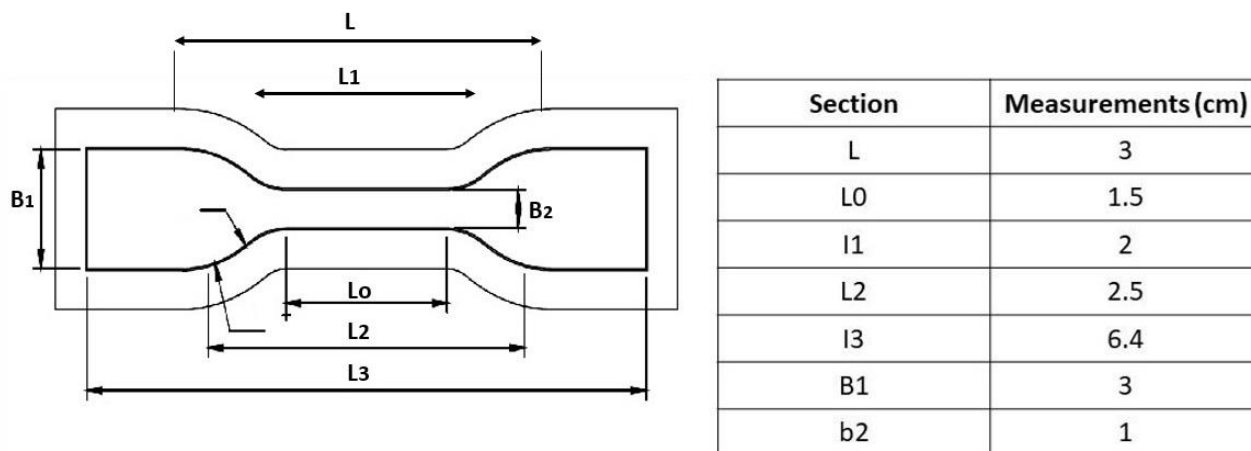


Figure 8 Dimensions of specimens for mechanical tests

5.17 Scanning electron microscope

The surface morphology of the films with and without loading of extracts was analyzed. Before analysis, the samples were meticulously prepared by cutting them into 1 x 1 cm dimensions and securing them onto cylindrical copper supports. The films were dried in a desiccator. The samples were analyzed under vacuum conditions and applying 15-20 Kv.

5.18 Antimicrobial study of hydrogel films with GME and PGE

The in vitro antibacterial efficacy of hydrogel films was assessed using the disc diffusion method against *Staphylococcus aureus* and *Escherichia coli*. The essay was carried out using the methodology previously described in antimicrobial studies of the extracts of GME and PGE. The modification was based on the change in the use of Whatman paper for films without extracts and with different mixtures of GME and PGE. Before testing, the films were dried in a desiccator for 24 hours and then cut to match the dimensions of the discs used in the diffusion tests, specifically 6 mm in diameter. The films were irradiated with ultraviolet light on each side for 30 minutes.

Agar plates were inoculated with *Staphylococcus aureus* and *Escherichia coli* and incubated for 16 hours at 37°C in a CO₂-enriched atmosphere. The inhibition zones for films containing extracts and those without extracts were measured to evaluate their antibacterial activity. The experiment was conducted in triplicate to ensure the reliability of the results.

5.19 Cell culture

The hydrogel films were prepared in a laminar flow cabinet to avoid contamination. After drying at room temperature in an isolated environment according to the film synthesis methodology, 3 mL of PBS was added to each well. The films were placed at 37°C in an oven for 24 hours to achieve maximum swelling. Subsequently, the films were irradiated with UV light for 15 minutes, and the excess PBS was removed. Following this, the previously established wound healing procedure was carried out, omitting the scratching step. Cellular behavior on the hydrogel films was monitored at 0 and 24 hours using a trinocular microscope at 10x magnification.

6 RESULTS AND DISCUSSION

6.1 GME and PGE Extracts

6.1.1 Qualitative phytochemical analysis

Plant parts, including their fruits, contain a variety of phytochemicals, categorized as primary and secondary metabolites, known for their healing, anti-inflammatory, antibacterial, and other beneficial properties crucial for wound dressing development [105], [106]. Phytochemical screening of mangosteen and pomegranate pericarps has identified several bioactive compounds, as depicted in Table 4. The ethanolic extract of mangosteen peel contained flavonoids, phenols, tannins, coumarins, saponins, proteins, and amino acids [107]. These compounds were extracted using ethanol as a polar solvent. [108]. The extracted compounds have a hydrophilic character; they are poorly soluble in water. Similarly, the pericarp of pomegranate is rich in flavonoids, phenols, tannins, coumarins, and saponins [109]. Contrary to the Mangosteen, this extract is hydrophilic. The phytochemical profiles of both mangosteen (GME) and pomegranate (PGE) extracts confirm their enrichment with phenols, tannins, flavonoids, saponins, proteins, and amino acids, detailed in Images illustrating these assays are shown in Figure 9. Alkaloids were absent in both extracts, confirmed by Dragendroff's and Wagner's tests, while tests for phytosterols were negative using Acetic Anhydride and Hesse's test. Several constituents analyzed in this study are pertinent to wound healing and skin maintenance [110].

Ethanolic extract	Mangosteen	Pomegranate
Flavonoids	++	+++
Phenols	+	++
Tannins	+++	++
Coumarins	++	+
Alkaloids	-	-
Phytosterols	-	-
Saponins	+	++
Proteins and amino acid	++	-

Table 4 Screening of major phytochemical compounds in the peel Mangosteen and pomegranate.

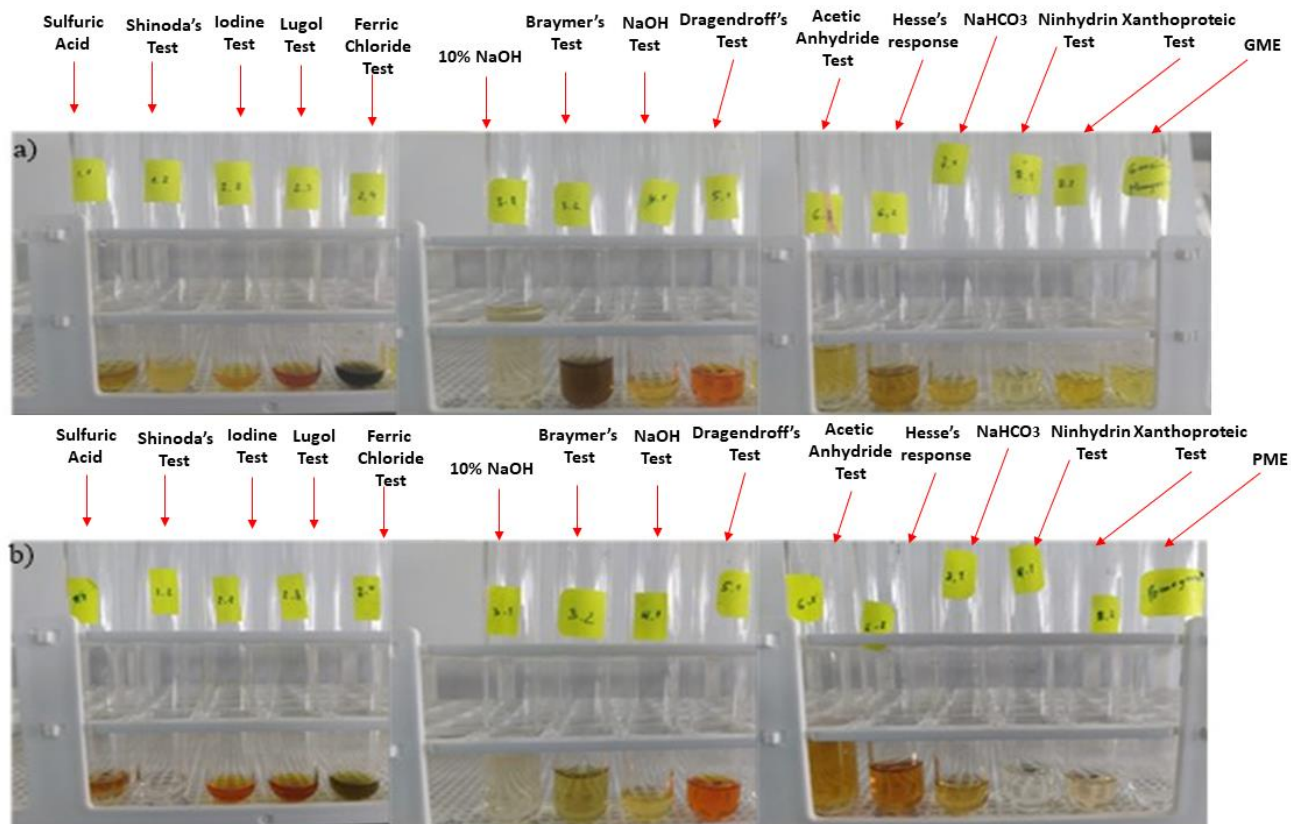


Figure 9 Reactions of screening of major phytochemical compounds in the peel a) Mangosteen and b) pomegranate.

6.1.2 Analysis of extracts using FTIR Spectrophotometer

The FTIR spectra of mangosteen pericarp extract detail in Figure 10 exhibit characteristic signals of xanthenes. A broad absorption band at 3343 cm^{-1} corresponds to the stretching vibrations of O-H, attributed to water molecules, hydroxyl groups, and hydrogen bonds. The signals at 2966 cm^{-1} and 2922 cm^{-1} indicate the asymmetric stretching vibrations of methyl (CH_3) and methylene (CH_2) groups, respectively, while the signal at 2854 cm^{-1} arises from the symmetric stretching vibration of methylene (CH_2) groups. Signals at 1605 cm^{-1} , 1579 cm^{-1} , and 1459 cm^{-1} suggest the presence of aromatic structures, whereas signals at 1278 cm^{-1} and 1222 cm^{-1} are associated with phenolic C-O stretching, characteristic of polyphenolic compounds. The strong band at 1433 cm^{-1} arises from CH_2 bending, and bands at 1374 cm^{-1} correspond to CH_3 bending. Furthermore, bands at 1184 cm^{-1} , 1154 cm^{-1} , and 1044 cm^{-1} denote the stretching vibrations of C-O from the ether and hydroxyl groups. Bands at 901 cm^{-1} , 774 cm^{-1} , and 681 cm^{-1} originate from $-\text{HC}=\text{CH}-$ (trans) out-of-plane bending, $-\text{HC}=\text{CH}-$ (cis) out-of-plane bending, and $-(\text{CH}_2)_n-$; $-\text{HC}=\text{CH}-$ bending, respectively. Signals at 1717 cm^{-1} and 1770 cm^{-1} arise from the stretching vibrations of carbonyl

(C=O) groups in carboxylic acids, ketones, and esters, or both [111], [112]. All signals corresponding to GME are summarized in Table 5.

In the infrared spectrum of pomegranate extract (PGE) depicted in Figure 10, a broad signal at approximately 3307 cm^{-1} is attributed to the stretching vibrations of hydroxyl groups in carboxylic acids, alcohols, and phenols. The signals at 2971 cm^{-1} and 2931 cm^{-1} represent the asymmetric stretching vibrations of methyl (CH_3) and methylene (CH_2) groups, respectively, while the signal at 2880 cm^{-1} is due to the symmetric stretching vibration of methylene (CH_2) groups. The signal at 1716 cm^{-1} corresponds to the stretching vibration of carbonyl groups in carboxylic acids, ketones, and aldehydes, or both. The signal at 1603 cm^{-1} represents the stretching vibration of C=C bonds in aromatic structures. Additionally, a significant band in the PGE spectrum occurs at 1029 cm^{-1} , associated with the stretching vibration of C-O bonds in alcohols. All signals corresponding to PGE are summarized in Table 6.

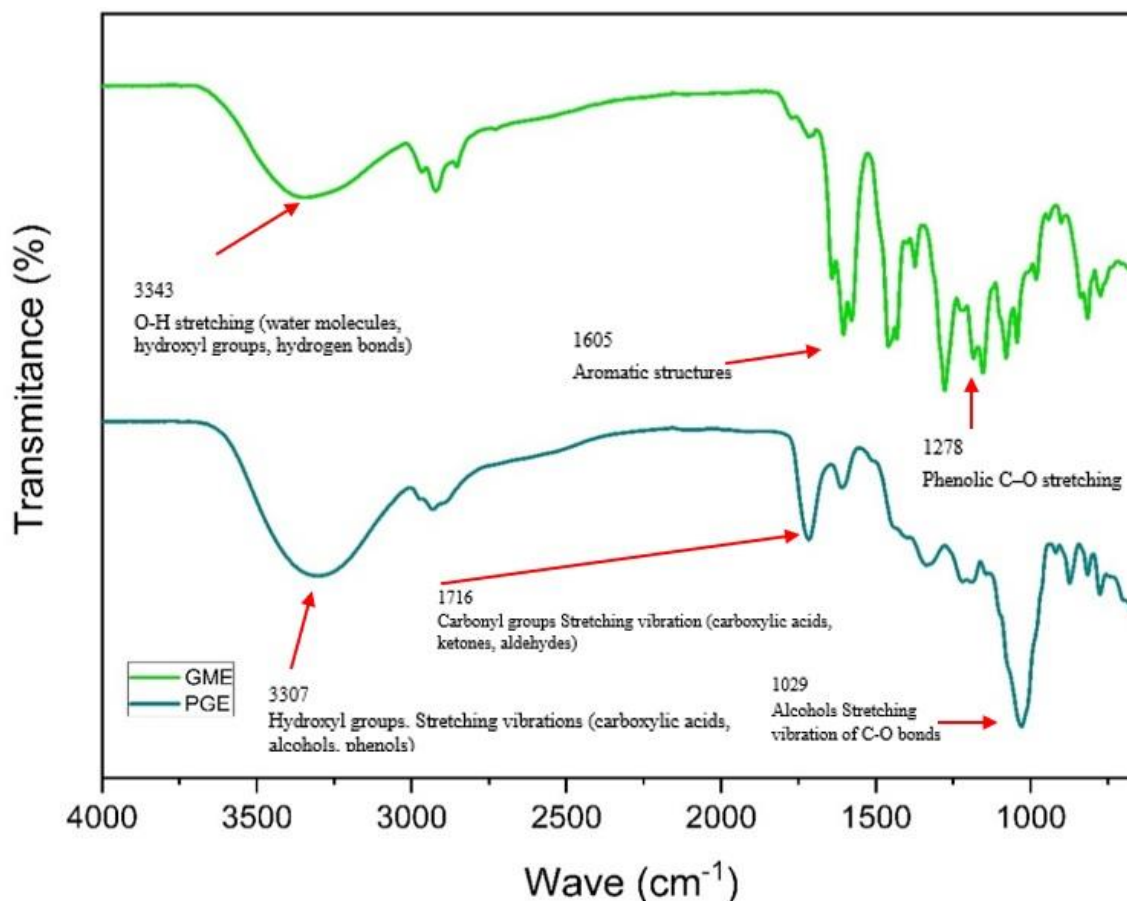


Figure 10 FTIR extracts GME and PGE

Wavenumber (cm ⁻¹)	Functional Group/Observation
3343	O-H stretching (water molecules, hydroxyl groups, hydrogen bonds)
2965	Asymmetric CH ₃ stretching
2923	Asymmetric CH ₂ stretching
2854	Symmetric CH ₂ stretching
1771	(C=O) groups stretching vibration of unconjugated carbonyl
1717	(C=O) groups stretching vibration of unconjugated carbonyl
1642	unconjugated C=C stretching vibration
1605	Aromatic structures
1579	Aromatic structures
1459	Aromatic structures
1433	CH ₂ bending
1374	CH ₃ bending
1278	Phenolic C–O stretching
1222	Phenolic C–O stretching
1184	C–O stretching (ether and hydroxyl groups)
1154	C–O stretching (ether and hydroxyl groups)
1044	C–O stretching (ether and hydroxyl groups)
901	-HC=CH- (trans) out of plane bending
774	-HC=CH- (cis) out of plane bending
681	-(CH ₂) _n ; -HC=CH- bending

Table 5 IR Band Assignments of Mangosteen Ethanolic Extract.

Wavenumber (cm ⁻¹)	Functional Group/Observation
3307	Hydroxyl groups. Stretching vibrations (carboxylic acids, alcohols, phenols)
2971	CH ₃ groups Asymmetric stretching vibrations
2929	CH ₂ groups Asymmetric stretching vibrations
2880	CH ₂ groups Symmetric stretching vibration
1716	Carbonyl groups Stretching vibration (carboxylic acids, ketones, aldehydes)
1612	Aromatic structures Stretching vibration of C=C bonds
1029	Alcohols Stretching vibration of C-O bonds

Table 6 IR Band Assignments of Pomegranate Ethanolic Extrac

6.1.3 HPLC Profiling of Mangosteen and Pomegranate

The characteristic UV-Vis absorption spectra of each component were used to identify it, providing valuable insights into the composition of both extracts.

Figure 11 illustrates the chromatogram of the ethanolic extract of pomegranate, and Figure 12 shows the UV-vis spectra of each component. The chromatogram indicates that the extract consists of three major components with retention times of 1.73, 2.08, and 2.49 minutes. The UV spectra were recorded to identify the compounds and compared with reference data from the literature from Sigma standards. The spectra UV-vis of all components shows absorptions maximus characteristics of flavonoids between 250-270 nm associated with the A-ring benzoyl system and between 350-385 nm associated with the B-ring cinnamoyl system[113].

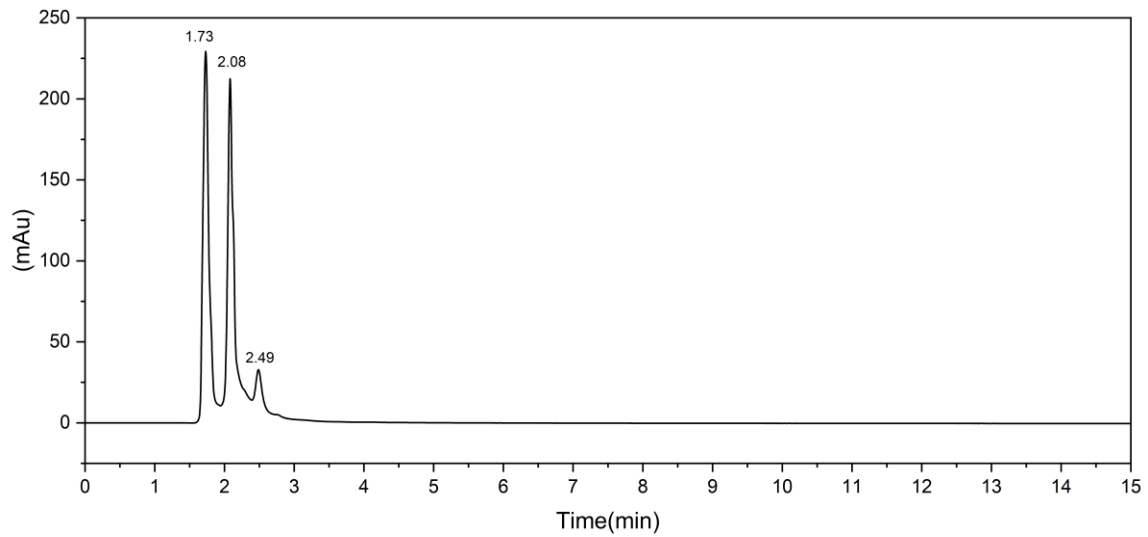


Figure 11 HPLC chromatogram of *P. Granatum* ethanolic extract

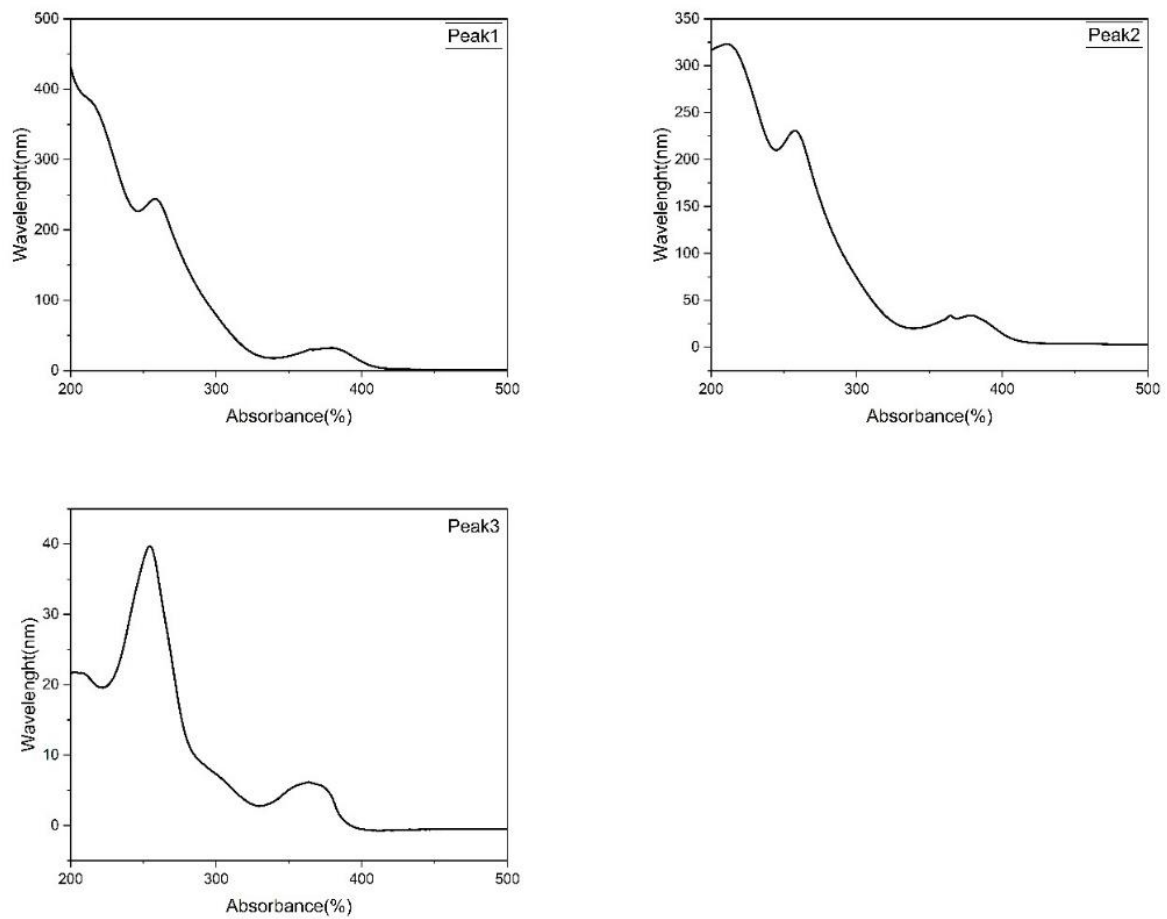


Figure 12 UV-Vis spectra from *P. Granatum* extract ethanolic.

Figure 13 displays the chromatogram of the ethanolic extract of Mangosteen, while Figure 14 shows the UV-Vis spectra of each component. The chromatogram of the mangosteen pericarp extract indicates that the extract consists of two major components with retention times of 4.04 minutes and 5.46 minutes. The UV-vis spectra of both components exhibit characteristic absorption maxima of an aromatic benzene chromophore, indicating the presence of a xanthone nucleus. The UV spectra were recorded to identify the compounds and compared with reference data from the literature from Sigma standards. Detailed spectral analysis permitted the identification of both components as γ -MG and α -MG, consistent with the literature on mangosteen pericarp [114], [115]

The UV-vis spectra of α -MG and γ -MG exhibited maximum absorption peaks at 243, 317, and 352 nm, consistent with the reported literature [116]. The peak at 243 nm corresponds to the C=C chromophore involving $\pi \rightarrow \pi^*$ transitions, while the peak at 317 nm is attributed to the C=O chromophore with $n \rightarrow \pi^*$ transitions. Additionally, a shoulder observed at 265 nm suggests the presence of the C-O-C chromophore involving $n \rightarrow \sigma^*$ transitions [117].

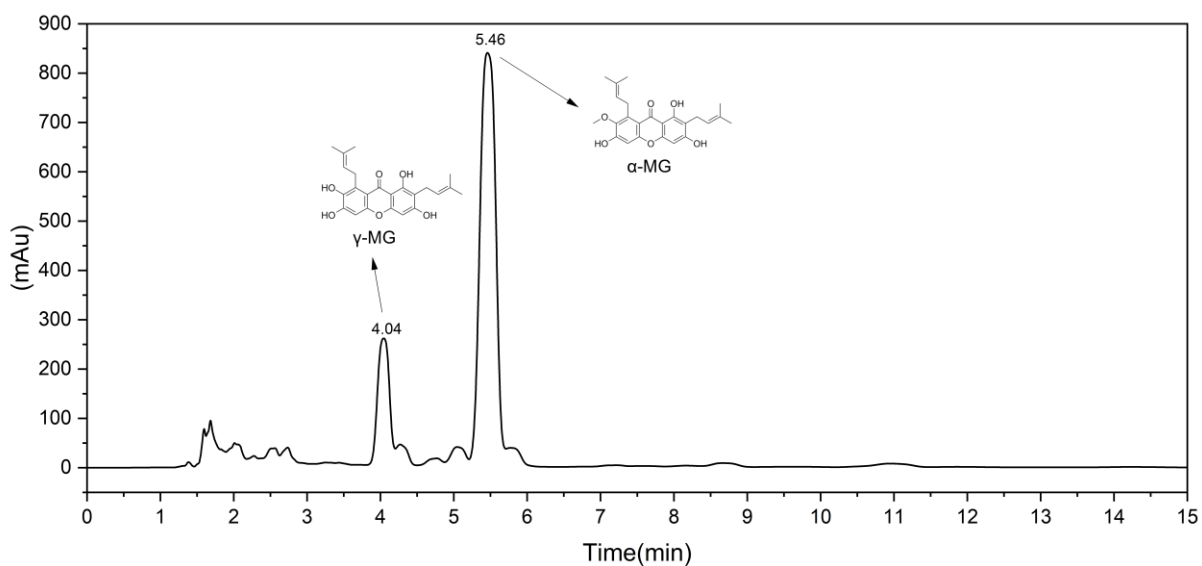


Figure 13 HPLC chromatogram of *G. Mangostana* ethanolic extract

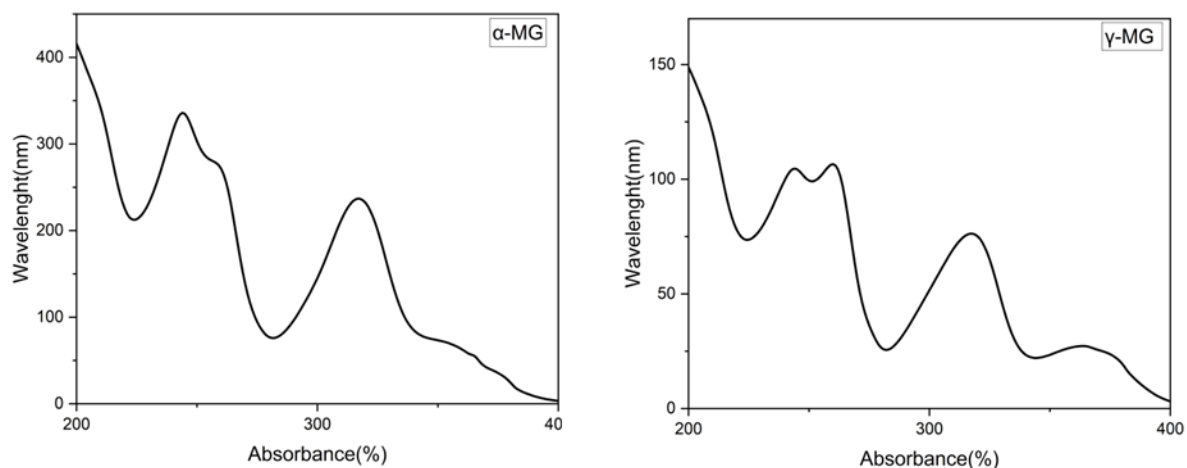


Figure 14 UV-Vis spectra from *G. Mangostana* extract ethanolic.

6.1.4 Total phenol content of Pomegranate and Mangosteen Peel

The total polyphenolic compound content analysis provides valuable insights into the bioactive components found in plants. These compounds are known for their potential to protect against skin injuries, and their therapeutic effects include anti-inflammatory, anticancer, and antioxidant properties [118], [119]. As a result, the highest extraction yield, 5.55 g, was obtained from the ethanolic extract of pomegranate (GE), followed by mangosteen (GM) with 1.17 g. The total phenolic content of these extracts was assessed using a standard curve constructed with gallic acid, correlating absorbance with concentration. The gallic acid analysis produced a linear curve, depicted in Figure 15, with the equation $y = 0.0049x + 0.0046$ and an R^2 value of 0.9902. The total phenolic results for each extract are represented in Table 7. Additionally, Figure 16 represents the standards used for testing the total phenolic content of the extracts.

Biologically active substances are present in plant-based foods, but a substantial quantity of this raw material is lost during processing without being consumed or utilized. This loss, which occurs yearly and is estimated at 1300 million of food, by-products, and waste, including fruit peels and other agricultural leftovers, is a significant concern [120]. The peel of Pomegranate fruit constitutes between 40% and 50% of its total weight. It contains bioactive compounds such as phenolic acids, polyphenols, and flavonoids, known for their physiological effects, including anti-inflammatory, antibacterial, antioxidant, and anticancer properties [121], [122]. Approximately

73.47% of the mangosteen fruit's weight is accounted for by its peel. The pericarps of mangosteen are rich in various compounds, including xanthenes, tannins, triterpenoids, benzophenones, flavonoids, anthocyanins, and phenolic compounds[76], [123].

According to the results obtained, it is appreciated that the total phenolic content is higher for GM than for PG. According to our results, the total phenolic content of PG and GM peels were 362.5 and 287.90 GAE/g, respectively. Results compatible with pomegranate extracts in the 276 to 413 GAE/g reported by Derakhshan[124]. On the other hand, the total phenol content of GME by maceration is below that of ethanolic extraction using the Soxhlet apparatus obtained by Udaya of 413 mg GAE/g obtained by Udaya[125]. When a wound occurs, reactive oxygen species are released to repair damaged tissues implicated in granulation, cellular proliferation, inflammation, angiogenesis, and extracellular matrix synthesis [126], [127]. However, an excess of these species can prolong the healing processes, ceasing to be beneficial[128]. Phenolic extracts have the potential to reduce oxidant species during the wound healing process, but more clinical trials are required[129], [130], [131], [132].

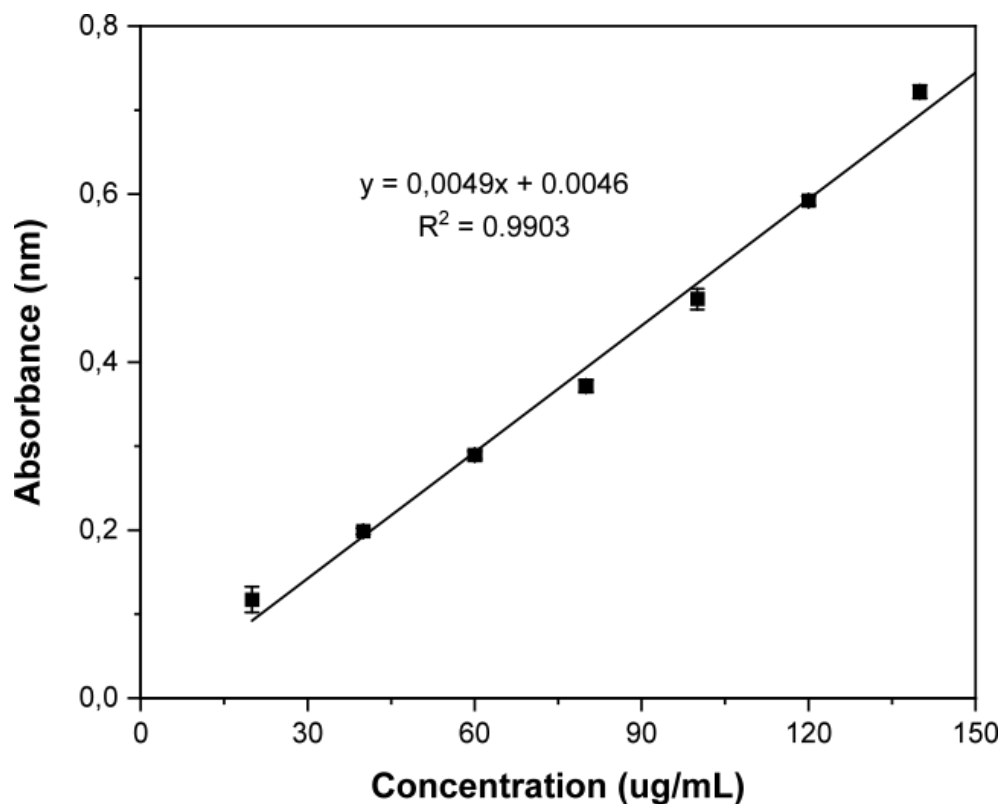


Figure 15 Gallic acid standard calibration curve for the quantification of total phenolic compound

Extract	Yield of crude extract g/100 g sample	Total phenolics (mg GAE/g)
GME	0,5	287.90
PGE	0,15	362.5

Table 7 Extraction yields, total phenolics from *G. mangostana* and *P granatum* ethanolic extracts

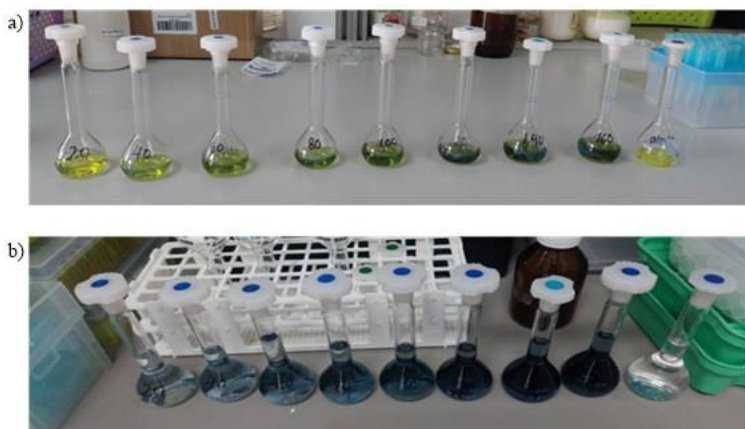


Figure 16 Calibration standards before and after 2 hours for measurements for the calibration standard curve

6.1.5 Antioxidant DPPH assay protocol

Free radicals have been demonstrated to regulate oxidative stress levels and facilitate tissue regeneration [133]. Physiologically, forming free radicals and antioxidant defenses leads to oxidative stress, which prompts mitochondrial and membrane-level alterations and mutations[134]. Free radicals are generated by the electron transport chain and the membrane-associated nicotinamide adenine dinucleotide phosphate (NADPH) oxidase (NOX) enzyme complex[129], [133]. These biological oxidants are often described as damaging. However, an appropriate level of them is vital for wound healing, as angiogenesis, hemostasis, and re-epithelialization benefit from these compounds[135], [136].

The antioxidant capabilities of two extracts, GME and PGE, were assessed relative to gallic acid. This comparative analysis involved determining their IC50 values plotted on a concentration versus DPPH inhibition graph. As depicted in Figure 17 and summarized in Table 8, GME

exhibited an IC₅₀ of 3.34 µg/mL, while PGE showed an IC₅₀ of 11.70 µg/mL, both compared to gallic acid's IC₅₀ of 1.02 µg/mL.

These results suggest that mangosteen extract exhibits the highest antioxidant activity compared to pomegranate. The GME extract approaches the standard closely, serving as a strong indicator of its antioxidant capacity. In contrast, pomegranate demonstrates the lowest effect. Tjahjani et al. [137] report the mangosteen peel extract using different solvents, one of them being 96% ethanol, finding an IC₅₀ of 7.48 µg/mL, concluding that mangosteen has potential antioxidant properties. Another study conducted in Malaysia, using microwave-assisted extraction of both mangosteen seed and rind, found IC₅₀ values of 37.54 and 9.40 µg/mL, respectively[138]. On the other hand, a study in Egypt found that the IC₅₀ for pomegranate extracted with ethanol and under heating conditions had an antioxidant activity with an IC₅₀ of 14.6 µg/mL[139]. Therefore, the incorporation of these types of extracts into biomaterials, such as films and hydrogels, may potentially encapsulate and release these active compounds to wounds, potentially improving the healing processes[140], [141], [142], [143].

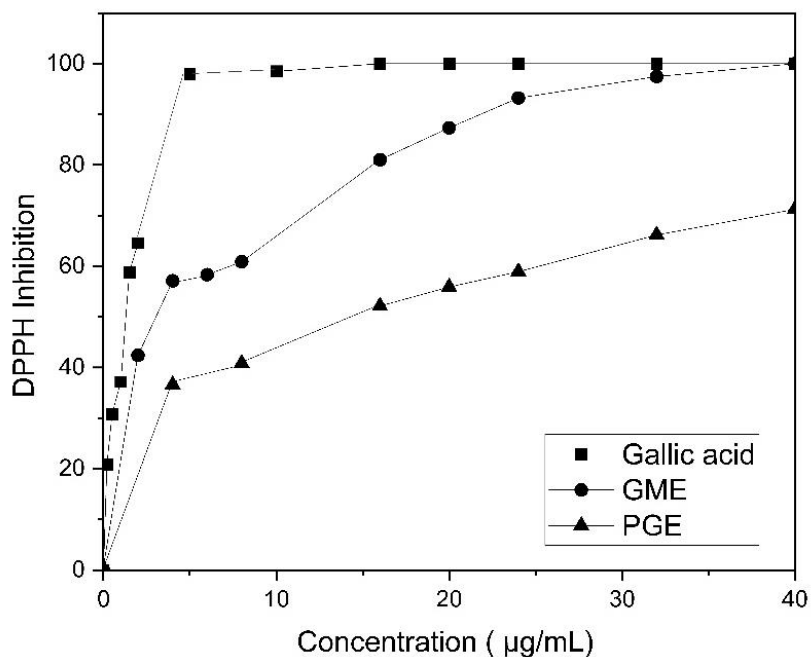


Figure 17 Graph of ethanolic extracts concentration versus % DPPH inhibition.

	Extract	IC ₅₀ (ug/mL)
1	GA	1.02
2	GME	3.34
3	PGE	11.70

Table 8 EC50 in DPPH radical scavenging activity.

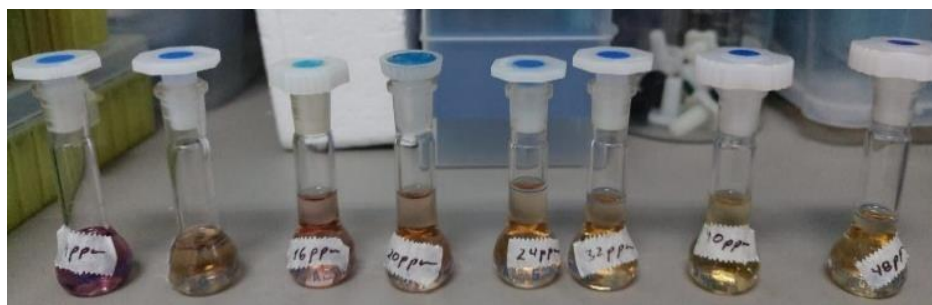


Figure 18 Mangosteen assay DPPH

6.1.6 Extracts of mangosteen and pomegranate peel antimicrobial studies

Antibacterial agents can help reduce bacterial colonization, preventing infections and inflammation that can disrupt healing processes. By reducing bacterial agents, the efficacy of active drugs or compounds that promote effective and quick wound healing is improved[144].

This comprehensive study meticulously analyzed the antibacterial effect of mangosteen (GME) and pomegranate (PGE) extracts. The inhibition of both extracts shown in Table 9 and Figure 19 against *E. Coli* and *S. Aureus* were thoroughly analyzed, with ampicillin used as a control. GME was studied in the following range of concentrations (100-0.01) mg/mL, showing bacterial susceptibility for both strains *S. Aureus* and *E. Coli*, respectively, applying 10 μ L of each extract. The extract produced inhibition zones from (9.30-10.45) mm to *S. Aureus*. On the other hand, using the extract had lower susceptibility to *E. Coli* than *S. Aureus*, obtaining inhibitions from 7.44 to 9.10 mm for *E. Coli*. The MBC found for GME in this study were 0.125 mg/mL and 5 mg/mL for *S. Aures* and *E. Coli*, respectively, as indicated in Table 10. These findings are consistent with and even slightly more inhibition than reported Chaiwarit and colleagues reported antibacterial

activities of GME utilizing 20 μ l at a concentration of 10 mg/mL, resulting in inhibition zones measuring 9.19 mm and 8.94 mm for *S. Aureus* and *E. Coli* respectively [145]. In our study, we used half the volume and obtained effects similar to those reported in the literature.

The inhibition zones observed in this study are attributable to the active compounds present in the GM extract. This finding aligns with previous research that has demonstrated the inhibition of both Gram-positive and Gram-negative bacteria by GM ethanolic extract [145], [146]. Specifically, the extract effectively inhibits *E. coli* and *S. Aureus* due to flavonoids and phenolic compounds, which are extracted via maceration. Compounds such as α -mangostin and γ -mangostin in the extract have been particularly noted for their efficacy against Gram-negative bacteria [74]. Our study further confirms the presence of xanthenes, tannins, saponins, and flavonoids, all exhibiting inhibitory activity against Gram-positive and Gram-negative bacteria. The mechanism of inhibition involves peptides that bind to the genetic material, leading to membrane damage and subsequent cell death [147].

Pomegranate extract (PGE) within the 100 mg/mL concentration range to 0.01 mg/mL exhibits inhibitory effects against *Staphylococcus aureus* and *Escherichia coli*. PGE is particularly effective against *S. aureus* at higher concentrations, with the minimum bactericidal concentration (MBC) determined to be 25 mg/mL, resulting in an inhibition zone of 8.5 mm. For *E. coli*, a higher concentration of 75 mg/mL is required to achieve an inhibition zone of 6.5 mm, as shown in Table 10. According to Mahmood et al., the ethanolic extract of pomegranate demonstrates significant inhibition, with 50 μ l producing inhibition zones of 25 mm for *S. aureus* and 9 mm for *E. coli*, respectively [148]. In contrast to our study, the results of better antibacterial effectiveness and a lower volume used may be related to the maceration method and the 96% ethanol solvent.

The compounds present in pomegranate extract have been shown to have biological activity, which resulted in the formation of zones of inhibition more significant for *S. aureus* than for *E. coli*. Analogous studies have reported the effectiveness of PGE against *E. coli* and *S. aureus*[149], [150]. The antibacterial effect is based on the fact that most of the components are antioxidant polyphenols by the presence of tannins and flavonoids[151]. Polyphenols provide plants with protection against bacteria and fungi[152]. The study confirmed the presence of flavonoids, phenolic compounds, tannins, coumarins, and saponins. The priority of polyphenols can explain the mechanism of bacterial death. Phenolic compounds can diminish virulence by reducing cells'

biofilms, forming ligands, and neutralizing bacterial toxins. Consequently, this decreases energy metabolites or nucleic acid production [153]. The extracts show antibacterial activity against the two bacterial strains used, demonstrating potential for inclusion in biomaterials for wound healing applications.

GME Concentration (mg/mL)	<i>Staphylococcus aureus</i> inhibition (mm)	<i>Escherichia coli</i> inhibition (mm)	PGE Concentration (mg/mL)	<i>Staphylococcus aureus</i> inhibition (mm)	<i>Escherichia coli</i> inhibition (mm)
GME			PGE		
100	10,45 ± 1.20	9,10 ± 0.50	100	16.83 ± 0.25	7,5± 0.15
75	10,20 ± 0.50	9,02 ± 0.35	75	15,21± 0.15	6,5± 0.46
50	9,86 ± 0.25	8,55 ± 0.41	50	11,7± 0.34	-
25	9,71 ± 0.47	8,15 ± 0,33	25	8,5 ± 0.29	-
10	9,70 ± 0.29	7,53 ± 0.15	10	-	-
5	9,52 ± 0.46	7,44 ± 0.14	5	-	-
1	9,40 ± 0 ,25	-	1	-	-
0,25	9,38 ± 0,29	-	0,25	-	-
0,125	9,30 ± 0,66	-	0,125	-	-
0,01	-	-	0,01	-	-

Table 9 GME and PGE extracts against S Aureus and E Coli

GME Concentration (MBC) (mg/mL)	<i>S. Aureus</i> inhibition (mm)	<i>E. Coli</i> inhibition (mm)	PGE Concentration (MBC) (mg/mL)	<i>S. Aureus</i> inhibition (mm)	<i>E. Coli</i> inhibition (mm)
GME			PGE		
0,125	9,30± 0,66	-	25 mg/mL	8,5 ± 0.29	-
5	-	7,44 ± 0.14	75 mg/mL	-	6,5± 0.46

Table 10 MBC for GME and PGE extracts against S. Aureus and E. Coli

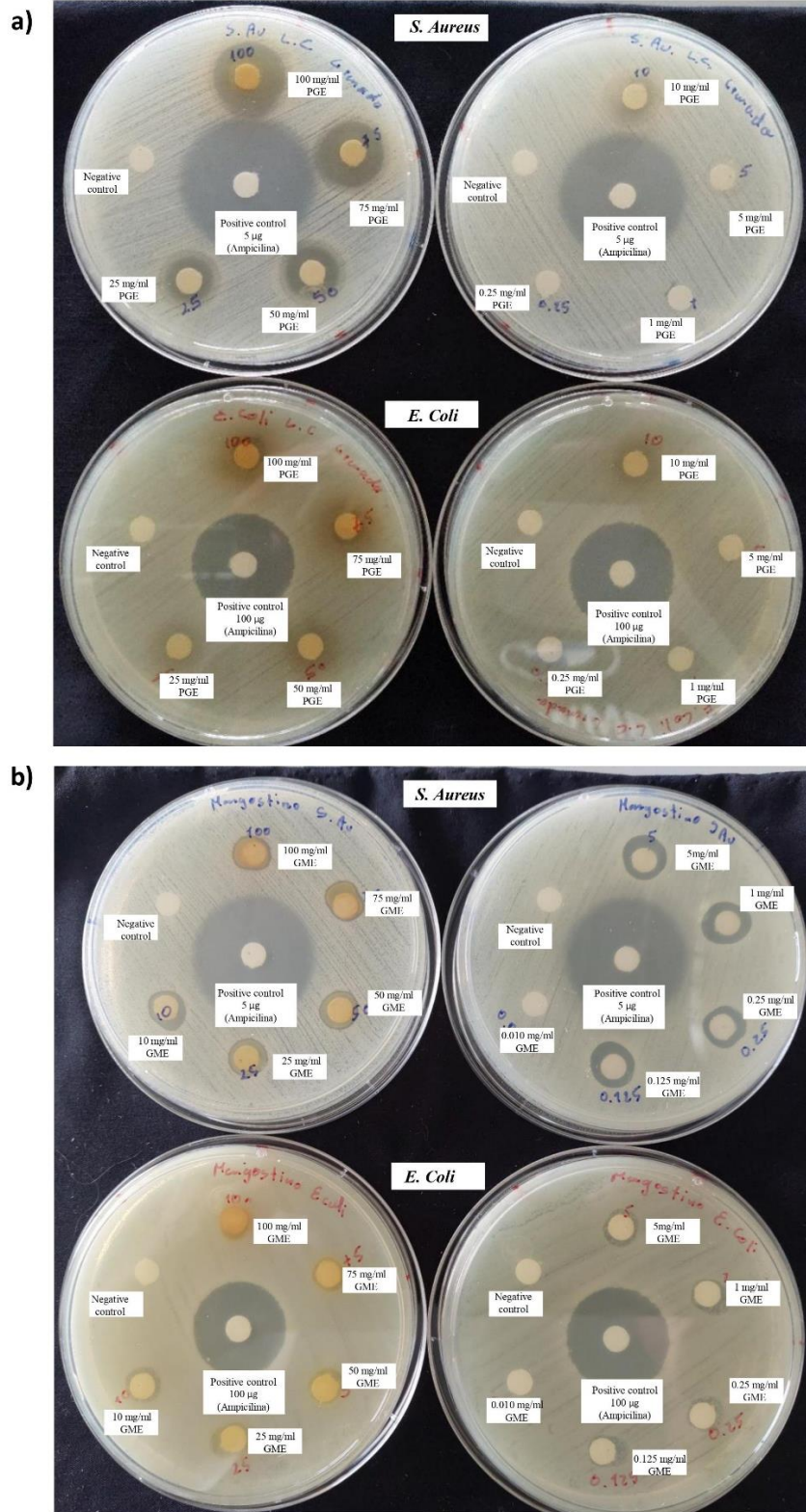


Figure 19 Diffusion disk of GME and PGE extracts against *S. Aureus* and *E. Coli* and inverted microscope

6.1.7 Wound healing assay

Images of NIH3T3 cells for control and inclusion of GME and PGE extracts for the wound assay are depicted in Figure 20. Calculation of confluence using Welch's t-test analysis and the ImageJ program to quantify wound confluence indicates an increase in fibroblast migration was observed in the sample treated with 50 $\mu\text{g/mL}$ GME compared to the control, showing an increase from 33% to 44% in wound closure at 24 hours. At 48 hours, the wound closed entirely without evidence of significant changes within the control and GME.

The results suggest that GME extract could contribute to a more efficient and safe healing process by improving the cell migration rate. These findings align with experiments comparing povidone to Mangosteen at 100 $\mu\text{g/mL}$, where mangosteen extract demonstrated more effective induction of fibroblast migration in 3T3-CCL92 [154]. Siri wattanasatorn et al. [155] reported on Thai medicinal plants, the Mangosteen ethanolic extract of pericarp in the concentrations (1-10) $\mu\text{g/mL}$, indicating that 2.5 $\mu\text{g/mL}$ of GME ethanol extract can reduce wound area to 48.42% of the original wound area at 24 hours. Pugar et al. [156] the combination of alginate and mangosteen pericarp extract was studied, finding an increase in fibroblasts, collagen density, and macrophages in diabetic wounds. Xanthonenes exhibit antioxidant and anti-inflammatory activities and can also scavenge free radicals in diabetic patients. Tatiya-aphiradee and colleagues [157] report studies on wounds in mice found that garcinia mangosteen extract reduces proinflammatory cytokines, shows antimicrobial activity, and helps wound healing. The possible mechanism of wound healing and proliferation could be related to lowering superoxide anion levels and decreasing nitric oxide [155]. The studied extract holds promise for treating acute wounds and diabetic ulcers.

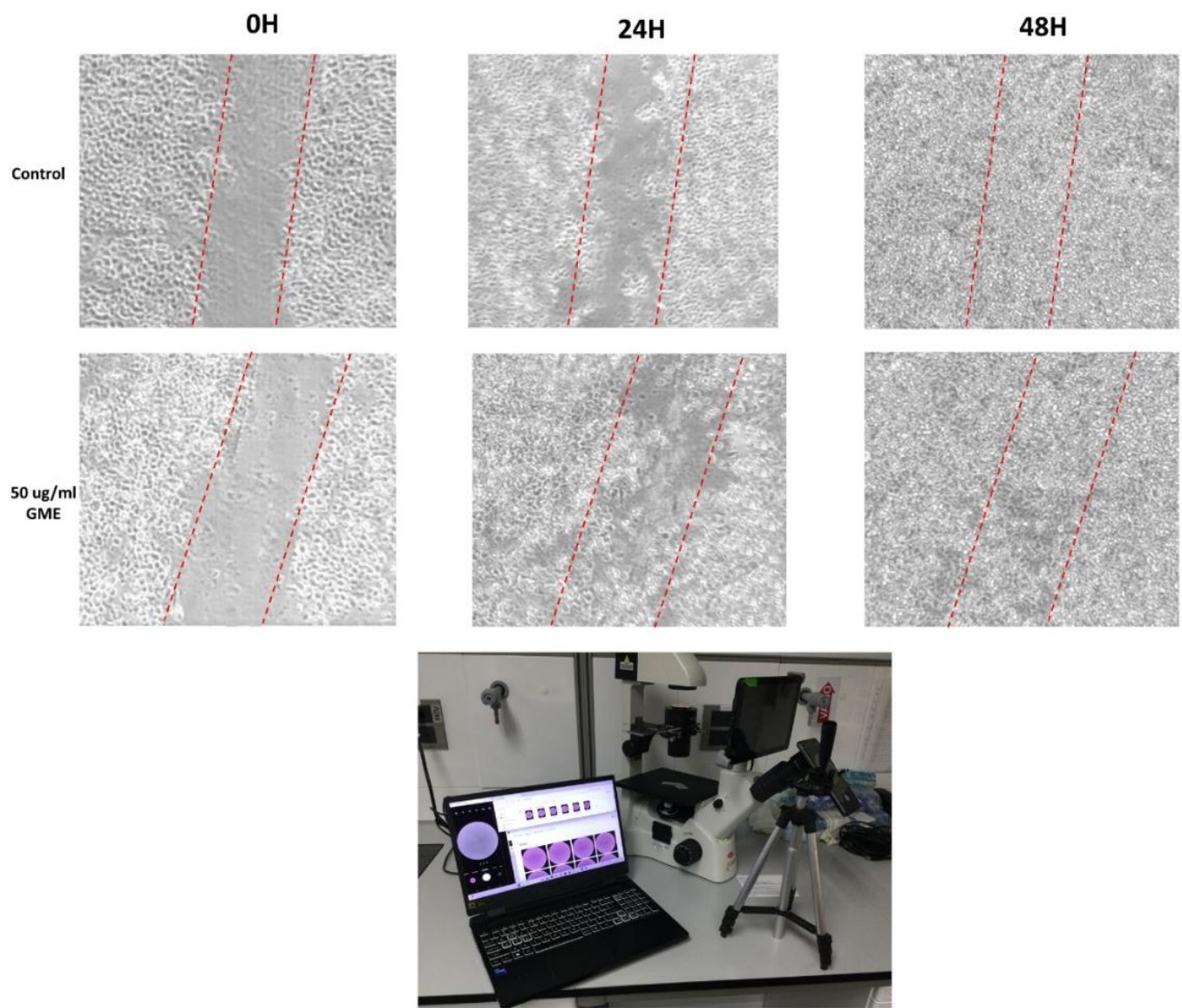


Figure 20 Representative images Scratch assay 10x for control and GME 50 ug/mL in the following time intervals 0h, 24h y 48h.

6.2 Characterization of Composite Hydrogel CHHEC

6.2.1 Fourier transform infrared FT-IR

The FTIR structural differences between CH and CHHEC spectra confirmed the chemical and physical crosslinking of the composite hydrogel. Figure 21 compares the spectra of chitosan with that of the composite hydrogel, revealing notable distinctions. In the chitosan spectrum, a band centered at 3325 cm^{-1} is observed, resulting from overlapping the $-\text{OH}$ and $-\text{NH}_2$ stretching vibrations; its widening is due to intramolecular hydrogen bonds. Moreover, it was possible to distinguish the signals associated with N-H stretching of the NH_2 group at 3360 and 3295 cm^{-1} . These distinctions significantly impact our understanding of the composite hydrogel's structure and properties.

In the hydrogel composite spectrum, this band exhibited a shift, broadening and increased intensity, suggesting a physical crosslinking due to the formation of hydrogen bonding and ionic interaction between the amine groups from chitosan and both the COO^- groups of citric acid and hydroxyl groups of HEC, or both. Also, an increase in the intensity of the signals between 1700 - 1200 cm^{-1} compared to the bands of saccharide chains is observed; this could indicate the formation of new amide bonds and the presence of free COO^- groups from citric acid forming ionic interactions with the NH_3^+ group of chitosan. The second derivative of both spectra was obtained to analyze this region in more detail, as shown in Figure 22.

In the second derivative of the chitosan spectrum, it is possible to distinguish the signals corresponding to amide I ($\text{C}=\text{O}$ stretching band from $-\text{NHCOCH}_3$) at 1656 cm^{-1} , amines groups (NH bending band from free $-\text{NH}_2$) at 1591 cm^{-1} , amide II (NH - bending band from $-\text{NHCOCH}_3$) at 1550 cm^{-1} and amide III ($\text{C}-\text{N}$ stretching band from $-\text{NHCOCH}_3$) at 1313 cm^{-1} .

The second derivative of the CHHEC spectrum reveals that the bands corresponding to amide I and amide II have increased in intensity and are shifted to 1648 cm^{-1} and 1528 cm^{-1} , respectively. Furthermore, the intensity of the amide III signal at 1313 cm^{-1} also increased; this confirms the formation of amide bonds [158], [159]. Additionally, the second derivate of CHHEC shows the apparition of a new signal at 1410 cm^{-1} . This signal is associated with the citric acid's asymmetric COO^- groups, suggesting that the signal at 1560 cm^{-1} overlaps the NH_3^+ groups of chitosan and the symmetric COO^- group of the citric acid. The signal of the symmetric COO^- group should

appear at approximately 1600 cm^{-1} . Their shift to 1560 cm^{-1} could be attributed to strong physical interaction between COO^- groups of citric acid and NH_3^+ groups of chitosan.

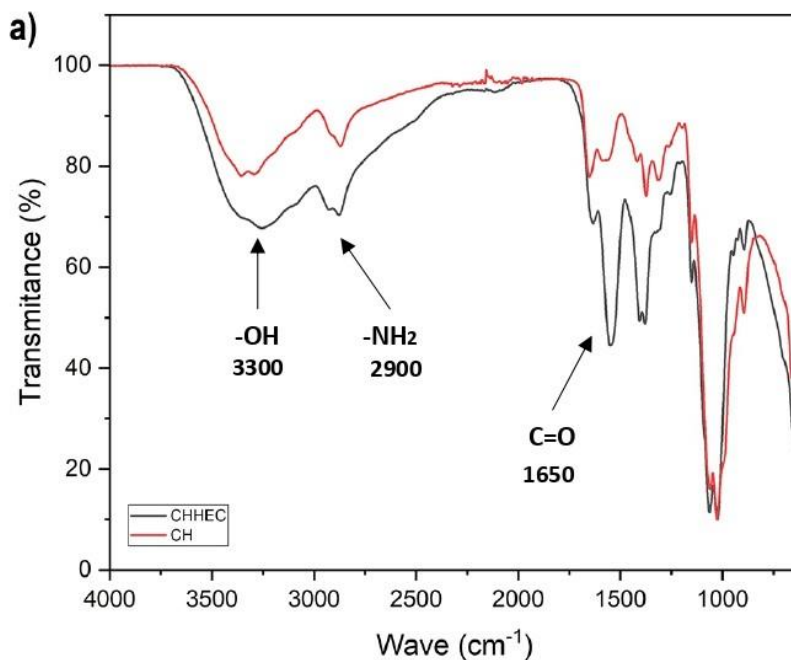


Figure 21 FTIR CH Film and CHHEC

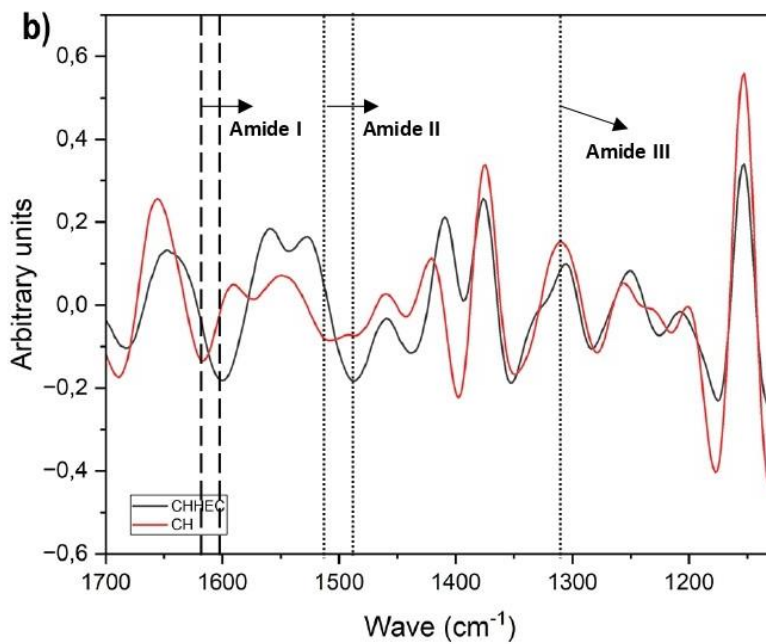
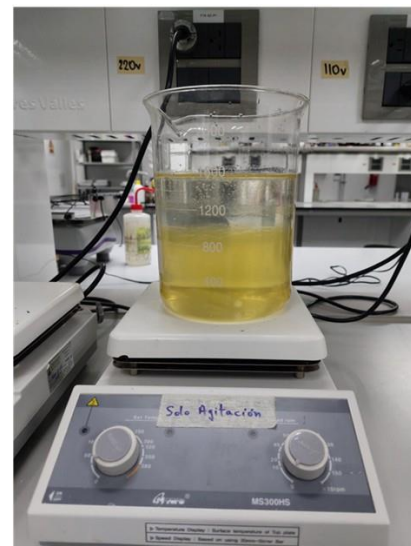
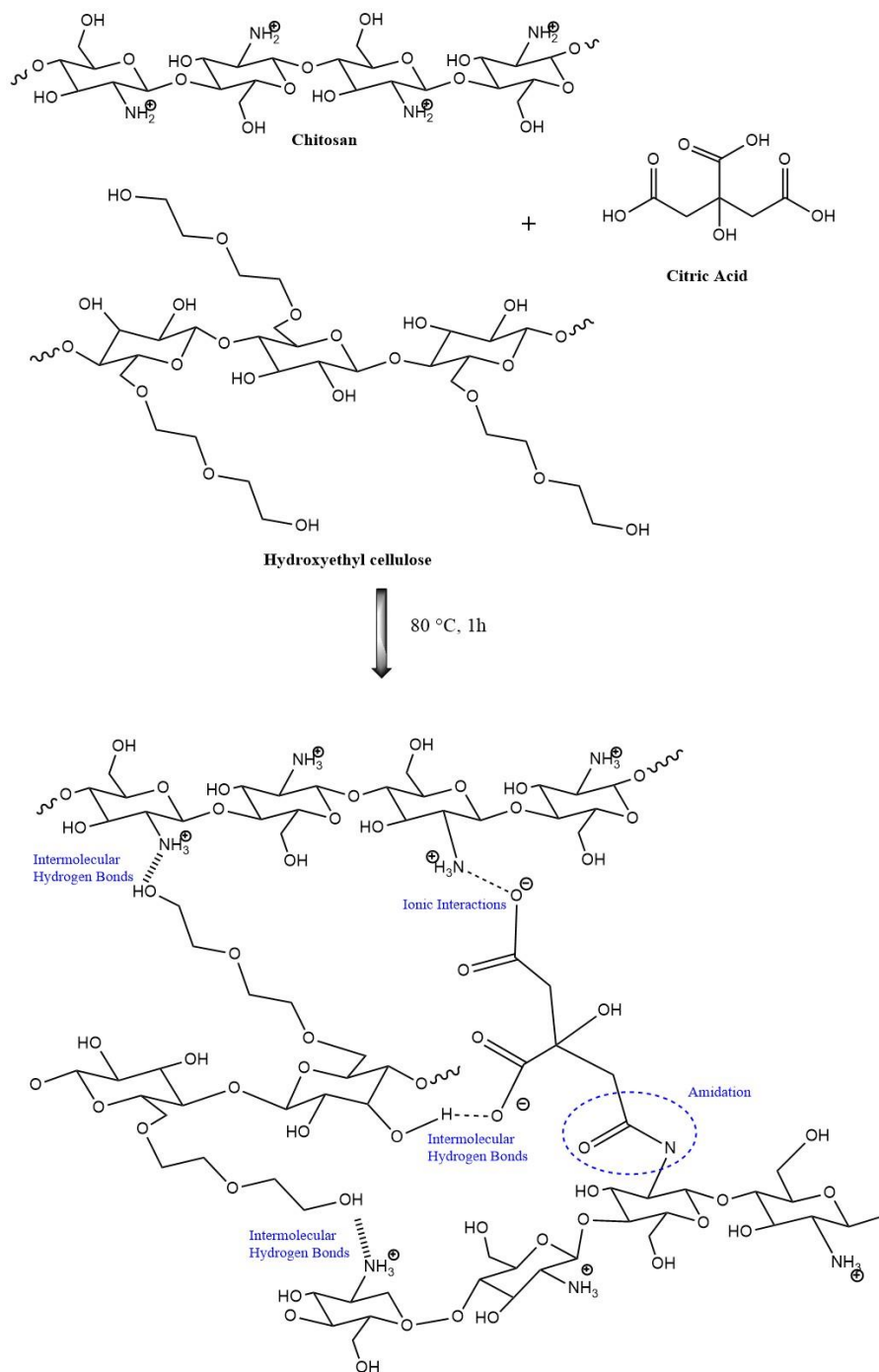
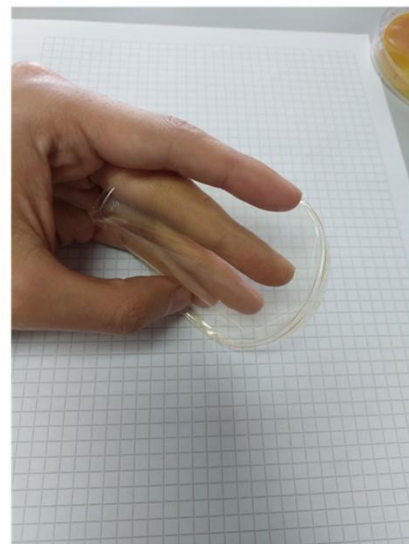


Figure 22 Second derivative of FTIR CH Film and CHHEC

Based on these findings confirming chemical and physical crosslinking, we propose a chemical structure for the composite hydrogel and its reaction mechanism. Figure 23 depicts the proposed reaction mechanism for forming the composite hydrogel. The following spectroscopic observations confirm the suggested average structure of the hydrogel film:



Mixing process



Hydrogel film appearance CHHEC

Figure 23 Reaction equation for the formation of the hydrogel film

6.2.2 Swelling ratio

Figure 24 depicts the behavior of hydrogel films identified as CHL3-HEC1-CA5-GL1, CHL1-HEC1-CA5-GL1, CHL3-HEC1-CA10-GL1, CHL1-HEC1-CA10-GL1, CHL3-HEC1-CA5-GL5, and CHL1-HEC1-CA5-GL5. The study varied the polysaccharide content in CH-HEC ratios of 3-1 and 1-1. In addition, the effects of two concentrations of citric acid and glycerol were studied.

In this study, we investigated the relationship between polysaccharide concentration and the swelling behavior of hydrogel films. Films with a CH-HEC content ratio of 3:1 demonstrated reduced swelling compared to those with a 1:1 ratio, suggesting that higher chitosan content correlates with lower swelling percentages relative to films with higher hydroxyethyl cellulose content. For instance, samples CHL3-HEC1-CA5-GL1 and CHL1-HEC1-CA5-GL1 exhibited swelling percentages of 237.75% and 411.86%, respectively. This trend was consistent across other samples, indicating the presence of hydroxyl (-OH) and carboxyl (-COOH) groups, known for their hydrophilic properties and water retention[160].

The effect of citric acid on the polymeric matrix was examined. The results indicate that increasing the citric acid content in the samples led to a decrease in the swelling capacity of the films. For instance, in samples CHL3-HEC1-CA5-GL1 and CHL3-HEC1-CA10-GL1, a reduction in swelling percentage was observed, decreasing from 237.75% to 103.33%, which represents a decrease of 43.46%. The same trend is observed for the other samples. This behavior is attributed to citric acid acting as a physical crosslinking agent, facilitating interactions such as hydrogen and ionic bonding within the matrix[161].

Incorporating glycerol as a plasticizing agent in the samples had a notable effect. The results indicate that an increase in glycerol concentration also increases the swelling capacity of the materials. For instance, the CHL1-HEC1-CA5-GL1 and CHL1-HEC1-CA5-GL5 reached 237.75% and 633.71%, respectively. Glycerol is a plasticizer known to enhance the flexibility and malleability of polymers. Its three hydroxyl groups contribute to the observed increase in the swelling percentage[162].

Adequate swelling is associated with hydration, accelerating the healing process[163]. Furthermore, it is related to the ability to absorb exudate and release pharmaceutical components and organic compounds with clinical efficacy in the treatment of wounds[164].

The following materials, CHL1-HEC1-CA5-GL5, CHL1-HEC1-CA10-GL1, and CHL1-HEC1-CA5-GL1, were discarded due to their excessively high swelling, which caused them to break into small pieces. Additionally, CHL3-HEC1-CA5-GL5 was eliminated because it released an excess of glycerin, resulting in an oily consistency. Therefore, the selected materials were CHL3-HEC1-CA5-GL1 and CHL3-HEC1-CA10-GL1.

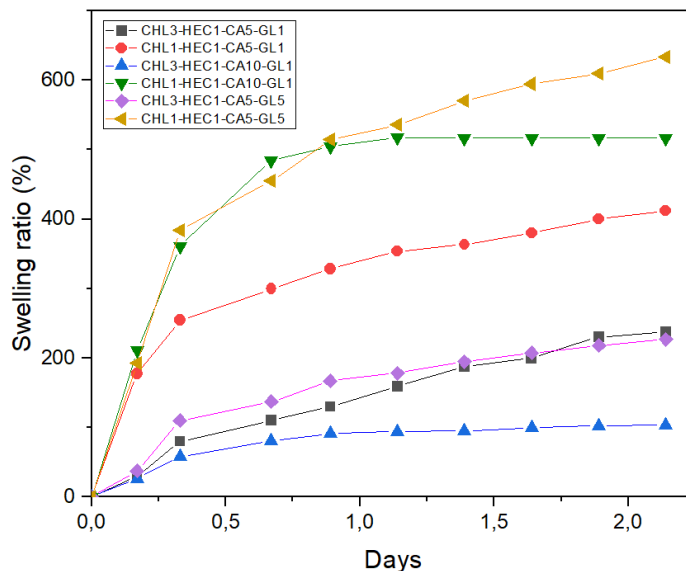


Figure 24 Swelling ratios of the different polymer compositions of the hydrogel films

6.2.3 Mechanical Properties

The previously prepared materials CHL3-HEC1-CA5-GL1, CHL1-HEC1-CA5-GL1, CHL3-HEC1-CA10-GL1, CHL1-HEC1-CA10-GL1, CHL3-HEC1-CA5-GL5, and CHL1-HEC1-CA5-GL5 underwent mechanical tests including tensile strength, elongation at break, and Young's modulus. Most films exhibited high rigidity mechanical tests cannot be reproduced and were discarded. Consequently, we selected the sample CH45HEC30CA5GL1 for further study, where we investigated two types of chitosan with low and high molecular weights, as detailed in Figure 25.

The Figure 25. show analyses of the dry-state samples CHL45HEC30CA5GL1 with CH with low molecular weight and CHH45HEC30CA5GL1 with high molecular weight. Tensile strength, elongation at break, and young module slightly increase by incorporating high molecular weight

chitosan. Specifically, films fabricated with low molecular weight chitosan exhibited a tensile strength of 67.85 MPa, whereas those with higher molecular weight recorded a remarkable increase to 98.77 MPa. Similarly, the elongation at break for low molecular weight samples measured at 14.39%, whereas the high molecular weight counterparts showed a slight increment of 0.60%. This trend is similar to Young's modulus, escalating from 3327.72 to 3618.07 MPa. The chitosan's molecular weight significantly influences film properties such as flexibility, strength, and water swelling capacity. Films comprising high molecular weight chitosan tend to possess superior mechanical strength and rigidity compared to those with low molecular weight, which lean towards flexibility.

Furthermore, crosslinking with citric acid enhances film rigidity. High-molecular-weight chitosan films exhibit elongated structures, facilitating enhanced 3D assembly. The higher proportion of amino groups also promotes hydrogen bonding[165]. To embed mangosteen (GME) and pomegranate (PGE) extracts directly into the material, low-molecular-weight chitosan was selected due to minimal discernible differences in the elongation break observed between the two types of chitosan evaluated.

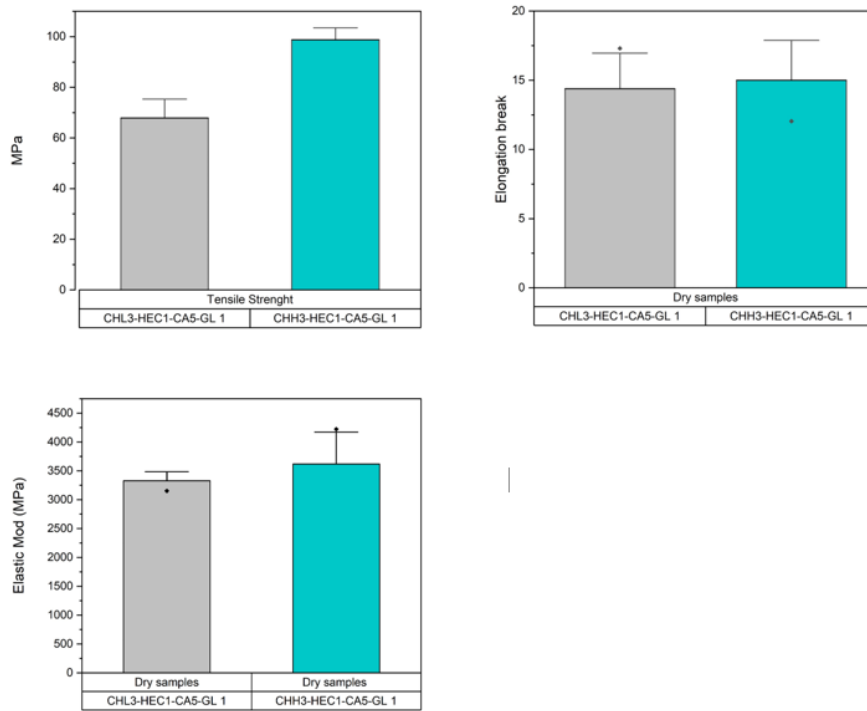


Figure 25 Tensile strength (a), Elongation (b), and Young's Modulus (c) of dried samples CHL45HEC30CA5GL1 and CHH45HEC30CA5GL1.

6.3 Hydrogel films loaded with and without GME and PGE extracts

The preceding chapters examined the chemical and biological aspects of GME and PGE extracts. The above chapter analyzes the physicochemical part of the polymeric matrix suitable for including extracts. The current chapter explores the impact of these extracts on the hydrogel film, covering physicochemical approaches, thermal and mechanical properties, morphology analysis, and a study of fibroblasts on the developed material.

6.3.1 Thickness and Weight Variation

Table 11 summarizes the physical dimensions of different film formulations used in the study, identified by their formulation codes: CHHEC, GME1, GME2, PGE1, PGE2, and GME1PGE1. The hydrogel films studied show high consistency and reproducibility regarding thickness and weight. Thicknesses range from 0.0882 mm to 0.1228 mm, with low standard deviations, for example, CHHEC: 0.0882 mm \pm 0.0057. The film weights range from 0.5714 g to 0.8033 g, with low standard deviations, for example, GM1: 0.8033 g \pm 0.0135. This low variability in the measured parameters indicates precise control of manufacturing conditions, such as temperature and curing time. It suggests that the processing methods and equipment are reliable and produce consistent results. Furthermore, the specific formulations with and without extract loading are well-defined and controlled, demonstrating that including extracts does not introduce significant variability in the measured physical properties. Figure 25 indicates the final appearance of the synthesized hydrogel films.

Formulation Code	Thickness(mm)	Weight (g)
CHHEC	0.0882 (\pm 0.0057)	0.5714 (\pm 0.0070)
GME1	0.0885 (\pm 0.0049)	0.8033 (\pm 0.0135)
GME2	0.1228 (\pm 0.0102)	0.7262 (\pm 0.0156)
PGE1	0.0983 (\pm 0.0043)	0.6550 (\pm 0.0081)
PGE2	0.1185 (\pm 0.0017)	0.7426 (\pm 0.0108)
GME1PGE1	0.1105 (\pm 0.052)	0.7540 (\pm 0.0159)

Table 11 Films with and without extract loading, thickness, weight variations

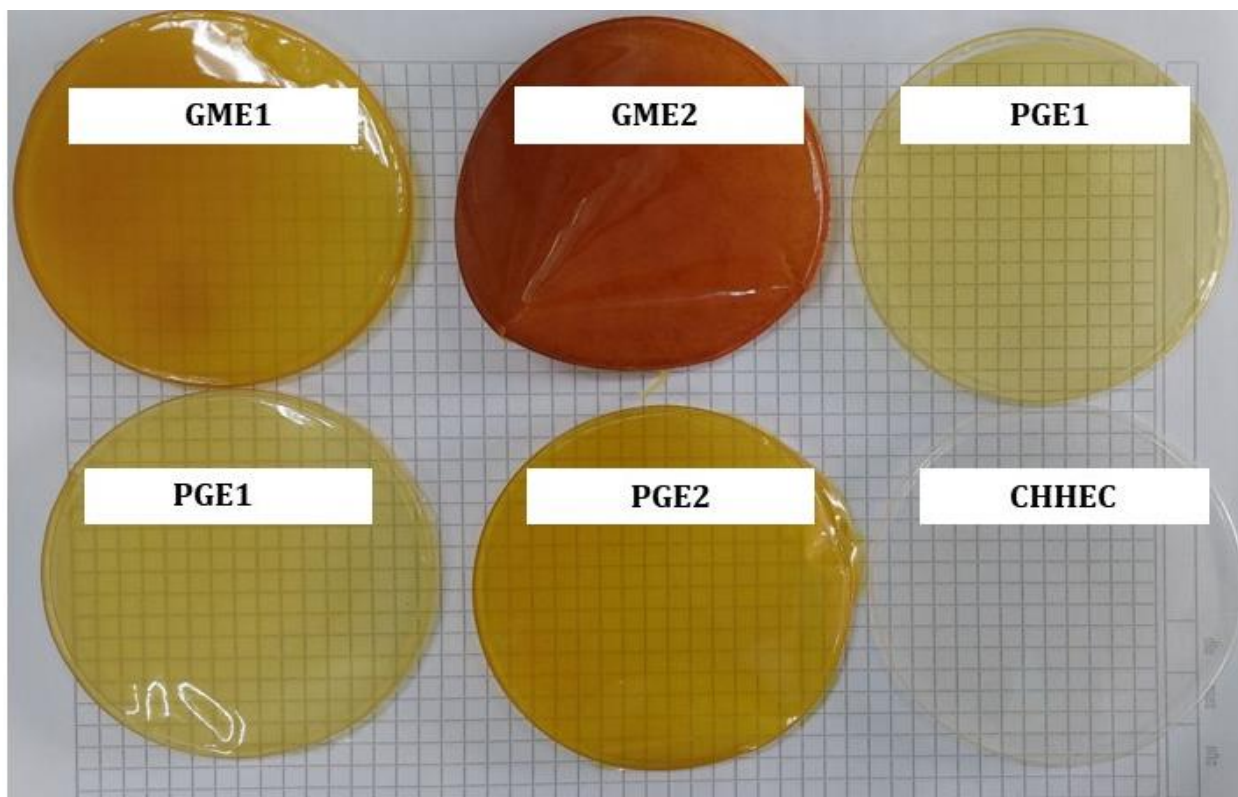


Figure 26 Photography of the synthesized films without extract and with extracts

6.3.2 Swelling ratio of Hydrogel films with GME and PGE

Researching swelling characteristics helps gauge the absorption capacity of wound dressings, which can be used to maintain moisture levels, manage exudate fluids, ensure wound adaptability and comfort, and facilitate the controlled release of active compounds or medications [166], [167].

According to Figure 27., the films with and without loading of GME and PGE extracts were analyzed in three media: deionized water (DI), phosphate-buffered saline (PBS), and simulated body fluid (SBF). The films were cut into 1 cm x 1 cm dimensions. The samples were tested for 180 minutes in 10-minute intervals.

Figure 27. a details the swelling behavior in deionized water of the hydrogel film results for materials with and without extract. The CHHEC film, without extract content, reaches the highest swelling percentage of 148% for this group. For hydrogel films loaded with extracts, it is observed that an increase in the concentration of the extract produces a decrease in swelling. However, films

with higher extract content show lower swelling percentages, with values of 83.43% and 80.50% for the GME2 and PGE2 films, respectively. The GME1 and PGE1 samples with the lowest concentrations reached 142.03 and 118.33% respectively. Additionally, combining the two extracts used in the GME1PGE1 sample shows a synergistic effect reduction in the swelling of 108.94%. This effect may be influenced by the presence of hydroxyl groups (-OH), amino groups (NH₂), and carboxyl groups (-COOH), which are hydrophilic and enhance water retention[168].

Figure 27. b shows the swelling behavior of hydrogel films in phosphate-buffered saline (PBS), simulating extracellular fluid[169]. PBS, composed of salts and a pH similar to the physiological, offers an aqueous environment conducive to cellular processes[170]. The CHHEC film exhibits the highest degree of swelling within the group, analogous to the study in deionized water. The CHHEC film reached a swelling of 278.57%. On the other hand, it is observed that swelling is reduced by increasing the concentration of the GME and PGE extracts. Films with high extract content reduced their swelling to 104.24% and 62.78% GME2 and PGE2, respectively. The presence of amino groups (-NH₂) and carboxylic acids (-COO-) causes interactions with the ions present in the PBS, modifying water absorption and, therefore, swelling[171] Similar findings were observed in a hydrogel made from polyvinyl alcohol and pectin that incorporated Hippophae rhamnoides extract, according to Kim et al. [172], the extract has a higher concentration of flavonoids, which are less soluble and reduce swelling in PBS.

Figure 27. c illustrates the swelling behavior of hydrogel films in SBF, which simulates blood plasma conditions due to their ion concentration and is widely studied for biocompatibility and biodegradability of materials [173]. The films in SBF exhibit the highest swelling to CHHEC compared to DI and PBS. The CHHEC film without extracts reaches a percentage of 875.47%. Conversely, higher extract content results in lower swelling, with 159.25% and 90.72% values for the GME2 and PGE2 films, respectively. The increased swelling in SBF is likely due to the ions affecting the polymer matrix structure, facilitating fluid penetration [171].

Figure 27. d displays the films' appearance in a dry state and swelling after 24 hours of immersion in various media. CHHEC samples without extract expand in SBF, with a minor expansion observed in PBS. Conversely, increasing the extract content enhances the films' dimensional stability, allowing them to retain dimensions similar to their original state[174]. Table 12 indicates

the maximum swelling achieved for each film with and without GME and PGE extracts loading for times greater than 180 minutes for DI, PBS, and SBF.

Hydrogels with swelling percentages below 150 exhibit dimensional stability, long-term moisture retention, and good mechanical strength. However, due to their design with chemical cross-linking, they have low drug loading and release capacities and poor cell adhesion. These hydrogels are suitable for tissue engineering and bioelectronics [175], [176], [177], [178], [179], [180]

On the other hand, hydrogels with swelling percentages above 150 are considered high-swelling hydrogels. They possess high levels of exudate absorption and high cell recruitment and facilitate drug entrapment and diffusion. However, they exhibit dimensional expansion and poor mechanical properties, making them also suitable for tissue engineering and drug delivery applications [181], [182], [183], [184], [185], [186], [187].

Physical and chemical cross-linking mechanisms are attributed to the dimensional stability and fluid absorption reduction. FTIR analysis confirmed the formation of amide bonds and the presence of ionic interactions and hydrogen bonding, which enhance the polymer matrix by compacting the space between polymer chains and restricting their movement within the CHHEC film [185].

Our research emphasizes the versatility of these properties by incorporating extracts into the base film, resulting in swelling percentages below 150 in deionized water (DI), which is ideal for tissue engineering applications. The inclusion of extracts notably enhances the polymer's dimensional stability and reduces swelling in various fluids. Hydrogel films containing extracts achieved swelling percentages below 150 in phosphate-buffered saline (PBS). In contrast, films without extracts show higher swelling properties, making them suitable for tissue engineering and drug delivery applications, as demonstrated in simulated body fluid (SBF).

These characteristics of the hydrogel films with extracts suggest various applications. The enhanced dimensional stability and controlled swelling behavior suggest potential uses in biomedical fields such as wound healing dressings. Furthermore, their adaptability to different swelling environments makes them suitable for targeted drug delivery systems, ensuring controlled release kinetics in specific physiological conditions.

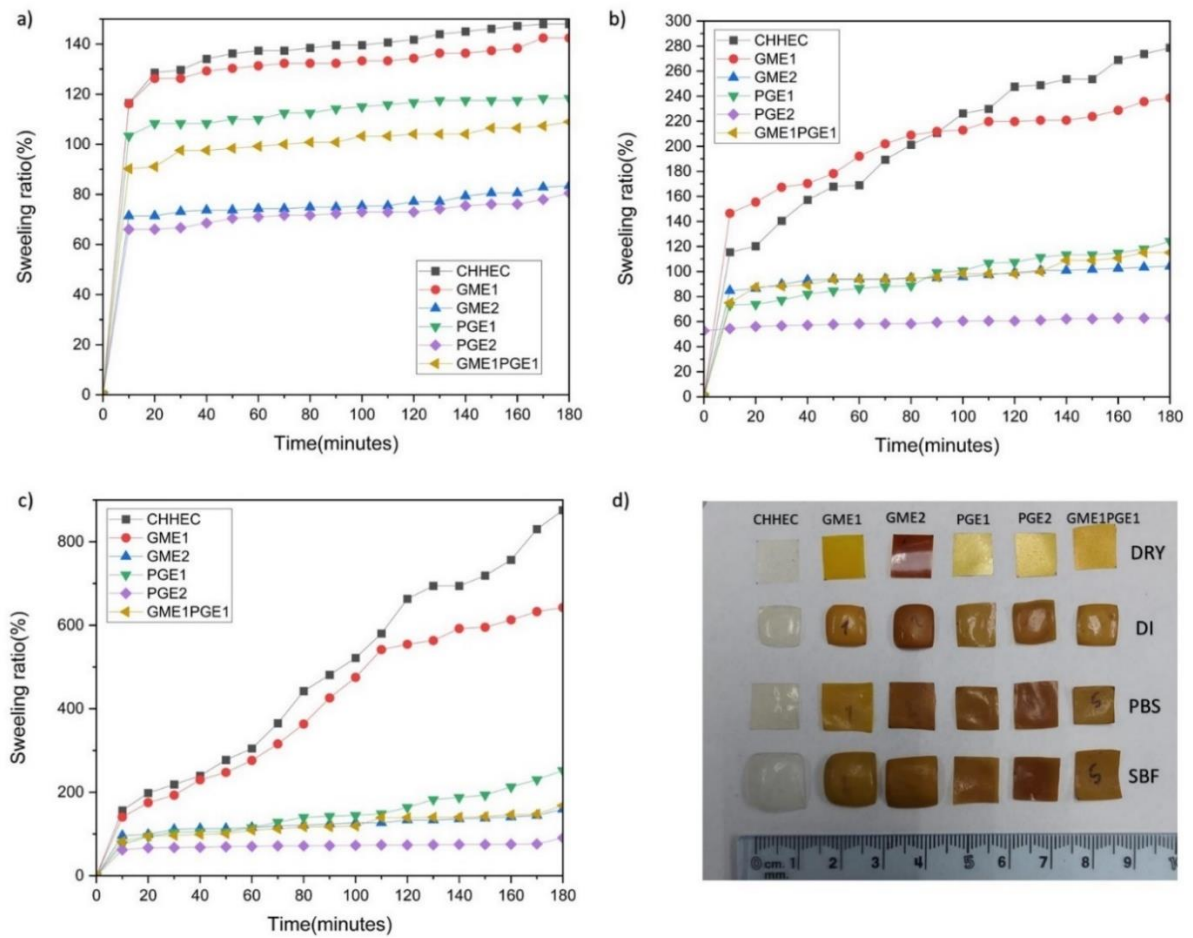


Figure 27 Swelling behavior of hydrogel films in different fluids: a) Deionized water (DI), b) phosphate buffered saline (PBS), c) simulation of blood plasma (SBF) and d) Appearance of the films 24 hours after immersion in each fluid

	Swelling in deionized water (%)	Swelling in PBS (%)	Swelling in SBF (%)
	180min	180min	180min
CHHEC	148.24	278.57	875.47
GME1	142.03	238.61	642.57
GME2	83.43	104.24	159.29
PGE1	118.33	124.16	252.26
PGE2	80.50	62.78	90.82
GME1PGE1	108.94	115.18	168.33

Table 12 Maximum swelling of hydrogel films achieved for time > 180 minutes for DI, PBS, and SBF

6.3.3 Transparency/Opacity

Transparency or opacity is an essential physical property in developing wound dressings, allowing adequate control by medical personnel[188]. Adequate transparencies are related to low absorbances because light at 600 nm can better pass through polymeric films[189]. Figure 28 and Table 13. indicate the transparency and opacity analyses. The film's transparency decreases as the concentration of the extracts increases. The sample CHHEC, composed mostly of chitosan and hydroxyethylcellulose, achieved a transparency of 0.96 with 0.04 opacity.

The GME1 and GME2 samples presented transparencies of 0.89 and 0.60, respectively. On the other hand, samples PGE1 and PGE2 obtained transparencies of 0.95 and 0.94. The previously mentioned samples show that the mangosteen extract's effect, compared to the pomegranate's effect, makes the films more opaque. The pomegranate effect at high concentrations does not reduce its transparency. Another notable result is that combining the two extracts at the lowest levels of GME1PGE1 reaches a transparency of 0.92. Qin and collaborators reported films composed of chitosan with pomegranate extract, indicating degrees of transparency reduction due to tannins[190]. Gómez-Estaca et al.[191] investigated the use of *Origanum Vulgare* and *Salvia Rosmarinus* extracts in gelatin films, finding that degrees of transparency decreased and opacity increased. Additionally, Kumar and collaborators[192] studied films composed of chitosan and pomegranate extract for developing edible films with results similar to those obtained in this research for packing films. Films with more significant transparency than 90% are considered suitable for hydrogel films in biomedical applications[193]. Incorporating extracts into our films facilitates effective, seamless monitoring of the stages or processes of wound healing.

Adequate transparency allows for continuous monitoring of the wound without the need to remove the dressing, which reduces trauma and decreases the risk of infection[194], [195]. In addition, these materials can reduce the need for frequent changes, which decreases pain and associated costs. Dressings with adequate transparency are especially useful in chronic wounds, where it is essential to constantly evaluate infection parameters, such as redness, exudate, and inflammation.

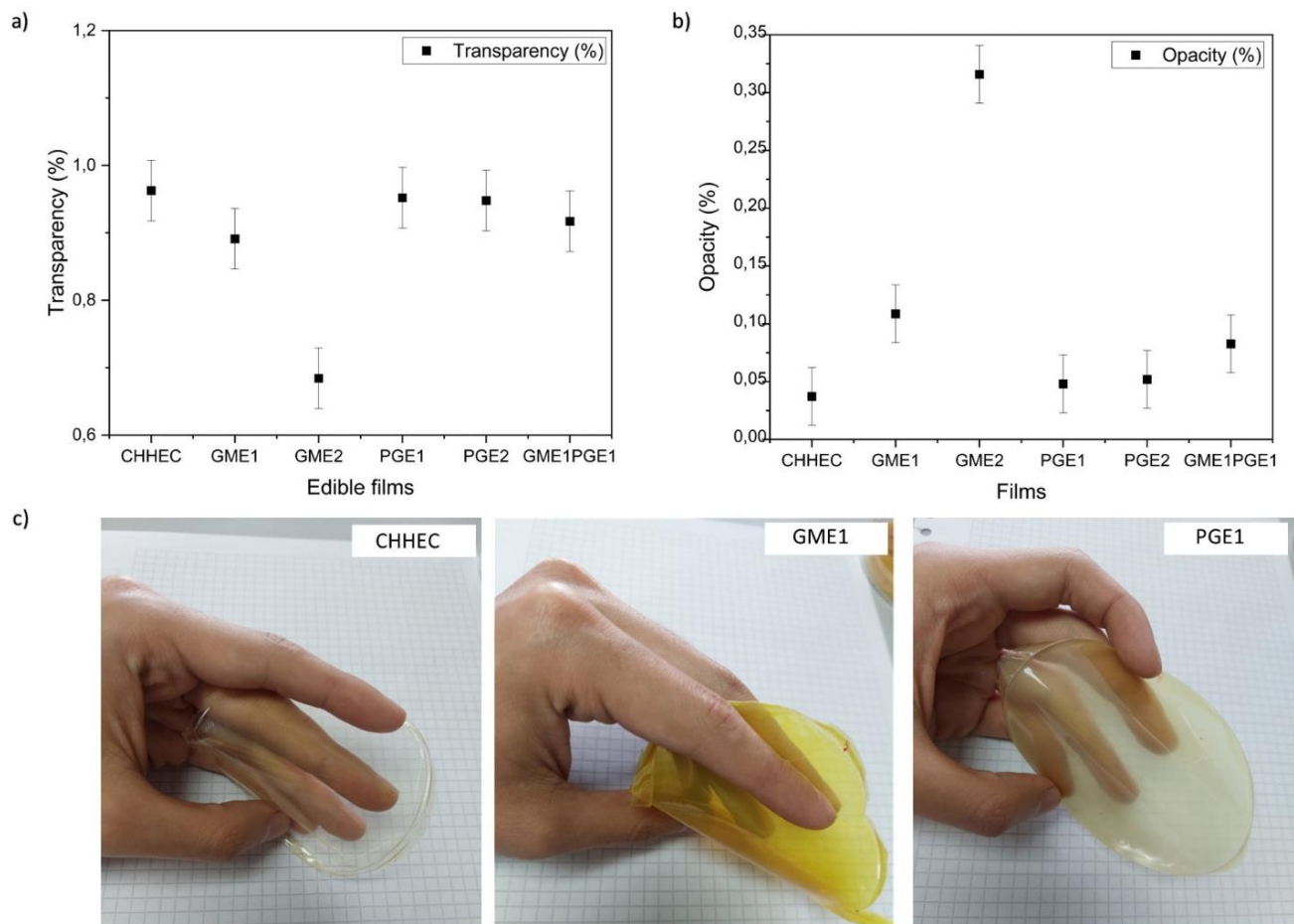


Figure 28 Effect of GME and PGE on the a) transparency, b) opacity in the films and c) appearance of the films. CH-HEC, GME-1, and PGE-1

	Transparency	Opacity
CHHEC	0.96	0.04
GME1	0.89	0.11
GME2	0.68	0.32
PGE1	0.95	0.05
PGE2	0.94	0.06
GME1PGE1	0.92	0.08

Table 13 Effect of the concentration of GME and PGE on the optical qualities transparency and opacity

6.3.4 Fourier transform infrared FT-IR

FTIR analysis was conducted to investigate the functional groups and interactions that likely occurred between the hydrogel composite and the components of both Mangosteen and pomegranate extracts.

Figure 29 a) presents the FTIR spectra of CHHEC film, Mangosteen extract (GME), and GME2 film. A comparative evaluation reveals the appearance of signals associated with the components of the ethanolic extract in the GME2 film. Signals at 1605 cm^{-1} , 1579 cm^{-1} , and 1459 cm^{-1} correspond to carbonyl groups and aromatic structures, while signals at 1278 cm^{-1} and 1222 cm^{-1} are associated with phenolic groups. Additionally, the disappearance of the signal at 1406 cm^{-1} , associated with carboxylate groups, in the CHHEC film is observed once the extract is incorporated into the film. These results suggest that the components of the ethanolic extract likely interact with the CHHEC film through hydrogen bond formation and/or protonation of the carboxylate groups.

Figure 29 b) shows the FTIR spectra of CHHEC, Pomegranate extract PGE, and PGE2 film. A comparative evaluation of the spectra reveals signals associated with carboxylic acids, ketones, and/or esters in the PGE2 hydrogel film. As in the case of the GME2 film, the signal associated with carboxylate groups in the CHHEC film disappears, suggesting hydrogen bond formation and/or protonation of the carboxylate groups.

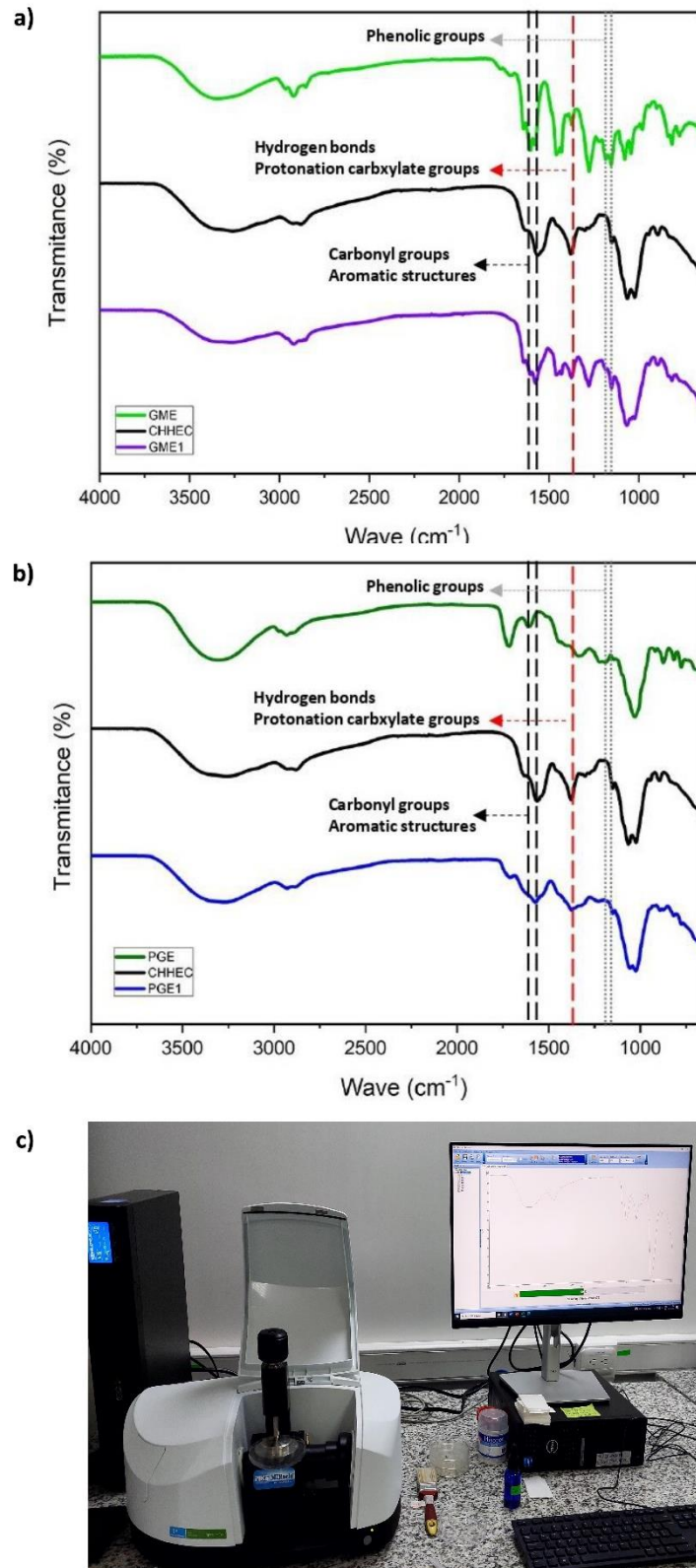
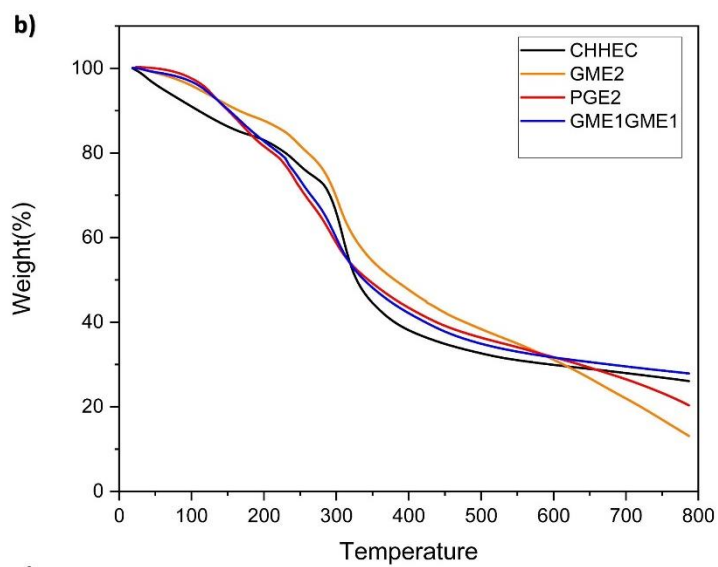
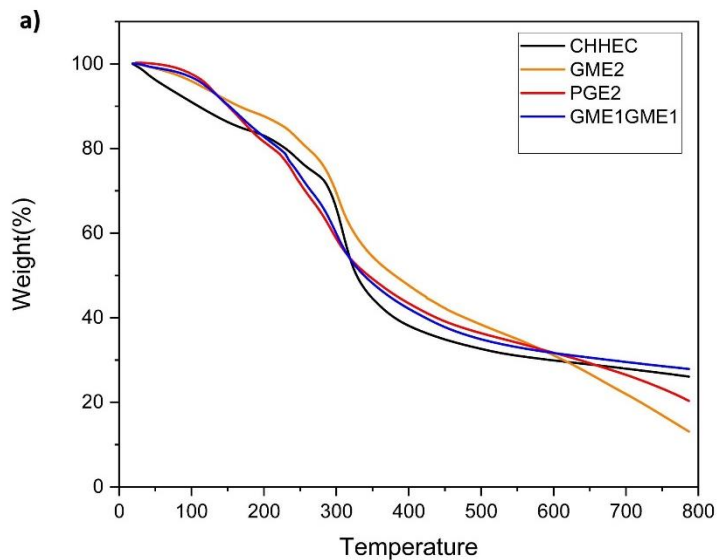


Figure 29 FTIR film compositions a) CH-HEC Film, b) CH-HEC-GM-1-PG-1 Film, c) CH-HEC-GM-1 Film and d) CH-HEC-PG-1 F

6.3.5 Thermogravimetric analysis TGA of Hydrogel films with GME and PGE

The results of films with extract and without content were examined by thermogravimetric analysis presented in Figure 30. The analysis reveals a first stage in which water evaporates from polymer films until reaching 150°C, similar to previous research[196], [197]. Subsequently, the CH component degrades, being less stable than HEC. Hydroxyethylcellulose, chitosan, and extracts degrade over a 220 C temperature to reach 350°C, accounting for between 52% and 55% of the total weight of different films[198], [199]. In contrast, hydroxyethylcellulose indicates lower thermal stability than other types of cellulose, such as methylcellulose and hydroxypropyl methylcellulose[197]. The main degradation of the polymer matrix is observed above 300°C. Multiple peaks or shoulders suggest complex thermal degradation by denaturation of chitosan and extracts[200], [201]. At the end of thermal degradation, CHHEC, GME2, PGE2, and GME1PGE1 were recorded as 26.07%, 13.107%, 20.34%, and 27,90%, respectively. In general, the thermal stability of the chitosan hydroxyethyl cellulose films was slightly altered due to the incorporation of GME and PGE.

The thermal stability of the film incorporating GME is affected. In contrast, the film containing PGE shows minor effects. Mixing both extracts at low concentrations does not change the thermal stability of the initial hydrogel film. Kanmani and colleagues [202], crafted films combining chitosan with carrageenan, finding no changes in thermal stability upon the adding of grapefruit extract. Furthermore, Pelissari and fellow [203] researchers conducted similar investigations on polymeric matrices comprising chitosan and starch, incorporating *Origanum vulgare* oil without observing alterations in thermal stability.



c)



Figure 30 Thermal gravimetric analysis of films CH-HEC, CH-HEC-GM-2, CH-HEC-PG-2 and CH-HEC-GM-1-PG-1 a) Weight (%) vs Temperature, b) Deriv. Weight (%/min) vs Temperature and c) representative image of TGA 5500

6.3.6 Mechanical Strength of Hydrogel films with GME and PGE

The mechanical properties of films with and without extracts, such as tensile strength, elongation at break, and Young's modulus, are detailed in Figure 31. Understanding how these materials modify the mechanical properties under different concentrations of extracts and in dry and hydrated states is essential. To apply wound dressings on patients, the films must protect the wounds from potential additional injuries, serve as a barrier against bacteria, and adapt to movement in the joints [199], [200]. This research covers the evaluation of tensile strength, which measures the material's ability to withstand forces without breaking, and elongation at break, which indicates the ability to stretch before fracture in percentage of the original measurement. Additionally, Young's modulus determines the material's rigidity against deformation under load.

Figure 31. a show an increase in GME concentration led to a reduction in the tensile strength of the films, with values of 61.55 ± 4.13 , 55.06 ± 8.60 , and 43.82 ± 3.78 MPa for CHHEC, GME1, and GME2, respectively. These findings are not in agreement with those reported by Zhen and collaborators, who analyzed that increasing the concentration of the mangosteen rind powder enhances the tensile strength of chitosan, as the powder acts as a reinforcing filler within the polymer matrix[204]. Further investigations involving cellulose nanofibers and chitosan nanofibers revealed significant decreases in tensile strength[205], [206], findings compatible with the films synthesized in this research. This reduction in tensile strength may be due to the interactions between the CHHEC film and the extracts through hydrogen bond formation and/or protonation of the carboxylate groups, thereby increasing the hardness and tensile strength[207].

This same pattern was observed in Figure 31. a where the films incorporating PGE, with values of 61.55 ± 4.13 , 40.39 ± 8.71 , and 31.47 ± 3.83 MPa for CHHEC, PGE1, and PGE2, respectively. The addition of pomegranate extract reduces tensile strength, which differs from the results reported in other studies[208]. The compounds found in pomegranate peel can reinforce chitosan, as polymer matrices might interact with the phenolic compounds in the peel, resulting in modifications that can potentially increase tensile strength[209]. This increase is due to the increase in molecular mobility of the chitosan chains in addition to flexibility and free volume. Other research on edible films has shown that gallic acid can enhance mechanical strength[210].

Additionally, this difference found in the films with GME and PGE might be due to the presence of hydroxyethyl cellulose. However, studies incorporating phenolic compounds into cellulose

derived from bananas have noted decreased tensile strength[211]. Hebat-Allah and colleagues report using hydroxyethyl cellulose loaded with mangiferin extract, citing a reduction in tensile strength due to the attenuation of hydrogen bonds between these components[212]. According to previously reported literature, increased chitosan extracts reinforce polymeric matrixes. On the other hand, an increase in extracts in cellulosic matrices leads to a reduction in tensile strength [209]. Therefore, in the materials synthesized in this research, a predominant effect of hydroxyethylcellulose with extracts is observed, which leads to the reduction of tensile strength [212]. The combination of both extracts in the sample GME1PGE1 reached an intermediate value of 51.12 ± 2.45 MPa.

Figure 31. b. shows the samples in the hydrated state reach values that decrease compared to dry values. The values reached by the films in the wet state were 7.56 ± 1.68 , 10.99 ± 1.43 , 6.16 ± 1.91 , 4.87 ± 1.12 , 3.70 ± 0.68 y 4.95 ± 0.25 , respectively, for CHHEC, GME1, and GME2, PGE1, PGE2, and GME1PGE1. Water acts as a plasticizer in hydrogels, reducing intermolecular forces between polymer chains, decreasing tensile strength, and causing an increase in elongation break[213], [214]. In addition, after rehydration of the films, the tensile strength values decreased significantly compared to the dried samples. This can be attributed to the behavior of glycerol and water[215].

Figure 31. c. shows that a higher GME content causes a critical reduction in the percentage values of the elongation at break compared to the material made up only of polysaccharides, obtaining values of 17.15 ± 2.71 , 7.40 ± 3.81 , and 3.47 ± 0.99 MPa for CHHEC, GME1, and GME2 respectively. These results are consistent with those obtained by Zhang et al., who found that an increase in mangosteen peel powder decreases the elongation at break[216]. Mangosteen contains insoluble molecules that cause discontinuities in the polymer structure, altering the interactions among the chitosan polymer chains [217]. Including mangosteen extract in the polymeric matrix produces a heterogeneous surface, which could generate irregularities and weaken the cohesion of the material, leading to defects before rupture[218]. Therefore, mangosteen achieved the lowest elongation percentages before rupture.

On the contrary, incorporating the PGE extract into the material does not alter the original material but improves the percentage of elongation at break with the following data of 17.15 ± 2.71 , 17.19 ± 1.57 , and 42.78 ± 42.78 MPa for CHHEC, PGE1, and PGE2 respectively. Kumar and collaborators[219] report on films made with chitosan and pomegranate extract, which

improve the elongation percentage due to the inclusion of methanolic extracts obtained from pomegranate peel. Pomegranate extract, soluble in water, produces a more homogeneous interface with fewer irregularities than mangosteen[218]. The combination of both extracts GME-1PGE-2 reached an intermediate state of 12.05 ± 3.25 .

Figure 31. d. shows the samples in the hydrated state reach values of 154.93 ± 25.14 , 110.90 ± 17.00 , 77.62 ± 20.12 , 97.26 ± 20.65 , 89.95 ± 14.04 y 112.91 ± 4.58 respectively for CHHEC, GME1, and GME2, PGE1, PGE2, and GME1PGE1. All hydrogel films indicate an improvement in elongation at break under rehydration conditions because the water content causes slippage between the polymer chains, reducing friction and generating greater material flexibility [213], [214].

The Young's modulus of the extract-loaded and unloaded films is assigned in Figure 31. e. The Young's moduli increase with the GME content reaching values of 2687 ± 613.67 and 2459 ± 68.62 MPa for GME1 and GME2. In contrast, CHHEC that reach 2181.30 ± 461.62 . On the other hand, Young's modulus is reduced using the PGE extract from 1106 ± 186.88 to 135.6 ± 106.66 MPa for PGE1 and PGE2, respectively. Figure 31. f shows the values of Young's modulus in the hydrated state with a drastic decrease with the following values of 4.29 ± 0.64 , 10.65 ± 2.42 , 9.80 ± 2.40 , 5.95 ± 1.64 , 4.02 ± 0.76 , and 4.38 ± 0.38 respectively for CHHEC, GME 1, and GME2, PGE1, PGE2, and GME1PGE1. Taokaew and his colleagues[220], fabricated cellulose nanofiber films, including mangosteen extract, and observed a significant decrease in tensile strength and elongation at break, along with an increase in Young's modulus.

Contrary to previous studies involving similar compounds in chitosan matrices, the findings reveal a decrease in tensile strength with increasing GME content. Similarly, films incorporating PGE extract also exhibit reduced tensile strength, diverging from expectations based on phenolic interactions with chitosan. Hydroxyethyl cellulose in these films likely contributes to this mechanical decline, disrupting hydrogen bonding within the polymer matrix. However, the hydration of these films led to an improvement in elongation at break. Interestingly, films with pomegranate peel extract showed improved elongation at break, indicating enhanced flexibility under stress. These observations underscore the intricate interplay between additives and polymer matrices in governing film properties.

A wide range of mechanical properties is accepted for films. Sharma et al.[221] reported chitosan-based hydrogels with silver nanoparticles, showing elongation at break ranging from 2.38 to 73.45%, suitable for wound dressings. Chopra et al. studied the tensile strength and elongation at break of chitosan-polyvinyl alcohol films with honey, finding tensile strengths ranging from 4.74 to 38.36 MPa and elongation at break values from 30 to 33.51% [222]. Other studies on quaternary ammonium-chitosan loaded with gentamicin sulfate reported tensile strengths ranging from 18.63 to 5.63 MPa and elongation at break from 23.11 to 84.92, indicating suitability for wound dressings [223]. Films prepared in our research exhibit mechanical properties within these ranges, making them suitable for application in wound dressing areas.

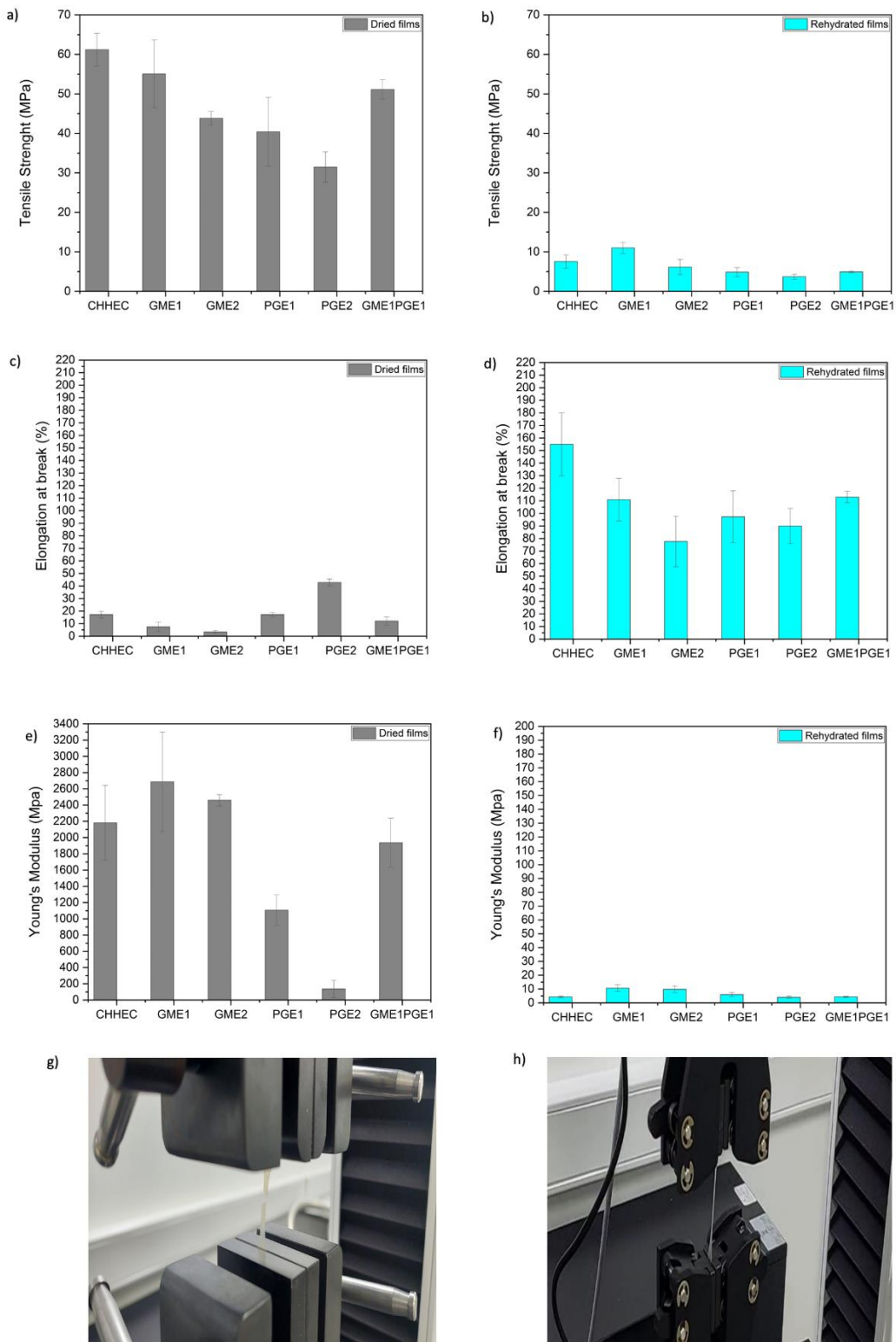


Figure 31 Tensile mechanical properties a) Tensile Strength b) Elongation at break c) Young's Modulus (MPa) and d) Representative Sample. Different films with and without extract content were evaluated in dry and wet conditions. Error bars indicate standard deviations

6.3.7 Scanning electron microscope

The Scanning Electron Microscopy (SEM) analysis results indicate that the morphology of the hydrogel films, including pore size, shape, and surface characteristics, affect the development of materials for biomedicine and controlled drug release. Pores can allow fibroblast infiltration for healing processes and facilitate exudate drainage and gas exchange[224]. The dense structure of the films could help restrict the passage of bacteria, reducing the risk of infections. Moreover, a smooth surface is less prone to bacterial accumulation, becoming an effective barrier between the skin and the wound, which can benefit wounds in areas with much movement[225].

The morphological characteristics of the CH-HEC, GM1, and PGE1 hydrogel films are detailed in Figure 32. The figure displays micrographs at low magnification to observe large areas of the film and visualize its integrity, capturing both sides of each film. The section in contact with the plastic wall of the Petri dish exhibited a shiny appearance, while the side exposed to environmental conditions until drying showed an opaque appearance, with a rough surface (Figure 32 b, d, f and are magnified regions of the inset in Figure 32 b.1, d.1, f.1). Generally, the shiny side demonstrated a smooth surface due to molding, in contrast to the drying side, which exhibited a rough texture. The films displayed good homogeneity, achieved by properly integrating different components through the casting method, with ethanol added to enhance homogeneity.

The control film CHHEC is shown in Figure 32.a, on the shiny side, presented a smooth, pore-free, continuous surface without fractures, which indicates a compact structure produced by the polymer chains[226]This can be explained by the excellent homogeneity of the mixture, which is attributed to the correct integration of the polymers, plasticizer, and cross-linking agent. The micrograph of the reverse side, indicated in Figure 32.b, shows slight roughness.

In Figure 32.c the GME1 film is observed with the side in contact with the Petri dish, showing a relatively smooth surface but displaying several notable features such as irregularly distributed holes or pores without fractures. Additionally, spherical structures are present. In contrast, the drying side in Figure 32.d exhibits roughness due to the presence of GME extract with more pores than the other side, consistent with the literature[227]Depressions also indicate variations in the sample's topography. These changes may result from the mangosteen extract's hydrophobic nature. The GME extract shows immiscibility with water, increasing as its concentration rises. Hence, it was pre-dissolved in ethanol.

On the other hand, the PGE1 film in Figure 32.e exhibits a smooth surface with no visible pores on the shiny side[222]In contrast, the dried side Figure 32.f shows a slight roughness compared to the GME1 film, potentially due to the hydrophilic pomegranate ethanol extract influencing the film's surface properties.

The results indicate that the films' optical, mechanical, swelling and other physicochemical properties can be modified by alterations in the surface morphology[228]. It is important to note that a highly rough surface could pose challenges in wound healing, as it might promote greater fibroblast adhesion [229], [230]. Therefore, it would be more beneficial to choose a smoother surface where cells such as fibroblasts and keratinocytes exhibit less adhesion [225]The results suggest that incorporating GME and PGE extracts significantly alters the films' surface properties, influencing their biocompatibility and potential applications in regenerative medicine.

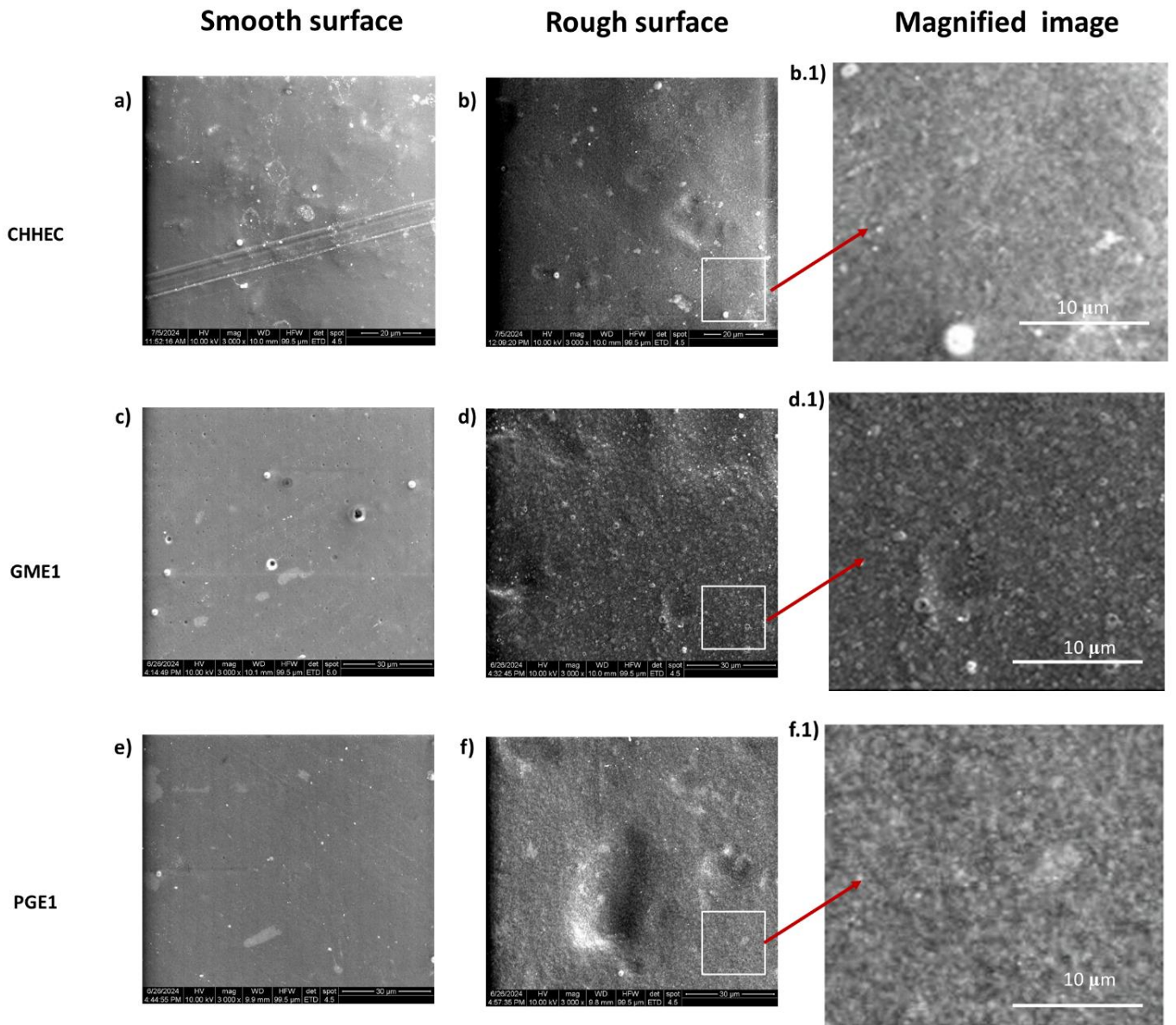


Figure 32 SEM micrographs a) CHHEC bright side 1000x; b) CHHEC opaque side 1000x; c) GME1 bright side 1000x; d) GME1 opaque side 1000x; e) PGE1 bright side 1000x; and f) PGE1 opaque side 1000x.

6.3.8 Disc diffusion of hydrogel films loaded with extracts

Gram-positive and gram-negative bacteria are found in the skin microbiota. Among gram-positive bacteria, species such as *Streptococcus* and *Staphylococcus* are commonly found on the skin[231]. Strains from the following bacteria, such as *Staphylococcus aureus* and *Staphylococcus epidermidis*, have been the most studied for cutaneous applications in tissue engineering areas[232]. *Staphylococcus* can cause infections, prolong wound healing processes, and increase the risk of complications[233]. Conversely, gram-negative bacteria like *Escherichia coli*, *Acinetobacter*, and *Pseudomonas* are also found on the skin. Unlike gram-negative bacteria, the latter can cause pathogenic diseases by entering through skin lacerations, where they can proliferate and cause severe infections and pathologies[234]. Understanding the balance of the skin microbiota is crucial, as it is involved in wound healing and protecting different surrounding tissues.

The disk diffusion test was carried out using the following concentrations in the films (0.20% w/v and 2% w/v) concerning the GME extract, the other samples with (1.05% w/v and 2.11% w/v) of PGE and a film with both extracts 0.20% w/v and 1.05% w/v respectively for GME and PGE. Two strains were studied: *Escherichia Coli* and *Staphylococcus aureus*. Figure 33 shows the films with partial halo inhibition, the values of which are tabulated in Table 14.

The inclusion of GME extracts did not exhibit inhibition. However, upon contact with agar-incorporated films, no growth of gram-negative bacteria was observed for GME1 and GME2, which was confirmed using a stereomicroscope. The literature suggests that larger polymers, for example, those with a molecular weight of 10 kDa, demonstrate reduced sensitivity to Gram-positive bacteria[235]. In this study, the chitosan used ranged from 5 to 19 kDa, and this effect could have been the cause of the non-release of the GME extract. Another significant consideration could be the low solubility of the Mangosteen ethanol extract in water in specific alpha-Mangostin[236]. DMSO, utilized in the individual testing of the GME extract, facilitated its diffusion, thereby highlighting its antibacterial activity against *S. aureus* and *E. coli* with the findings established in this research. The principal molecule in the GME is α -mangostin due to its

ability to destroy the plasma membrane of Gram-positive bacteria such as *S. aureus*[237], [238], [239].

Conversely, the presence of PGE within the polymeric material resulted in a partial inhibition zone measuring 15.5 mm for PGE2 film. The difference in charges between the microbial cell membrane and antibacterial agents can modify permeability respiration and increase the diffusion of the extract across bacterial membranes[240]. These results are similar to those obtained by Valdés and colleagues in synthesizing films based on gelatin and pomegranate seed extract[241]. They found that high extract concentrations enhance the antimicrobial effect with small inhibition radii. According to the literature, there is a clearer effect on Gram-positive bacteria than Gram-negative bacteria due to the phenolic compounds in pomegranate[242], [243].

Notably, the GMEPGE1 film exhibited an inhibition zone of 15.5 ± 0.55 mm, whereas the GME1 and PGE1 films showed no inhibition individually. It is observed that the two antimicrobial extracts at low concentrations do not have a significant effect when used separately in the membranes. However, when combined, the GME1PGE1 hydrogel film indicates antimicrobial activity against *S. Aureus*, demonstrating a synergistic effect. This effect probably arises from the non-release of GME, which remains inside the polymer matrix as a filler, thereby facilitating the diffusion of the PGE extract.

The findings in this study align closely with previous literature. Taokaew et al. [82] developed a film using nanocellulose fibers infused with an ethanolic extract from Mangosteen peel, demonstrating 4 mm inhibition zones against *Staphylococcus aureus*, *S. epidermidis*, and *Candida albicans*. Boonmak and colleagues[16] fabricated poly (vinyl acetate) films loaded with mangosteen at 1 to 3% concentrations. They found that these films were effective only against *S. aureus*, with a more substantial effect observed against Gram-positive than Gram-negative bacteria. Nascimento and colleagues[244] have reported a polymeric film made from a 1.25% w/v hydroalcoholic extract of pomegranate peel, prepared in situ within a polymeric matrix composed of starch and polyvinyl acetate. This film exhibits antimicrobial activity against *Staphylococcus Aureus*, with more than 1.8 cm inhibition zones. Faris and colleagues [245]synthesized a dressing gel containing Pomegranate and *Lignosus rhinocerotis* extracts. In their findings, they did not

observe antibacterial activity; thus, they only documented the activity of pomegranate, which is effective at high concentrations primarily due to tannins[246], [247].

The hydrogel films synthesized in our investigation showed activity against *Staphylococcus aureus* only, which could effectively inhibit the growth of pathogenic bacteria. This is a crucial element of care and integrity to the wound treatment process, ensuring a more effective and faster recovery for the patient.

CODE	<i>Escherichia coli</i> inhibition mL	<i>Staphylococcus aureus</i> inhibition mL
CHHEC	-	-
GME1	-	-
GME2	-	-
PGE1	-	-
PGE2	-	15.5 ± 0.55
GME1PGE1	-	12.0 ± 0.36

Table 14 Inhibition zones produced by films with and without GM and PG peel extract

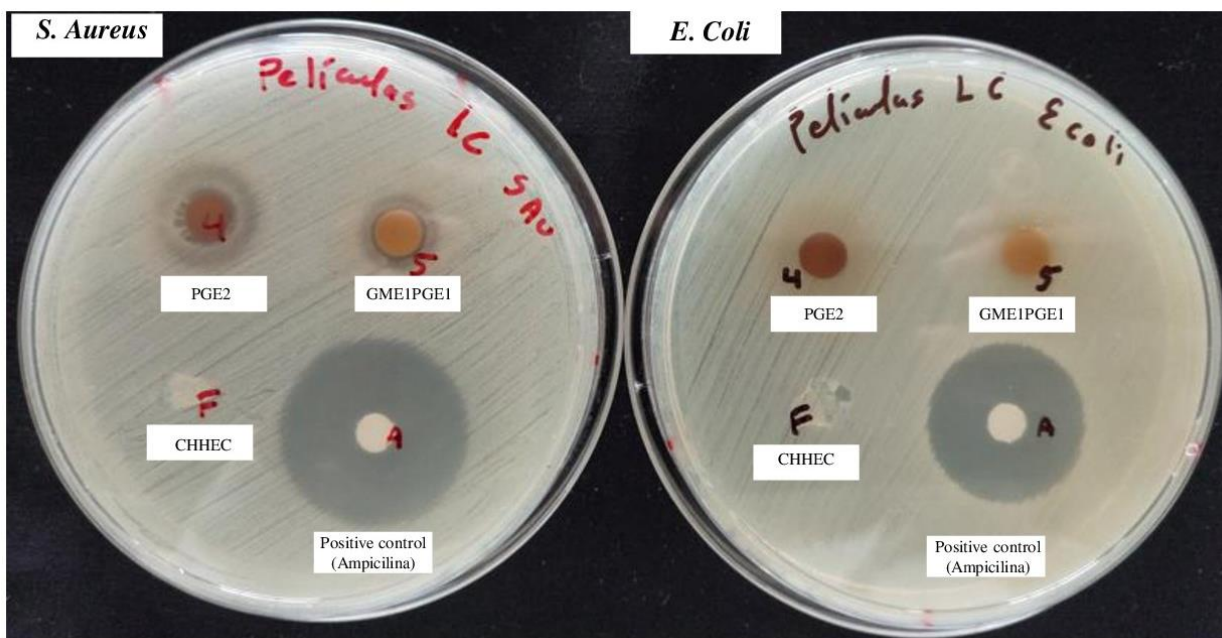


Figure 33 Hydrogel films. with extracts and without extracts against *S. Aureus* and *E. Coli*; CH-HEC-PG-1 (4); CH-HEC-PG-1 (5); CH-HEC(F); and Ampicilim (A)

6.3.9 Cell culture on hydrogel films

Figure 34 shows the control and the films CHHEC, PGE1, and GME1 at 0 and 24 hours post-cell incubation under 10x magnification. In certain instances, cell adhesion appears to surpass that of the control; however, accurately quantifying this increase is challenging due to the unique optical properties exhibited by each film.

Garcinia mangostana extracts have been tested on fibroblast, neutrophil, and macrophage cell lines, showing improved proliferation and collagen density[248]. Some compounds in *Garcinia mangostana* extracts may inhibit cancer cell growth[249]. However, further studies are needed to assess toxicity to normal cells and possible adverse effects on wound healing. No toxic effects of *Garcinia mangostana* have been found in skin studies. Chivapat et al.[250] reported oral administration studies, where mice were given doses of 10, 100, 500, 1000, and 1000 mg/kg/day for six months; long-term liver and kidney damage was observed in mice given 500 mg/kg/day. Elevated levels of alanine aminotransferase and aspartate aminotransferase are enzymes released when there is liver damage and elevated creatinine levels.

Kaci and collaborators [251] studied the *Punica granatum* extract in the WST-8 assay to study the induction or inhibition of cell proliferation in vitro through a colorimetric assay. Their results showed no toxic effects. Studies of these types of extracts in cancer cells B16F10, such as melanoma, have demonstrated cytotoxic effects, reducing angiogenesis and cell proliferation[252]. Jahromi et al.[253] reported studies where dermal injections of 224 mg/kg of *Punica granatum* ethanolic extract were administered to mice found no evidence of skin allergies. Additionally, the mice received doses of 0.5, 1.9, and 7.5 mg/kg over 22 days, and no toxic effects were observed, suggesting potential use in applications against diseases.

Based on the available literature, both extracts have shown no toxic effects on skin cells in vitro and in vivo. These extracts are commonly utilized in alternative medicine for extended treatments. While toxic effects have been reported with oral administration, these occur only under long-term exposure and in large doses. Notably, both extracts have demonstrated cytotoxic activity against various cancer cell lines, including melanoma. No adverse effects are anticipated for dermal applications, as the extracts are applied in minimal quantities to develop wound dressings.

NIH/3T3

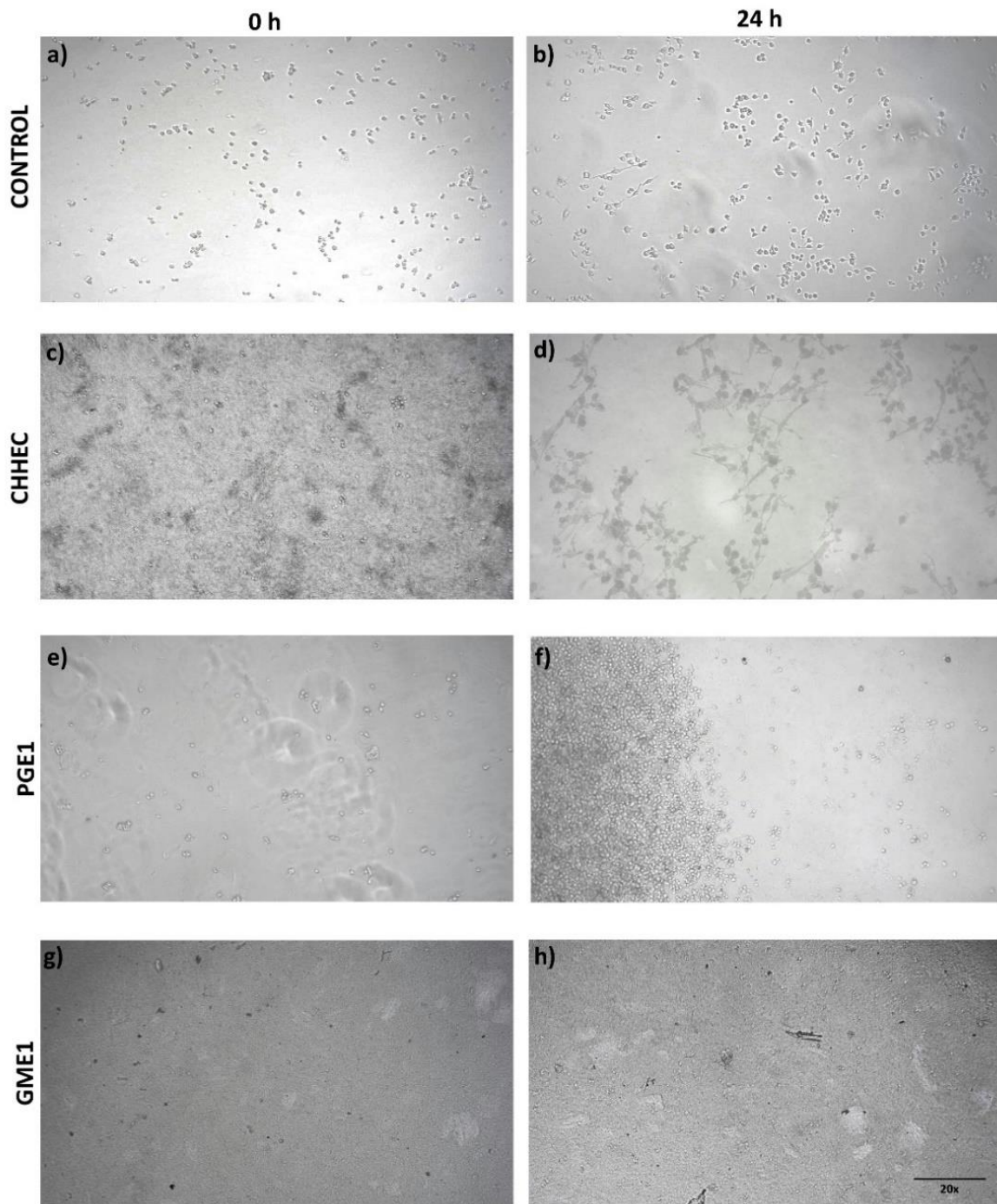


Figure 34 NIH/3T3 fibroblast cell culture on films after 24 h incubation images. Micrographs obtained with inversion microscope a) control $t=0$, b) control $t=24h$, c) CH-HEC $t=0$, d) CH-HEC $t=24h$, e) CH-HEC-PG-1 $t=0$, f) CH-HEC-PG-1 $t=24h$, g) CH-HEC-GM-1 $t=0$, and h) CH-HEC-GM-1 $t=24h$.

7 CONCLUSIONS

The *Garcinia mangostana* and *Punica granatum* peels are rich in phytochemical compounds with potential wound regeneration capabilities. The extracts are characterized by high phenolic content and exhibit significant antioxidant activity. Both extracts demonstrate antimicrobial efficacy against *S. aureus* and *E. coli*. Specifically, GME enhances NIH3T3 fibroblast migration within 24 hours. Using the casting method, we successfully synthesized a series of hydrogel films based on chitosan and hydroxyethyl cellulose, incorporating GME and PGE extracts. SEM micrographs reveal a slight increase in surface roughness correlating with higher extract concentrations. The FTIR spectra show characteristic bands of the extracts integrated into the polymeric matrix. Swelling studies conducted in simulated biological fluids reveal that increased extract concentrations reduce the swelling percentage. Furthermore, higher extract concentrations slightly reduce transparency, while TGA characterization shows a marginal decrease in the thermal stability of the films containing extracts. Antibacterial activity is more effective in films with PGE2 and GME1PGE1 against *S. aureus*. GME reduces the mechanical properties of the films, whereas PGE enhances elongation at break.

8 RECOMMENDATIONS

Conduct cellular toxicity studies of the extracts on the cells that make up the different layers of the dermis. Perform in vitro and in vivo tests on other strains of fibroblasts and keratinocytes. Establish an appropriate release study to determine the best concentration released into the biological medium. Use reference standards for the main compounds of interest involved in fibroblast cell migration and proliferation. Test other extracts in the polymer matrix that can be obtained with polar or non-polar solvents. Lastly, studies on cancer cells will be conducted, mainly focusing on the compounds GME and PGE, which are known to be capable of inhibiting cancer.

9 References

- [1] J. Li *et al.*, “Procedural Promotion of Multiple Stages in the Wound Healing Process by Graphene-Spiky Silica Heterostructured Nanoparticles,” *Int J Nanomedicine*, vol. 18, pp. 6585–6599, 2023, doi: 10.2147/IJN.S426552.
- [2] L. Ding *et al.*, “Research progress and challenges of composite wound dressings containing plant extracts,” *Cellulose*, vol. 30, no. 18, pp. 11297–11322, Dec. 2023, doi: 10.1007/S10570-023-05602-0.
- [3] M. Li *et al.*, “Smart and versatile biomaterials for cutaneous wound healing,” *Biomater Res*, vol. 27, no. 1, pp. 1–32, Dec. 2023, doi: 10.1186/S40824-023-00426-2/FIGURES/13.
- [4] H. M. Nguyen, T. T. Ngoc Le, A. T. Nguyen, H. N. Thien Le, and T. T. Pham, “Biomedical materials for wound dressing: recent advances and applications,” *RSC Adv*, vol. 13, no. 8, pp. 5509–5528, Feb. 2023, doi: 10.1039/D2RA07673J.
- [5] P. Monika, M. N. Chandrababha, A. Rangarajan, P. V. Waiker, and K. N. Chidambara Murthy, “Challenges in Healing Wound: Role of Complementary and Alternative Medicine,” *Front Nutr*, vol. 8, p. 791899, Jan. 2021, doi: 10.3389/FNUT.2021.791899.
- [6] H. Yao *et al.*, “Design strategies for adhesive hydrogels with natural antibacterial agents as wound dressings: Status and trends,” *Mater Today Bio*, vol. 16, p. 100429, Dec. 2022, doi: 10.1016/J.MTBIO.2022.100429.
- [7] M. H. Norahan, S. C. Pedroza-González, M. G. Sánchez-Salazar, M. M. Álvarez, and G. Trujillo de Santiago, “Structural and biological engineering of 3D hydrogels for wound healing,” *Bioact Mater*, vol. 24, p. 197, Jun. 2023, doi: 10.1016/J.BIOACTMAT.2022.11.019.
- [8] P. Monika, M. N. Chandrababha, A. Rangarajan, P. V. Waiker, and K. N. Chidambara Murthy, “Challenges in Healing Wound: Role of Complementary and Alternative Medicine,” *Front Nutr*, vol. 8, p. 791899, Jan. 2021, doi: 10.3389/FNUT.2021.791899.

- [9] S. Alven, S. Peter, Z. Mbese, and B. A. Aderibigbe, “Polymer-Based Wound Dressing Materials Loaded with Bioactive Agents: Potential Materials for the Treatment of Diabetic Wounds,” *Polymers (Basel)*, vol. 14, no. 4, Feb. 2022, doi: 10.3390/POLYM14040724.
- [10] S. P. Chen *et al.*, “Mangosteen xanthone γ -mangostin exerts lowering blood glucose effect with potentiating insulin sensitivity through the mediation of AMPK/PPAR γ ,” *Biomedicine & Pharmacotherapy*, vol. 144, p. 112333, Dec. 2021, doi: 10.1016/J.BIOPHA.2021.112333.
- [11] S. Melia, D. Novia, I. Juliyarsi, and E. Purwati, “The characteristics of the pericarp of *garcinia mangostana* (mangosteen) extract as natural antioxidants in rendang,” *IOP Conf Ser Earth Environ Sci*, vol. 287, no. 1, Aug. 2019, doi: 10.1088/1755-1315/287/1/012028.
- [12] Y. S. Kurniawan, M. R. G. Fahmi, and L. Yuliaty, “Isolation and optical properties of natural pigments from purple mangosteen peels,” *IOP Conf Ser Mater Sci Eng*, vol. 833, no. 1, Jun. 2020, doi: 10.1088/1757-899X/833/1/012018.
- [13] C. Bi, H. Xu, J. Yu, Z. Ding, and Z. Liu, “Botanical characteristics, chemical components, biological activity, and potential applications of mangosteen,” *PeerJ*, vol. 11, 2023, doi: 10.7717/PEERJ.15329.
- [14] K. Q. Sani, P. Paulina, and P. K. Insyira, “The Study Utilization of Mangosteen (*Garcinia mangostana* L.) Peel Extract as a Gel-Based Burn Wound Plaster,” *Equilibrium Journal of Chemical Engineering*, vol. 7, no. 2, p. 147, Oct. 2023, doi: 10.20961/EQUILIBRIUM.V7I2.76952.
- [15] M. E. Gondokesumo, Y. Antonius, and Y. E. Agustin, “Effectivity of Patch Herbal Mixture Composed of Mangosteen Peel Extract and Bacterial Cellulose for Wound Healing,” *Pharmacognosy Journal*, vol. 15, no. 3, pp. 461–466, May 2023, doi: 10.5530/pj.2023.15.102.
- [16] N. Boonmak, J. Niyompanich, P. Chuysinuan, P. Niamlang, P. Ekabutr, and P. Supaphol, “Preparation of mangosteen extract-loaded poly(vinyl acetate) for use as an antibacterial spray-on dressing,” *J Drug Deliv Sci Technol*, vol. 46, pp. 322–329, Aug. 2018, doi: 10.1016/J.JDDST.2018.05.033.

- [17] P. A. C. Wulandari *et al.*, “Wound Healing and Antioxidant Evaluations of Alginate from *Sargassum ilicifolium* and Mangosteen Rind Combination Extracts on Diabetic Mice Model,” *Applied Sciences* 2021, Vol. 11, Page 4651, vol. 11, no. 10, p. 4651, May 2021, doi: 10.3390/APP11104651.
- [18] F. Marra, B. Petrovicova, F. Canino, A. Maffia, C. Mallamaci, and A. Muscolo, “Pomegranate Wastes Are Rich in Bioactive Compounds with Potential Benefit on Human Health,” *Molecules*, vol. 27, no. 17, Sep. 2022, doi: 10.3390/MOLECULES27175555.
- [19] Y. Mo *et al.*, “Pomegranate Peel as a Source of Bioactive Compounds: A Mini Review on Their Physiological Functions,” *Front Nutr*, vol. 9, p. 887113, Jun. 2022, doi: 10.3389/FNUT.2022.887113.
- [20] J. Singh *et al.*, “Pomegranate Peel Phytochemistry, Pharmacological Properties, Methods of Extraction, and Its Application: A Comprehensive Review,” *ACS Omega*, vol. 8, no. 39, pp. 35452–35469, Oct. 2023, doi: 10.1021/ACSOMEGA.3C02586/ASSET/IMAGES/LARGE/AO3C02586_0003.JPEG.
- [21] M. H. Hashemi Poor, S. Hosseinzadeh, and M. Aminlari, “Wound healing potential of pomegranate peel extract in human dermal fibroblasts through regulating the expression of FN1 gene,” *South African Journal of Botany*, vol. 146, pp. 222–229, May 2022, doi: 10.1016/J.SAJB.2021.10.017.
- [22] N. N. Costa *et al.*, “Polymeric films containing pomegranate peel extract based on PVA/starch/PAA blends for use as wound dressing: In vitro analysis and physicochemical evaluation,” *Materials Science and Engineering: C*, vol. 109, p. 110643, Apr. 2020, doi: 10.1016/J.MSEC.2020.110643.
- [23] M. H. Hashemi Poor, S. Hosseinzadeh, and M. Aminlari, “Wound healing potential of pomegranate peel extract in human dermal fibroblasts through regulating the expression of FN1 gene,” *South African Journal of Botany*, vol. 146, pp. 222–229, May 2022, doi: 10.1016/J.SAJB.2021.10.017.
- [24] W. Widowati, L. Darsono, J. Suherman, N. Fauziah, M. Maesaroh, and P. putu Erawijantari, “Anti-inflammatory effect of mangosteen (*Garcinia mangostana* L.) peel extract and its

- compounds in lps-induced raw264.7 cells,” *Natural Product Sciences*, vol. 22, no. 3, pp. 147–153, 2016, doi: 10.20307/NPS.2016.22.3.147.
- [25] F. Gutierrez-Orozco and M. L. Failla, “Biological Activities and Bioavailability of Mangosteen Xanthones: A Critical Review of the Current Evidence,” *Nutrients*, vol. 5, no. 8, p. 3163, Aug. 2013, doi: 10.3390/NU5083163.
- [26] A. A. Saparbekova, G. O. Kantureyeva, D. E. Kudasova, Z. K. Konarbayeva, and A. S. Latif, “Potential of phenolic compounds from pomegranate (*Punica granatum* L.) by-product with significant antioxidant and therapeutic effects: A narrative review,” *Saudi J Biol Sci*, vol. 30, no. 2, p. 103553, Feb. 2023, doi: 10.1016/J.SJBS.2022.103553.
- [27] I. A. Duceac, L. Vereștiuc, A. Coroaba, D. Arotăriței, and S. Coseri, “All-polysaccharide hydrogels for drug delivery applications: Tunable chitosan beads surfaces via physical or chemical interactions, using oxidized pullulan,” *Int J Biol Macromol*, vol. 181, pp. 1047–1062, Jun. 2021, doi: 10.1016/J.IJBIOMAC.2021.04.128.
- [28] H. M. Ibrahim, E. M. R. E.- Zairy, H. M. Ibrahim, and E. M. R. E.- Zairy, “Chitosan as a Biomaterial — Structure, Properties, and Electrospun Nanofibers,” *Concepts, Compounds and the Alternatives of Antibacterials*, Dec. 2015, doi: 10.5772/61300.
- [29] X. Wang *et al.*, “Chitosan-Based Hydrogels for Infected Wound Treatment,” *Macromol Biosci*, vol. 23, no. 9, p. 2300094, Sep. 2023, doi: 10.1002/MABI.202300094.
- [30] P. Feng *et al.*, “Chitosan-Based Functional Materials for Skin Wound Repair: Mechanisms and Applications,” *Front Bioeng Biotechnol*, vol. 9, Feb. 2021, doi: 10.3389/FBIOE.2021.650598.
- [31] A. Naeem, C. Yu, X. Wang, M. Peng, Y. Liu, and Y. Liu, “Hydroxyethyl Cellulose-Based Hydrogels as Controlled Release Carriers for Amorphous Solid Dispersion of Bioactive Components of *Radix Paeonia Alba*,” *Molecules 2023, Vol. 28, Page 7320*, vol. 28, no. 21, p. 7320, Oct. 2023, doi: 10.3390/MOLECULES28217320.
- [32] G. F. El Fawal, M. M. Abu-Serie, M. A. Hassan, and M. S. Elnouby, “Hydroxyethyl cellulose hydrogel for wound dressing: Fabrication, characterization and in vitro

- evaluation,” *Int J Biol Macromol*, vol. 111, pp. 649–659, May 2018, doi: 10.1016/J.IJBIOMAC.2018.01.040.
- [33] E. E. Tudoroiu *et al.*, “An Overview of Cellulose Derivatives-Based Dressings for Wound-Healing Management,” *Pharmaceutics 2021, Vol. 14, Page 1215*, vol. 14, no. 12, p. 1215, Nov. 2021, doi: 10.3390/PH14121215.
- [34] S. Garg, A. Garg, A. Shukla, S. K. Dev, and M. Kumar, “A review on Nano-therapeutic drug delivery carriers for effective wound treatment strategies,” *Asian J Pharm Pharmacol*, vol. 4, no. 2, pp. 90–101, Apr. 2018, doi: 10.31024/AJPP.2018.4.2.1.
- [35] S. Singh, A. Young, and C. E. McNaught, “The physiology of wound healing,” *Surgery (Oxford)*, vol. 35, no. 9, pp. 473–477, Sep. 2017, doi: 10.1016/J.MPSUR.2017.06.004.
- [36] A. LaPelusa and H. D. Dave, “Physiology, Hemostasis,” *StatPearls*, May 2023, Accessed: Jun. 22, 2024. [Online]. Available: <https://www.ncbi.nlm.nih.gov/books/NBK545263/>
- [37] J. Davis and A. McLister, “Introduction to Wound Management,” *Smart Bandage Technologies*, pp. 1–35, Jan. 2016, doi: 10.1016/B978-0-12-803762-1.00001-1.
- [38] R. N. Gomes, F. Manuel, and D. S. Nascimento, “The bright side of fibroblasts: molecular signature and regenerative cues in major organs,” *NPJ Regen Med*, vol. 6, no. 1, Dec. 2021, doi: 10.1038/S41536-021-00153-Z.
- [39] E. M. Tottoli, R. Dorati, I. Genta, E. Chiesa, S. Pisani, and B. Conti, “Skin Wound Healing Process and New Emerging Technologies for Skin Wound Care and Regeneration,” *Pharmaceutics 2020, Vol. 12, Page 735*, vol. 12, no. 8, p. 735, Aug. 2020, doi: 10.3390/PHARMACEUTICS12080735.
- [40] N. Akhtari *et al.*, “Natural agents as wound-healing promoters,” *Inflammopharmacology*, vol. 32, no. 1, pp. 101–125, Feb. 2024, doi: 10.1007/S10787-023-01318-6.
- [41] Jr. Akanksha Yachmaneni, S. Jajoo, C. Mahakalkar, S. Kshirsagar, and S. Dhole, “A Comprehensive Review of the Vascular Consequences of Diabetes in the Lower Extremities: Current Approaches to Management and Evaluation of Clinical Outcomes,” *Cureus*, vol. 15, no. 10, Oct. 2023, doi: 10.7759/CUREUS.47525.

- [42] B. Cullen and A. Gefen, “The biological and physiological impact of the performance of wound dressings,” *Int Wound J*, vol. 20, no. 4, p. 1292, Apr. 2023, doi: 10.1111/IWJ.13960.
- [43] S. Guo and L. A. DiPietro, “Factors Affecting Wound Healing,” *J Dent Res*, vol. 89, no. 3, p. 219, Mar. 2010, doi: 10.1177/0022034509359125.
- [44] G. Olteanu *et al.*, “Advancements in Regenerative Hydrogels in Skin Wound Treatment: A Comprehensive Review,” *Int J Mol Sci*, vol. 25, no. 7, p. 3849, Apr. 2024, doi: 10.3390/IJMS25073849.
- [45] A. P. Serro *et al.*, “Hydrogels in Cutaneous Wound Healing: Insights into Characterization, Properties, Formulation and Therapeutic Potential,” *Gels 2024, Vol. 10, Page 188*, vol. 10, no. 3, p. 188, Mar. 2024, doi: 10.3390/GELS10030188.
- [46] E. M. Ahmed, “Hydrogel: Preparation, characterization, and applications: A review,” *J Adv Res*, vol. 6, no. 2, pp. 105–121, Mar. 2015, doi: 10.1016/J.JARE.2013.07.006.
- [47] M. Bustamante-Torres, D. Romero-Fierro, B. Arcentales-Vera, K. Palomino, H. Magaña, and E. Bucio, “Hydrogels Classification According to the Physical or Chemical Interactions and as Stimuli-Sensitive Materials,” *Gels*, vol. 7, no. 4, Dec. 2021, doi: 10.3390/GELS7040182.
- [48] O. Kapusta, A. Jarosz, K. Stadnik, D. A. Giannakoudakis, B. Barczyński, and M. Barczak, “Antimicrobial Natural Hydrogels in Biomedicine: Properties, Applications, and Challenges—A Concise Review,” *Int J Mol Sci*, vol. 24, no. 3, Feb. 2023, doi: 10.3390/IJMS24032191.
- [49] F. Fan, S. Saha, and D. Hanjaya-Putra, “Biomimetic Hydrogels to Promote Wound Healing,” *Front Bioeng Biotechnol*, vol. 9, Sep. 2021, doi: 10.3389/FBIOE.2021.718377.
- [50] B. Jia, G. Li, E. Cao, J. Luo, X. Zhao, and H. Huang, “Recent progress of antibacterial hydrogels in wound dressings,” *Mater Today Bio*, vol. 19, p. 100582, Apr. 2023, doi: 10.1016/J.MTBIO.2023.100582.
- [51] V. Gounden and M. Singh, “Hydrogels and Wound Healing: Current and Future Prospects,” *Gels*, vol. 10, no. 1, Jan. 2024, doi: 10.3390/GELS10010043.

- [52] H. M. Nguyen, T. T. Ngoc Le, A. T. Nguyen, H. N. Thien Le, and T. T. Pham, “Biomedical materials for wound dressing: recent advances and applications,” *RSC Adv*, vol. 13, no. 8, p. 5509, Feb. 2023, doi: 10.1039/D2RA07673J.
- [53] F. V. Borbolla-Jiménez *et al.*, “Films for Wound Healing Fabricated Using a Solvent Casting Technique,” *Pharmaceutics*, vol. 15, no. 7, Jul. 2023, doi: 10.3390/PHARMACEUTICS15071914.
- [54] S. Alven, S. Peter, Z. Mbese, and B. A. Aderibigbe, “Polymer-Based Wound Dressing Materials Loaded with Bioactive Agents: Potential Materials for the Treatment of Diabetic Wounds,” *Polymers (Basel)*, vol. 14, no. 4, Feb. 2022, doi: 10.3390/POLYM14040724.
- [55] S. Karki, H. Kim, S. J. Na, D. Shin, K. Jo, and J. Lee, “Thin films as an emerging platform for drug delivery,” *Asian J Pharm Sci*, vol. 11, no. 5, pp. 559–574, Oct. 2016, doi: 10.1016/J.AJPS.2016.05.004.
- [56] I. Savencu, S. Iurian, A. Porfire, C. Bogdan, and I. Tomuță, “Review of advances in polymeric wound dressing films,” *React Funct Polym*, vol. 168, p. 105059, Nov. 2021, doi: 10.1016/J.REACTFUNCTPOLYM.2021.105059.
- [57] A. Revete *et al.*, “Advancements in the Use of Hydrogels for Regenerative Medicine: Properties and Biomedical Applications,” *Int J Biomater*, vol. 2022, 2022, doi: 10.1155/2022/3606765.
- [58] W. Shu, Y. Wang, X. Zhang, C. Li, H. Le, and F. Chang, “Functional Hydrogel Dressings for Treatment of Burn Wounds,” *Front Bioeng Biotechnol*, vol. 9, Dec. 2021, doi: 10.3389/FBIOE.2021.788461.
- [59] J. Su, J. Li, J. Liang, K. Zhang, and J. Li, “Hydrogel Preparation Methods and Biomaterials for Wound Dressing,” *Life*, vol. 11, no. 10, Oct. 2021, doi: 10.3390/LIFE11101016.
- [60] A. Surowiecka, J. Strużyna, A. Winiarska, and T. Korzeniowski, “Hydrogels in Burn Wound Management—A Review,” *Gels*, vol. 8, no. 2, Feb. 2022, doi: 10.3390/GELS8020122.

- [61] A. P. Serro *et al.*, “Hydrogels in Cutaneous Wound Healing: Insights into Characterization, Properties, Formulation and Therapeutic Potential,” *Gels* 2024, Vol. 10, Page 188, vol. 10, no. 3, p. 188, Mar. 2024, doi: 10.3390/GELS10030188.
- [62] M. Ribeiro, M. Simões, C. Vitorino, and F. Mascarenhas-Melo, “Hydrogels in Cutaneous Wound Healing: Insights into Characterization, Properties, Formulation and Therapeutic Potential,” *Gels*, vol. 10, no. 3, Mar. 2024, doi: 10.3390/GELS10030188.
- [63] G. Satchanska, S. Davidova, and P. D. Petrov, “Natural and Synthetic Polymers for Biomedical and Environmental Applications,” *Polymers* 2024, Vol. 16, Page 1159, vol. 16, no. 8, p. 1159, Apr. 2024, doi: 10.3390/POLYM16081159.
- [64] A. P. Serro *et al.*, “Hydrogels in Cutaneous Wound Healing: Insights into Characterization, Properties, Formulation and Therapeutic Potential,” *Gels* 2024, Vol. 10, Page 188, vol. 10, no. 3, p. 188, Mar. 2024, doi: 10.3390/GELS10030188.
- [65] L. Jiang *et al.*, “Preparation and Characterization of Chitosan Films Containing Lychee (*Litchi chinensis* Sonn.) Pericarp Powder and Their Application as Active Food Packaging,” *Foods* 2021, Vol. 10, Page 2834, vol. 10, no. 11, p. 2834, Nov. 2021, doi: 10.3390/FOODS10112834.
- [66] K. Luo, J. Yin, O. V. Khutoryanskaya, and V. V. Khutoryanskiy, “Mucoadhesive and elastic films based on blends of chitosan and hydroxyethylcellulose,” *Macromol Biosci*, vol. 8, no. 2, pp. 184–192, Feb. 2008, doi: 10.1002/MABI.200700185.
- [67] Y. Balçık Tamer, “Development of citric acid crosslinked biodegradable chitosan/hydroxyethyl cellulose/organo-modified nanoclay composite films as sustainable food packaging materials,” *Polymer-Plastics Technology and Materials*, vol. 62, no. 9, pp. 1138–1156, Jun. 2023, doi: 10.1080/25740881.2023.2195908.
- [68] K. T. Le, C. T. Nguyen, T. D. Lac, L. G. T. Nguyen, T. L. Tran, and H. Tran-Van, “Facilely preparing carboxymethyl chitosan/hydroxyethyl cellulose hydrogel films for protective and sustained release of fibroblast growth factor 2 to accelerate dermal tissue repair,” *J Drug Deliv Sci Technol*, vol. 82, p. 104318, Apr. 2023, doi: 10.1016/J.JDDST.2023.104318.

- [69] E. Kızılkonca, E. Torlak, and F. B. Erim, "Preparation and characterization of antibacterial nano cerium oxide/chitosan/hydroxyethylcellulose/polyethylene glycol composite films," *Int J Biol Macromol*, vol. 177, pp. 351–359, Apr. 2021, doi: 10.1016/J.IJBIOMAC.2021.02.139.
- [70] A. Sharma, S. Khanna, G. Kaur, and I. Singh, "Medicinal plants and their components for wound healing applications," *Future Journal of Pharmaceutical Sciences 2021 7:1*, vol. 7, no. 1, pp. 1–13, Feb. 2021, doi: 10.1186/S43094-021-00202-W.
- [71] A. Fernandes, P. M. Rodrigues, M. Pintado, and F. K. Tavaría, "A systematic review of natural products for skin applications: Targeting inflammation, wound healing, and photo-aging," *Phytomedicine*, vol. 115, p. 154824, Jul. 2023, doi: 10.1016/J.PHYMED.2023.154824.
- [72] P. Schilrreff and U. Alexiev, "Chronic Inflammation in Non-Healing Skin Wounds and Promising Natural Bioactive Compounds Treatment," *International Journal of Molecular Sciences 2022, Vol. 23, Page 4928*, vol. 23, no. 9, p. 4928, Apr. 2022, doi: 10.3390/IJMS23094928.
- [73] I. Negut, G. Dorcioman, and V. Grumezescu, "Scaffolds for Wound Healing Applications," *Polymers (Basel)*, vol. 12, no. 9, pp. 1–19, Sep. 2020, doi: 10.3390/POLYM12092010.
- [74] A. R. Abubakar and M. Haque, "Preparation of Medicinal Plants: Basic Extraction and Fractionation Procedures for Experimental Purposes," *J Pharm Bioallied Sci*, vol. 12, no. 1, p. 1, Jan. 2020, doi: 10.4103/JPBS.JPBS_175_19.
- [75] X. Deng, M. Gould, M. Azam Ali, C. Azam Ali, and B. Sci, "A review of current advancements for wound healing: Biomaterial applications and medical devices," *J Biomed Mater Res B Appl Biomater*, vol. 110, no. 11, pp. 2542–2573, Nov. 2022, doi: 10.1002/JBM.B.35086.
- [76] S. R. M. Ibrahim *et al.*, "Garcixanthonones B and C, new xanthonones from the pericarps of *Garcinia mangostana* and their cytotoxic activity," *Phytochem Lett*, vol. 25, pp. 12–16, Jun. 2018, doi: 10.1016/J.PHYTOL.2018.03.009.

- [77] D. Rizaldy, R. Hartati, T. Nadhifa, and I. Fidrianny, "Chemical compounds and pharmacological activities of mangosteen (*Garcinia mangostana* L.)-updated review," *Biointerface Res Appl Chem*, vol. 12, no. 2, pp. 2503–2516, 2022, doi: 10.33263/BRIAC122.25032516.
- [78] V. Yuvanatemiya *et al.*, "A Review of the Influence of Various Extraction Techniques and the Biological Effects of the Xanthones from Mangosteen (*Garcinia mangostana* L.) Pericarps," *Molecules*, vol. 27, no. 24, Dec. 2022, doi: 10.3390/MOLECULES27248775.
- [79] V. Yuvanatemiya *et al.*, "A Review of the Influence of Various Extraction Techniques and the Biological Effects of the Xanthones from Mangosteen (*Garcinia mangostana* L.) Pericarps," *Molecules 2022, Vol. 27, Page 8775*, vol. 27, no. 24, p. 8775, Dec. 2022, doi: 10.3390/MOLECULES27248775.
- [80] N. Karim, M. A. Rahman, S. Changlek, and J. Tangpong, "Short-Time Administration of Xanthone From *Garcinia mangostana* Fruit Pericarp Attenuates the Hepatotoxicity and Renotoxicity of Type II Diabetes Mice," *J Am Coll Nutr*, vol. 39, no. 6, pp. 501–510, Aug. 2020, doi: 10.1080/07315724.2019.1696251.
- [81] S. Taokaew, N. Chiaoprakobkij, P. Siripong, N. Sanchavanakit, P. Pavasant, and M. Phisalaphong, "Multifunctional cellulosic nanofiber film with enhanced antimicrobial and anticancer properties by incorporation of ethanolic extract of *Garcinia mangostana* peel," *Materials Science and Engineering: C*, vol. 120, p. 111783, Jan. 2021, doi: 10.1016/J.MSEC.2020.111783.
- [82] S. Taokaew, N. Nunkaew, P. Siripong, and M. Phisalaphong, "Characteristics and anticancer properties of bacterial cellulose films containing ethanolic extract of mangosteen peel," *J Biomater Sci Polym Ed*, vol. 25, no. 9, pp. 907–922, Jun. 2014, doi: 10.1080/09205063.2014.913464.
- [83] S. Sreekumar, H. Sithul, P. Muraleedharan, J. M. Azeez, and S. Sreeharshan, "Pomegranate fruit as a rich source of biologically active compounds," *Biomed Res Int*, vol. 2014, 2014, doi: 10.1155/2014/686921.

- [84] Y. Mo *et al.*, “Pomegranate Peel as a Source of Bioactive Compounds: A Mini Review on Their Physiological Functions,” *Front Nutr*, vol. 9, p. 887113, Jun. 2022, doi: 10.3389/FNUT.2022.887113.
- [85] M. Čolić *et al.*, “Immunomodulatory Activity of Punicalagin, Punicalin, and Ellagic Acid Differs from the Effect of Pomegranate Peel Extract,” *Molecules*, vol. 27, no. 22, p. 7871, Nov. 2022, doi: 10.3390/MOLECULES27227871/S1.
- [86] P. Phimnuan, S. Yakaew, A. Yosboonruang, W. Luangbudnak, F. Grandmottet, and J. Viyoch, “Development of anti-acne film from bio-cellulose incorporating punica granatum peel extract,” *Walailak J Sci Technol*, vol. 16, no. 10, pp. 765–778, Oct. 2019, doi: 10.48048/WJST.2019.4702.
- [87] P. Gullón, G. Astray, B. Gullón, I. Tomasevic, and J. M. Lorenzo, “Pomegranate Peel as Suitable Source of High-Added Value Bioactives: Tailored Functionalized Meat Products,” *Molecules 2020, Vol. 25, Page 2859*, vol. 25, no. 12, p. 2859, Jun. 2020, doi: 10.3390/MOLECULES25122859.
- [88] M. Cedillo-Cortezano, L. R. Martinez-Cuevas, J. A. M. López, I. L. Barrera López, S. Escutia-Perez, and V. L. Petricevich, “Use of Medicinal Plants in the Process of Wound Healing: A Literature Review,” *Pharmaceuticals 2024, Vol. 17, Page 303*, vol. 17, no. 3, p. 303, Feb. 2024, doi: 10.3390/PH17030303.
- [89] M. Cedillo-Cortezano, L. R. Martinez-Cuevas, J. A. M. López, I. L. Barrera López, S. Escutia-Perez, and V. L. Petricevich, “Use of Medicinal Plants in the Process of Wound Healing: A Literature Review,” *Pharmaceuticals*, vol. 17, no. 3, Mar. 2024, doi: 10.3390/PH17030303.
- [90] W. Sun and M. H. Shahrajabian, “Therapeutic Potential of Phenolic Compounds in Medicinal Plants—Natural Health Products for Human Health,” *Molecules*, vol. 28, no. 4, Feb. 2023, doi: 10.3390/MOLECULES28041845.
- [91] S. B. Fialová, K. Rendeková, P. Mučaji, M. Nagy, and L. Slobodníková, “Antibacterial Activity of Medicinal Plants and Their Constituents in the Context of Skin and Wound Infections, Considering European Legislation and Folk Medicine—A Review,”

- International Journal of Molecular Sciences* 2021, Vol. 22, Page 10746, vol. 22, no. 19, p. 10746, Oct. 2021, doi: 10.3390/IJMS221910746.
- [92] A. Shedoeva, D. Leavesley, Z. Upton, and C. Fan, “Wound Healing and the Use of Medicinal Plants,” *Evidence-Based Complementary and Alternative Medicine*, vol. 2019, no. 1, p. 2684108, Jan. 2019, doi: 10.1155/2019/2684108.
- [93] R. S. Farag, M. S. Abdel-Latif, S. Emam, and S. Tawfeek, “Phytochemical screening and polyphenol constituents of pomegranate peels and leave juices,” 2014.
- [94] M. Niranjana, V. Vaishnav, and P. Mankar, “In-vitro analysis of antioxidant and antimicrobial properties of *Garcinia mangostana* L. (pericarp) and *Clitoria ternatea* (flower),” *The Pharma Innovation Journal*, vol. 9, no. 3, pp. 468–472, 2020, Accessed: Feb. 23, 2024. [Online]. Available: <https://www.thepharmajournal.com/archives/?year=2020&vol=9&issue=3&ArticleId=4516>
- [95] S. Kupina, C. Fields, M. C. Roman, and S. L. Brunelle, “Determination of Total Phenolic Content Using the Folin-C Assay: Single-Laboratory Validation, First Action 2017.13,” *J AOAC Int*, vol. 101, no. 5, pp. 1466–1472, Sep. 2018, doi: 10.5740/JAOACINT.18-0031.
- [96] S. Baliyan *et al.*, “Determination of Antioxidants by DPPH Radical Scavenging Activity and Quantitative Phytochemical Analysis of *Ficus religiosa*,” *Molecules*, vol. 27, no. 4, Feb. 2022, doi: 10.3390/MOLECULES27041326.
- [97] A. W. Bauer, W. M. Kirby, J. C. Sherris, and M. Turck, “Antibiotic Susceptibility Testing by a Standardized Single Disk Method,” *Am J Clin Pathol*, vol. 45, no. 4_ts, pp. 493–496, Apr. 1966, doi: 10.1093/AJCP/45.4_TS.493.
- [98] D. Stan *et al.*, “Formulation and Comprehensive Evaluation of Biohybrid Hydrogel Membranes Containing Doxycycline or Silver Nanoparticles,” *Pharmaceutics* 2023, Vol. 15, Page 2696, vol. 15, no. 12, p. 2696, Nov. 2023, doi: 10.3390/PHARMACEUTICS15122696.
- [99] H. Chopra, S. Bibi, S. Kumar, M. S. Khan, P. Kumar, and I. Singh, “Preparation and Evaluation of Chitosan/PVA Based Hydrogel Films Loaded with Honey for Wound Healing

- Application,” *Gels* 2022, Vol. 8, Page 111, vol. 8, no. 2, p. 111, Feb. 2022, doi: 10.3390/GELS8020111.
- [100] C. Ohtsuki, H. Kushitani, T. Kokubo, S. Kotani, and T. Yamamuro, “Apatite formation on the surface of ceravital-type glass-ceramic in the body,” *J Biomed Mater Res*, vol. 25, no. 11, pp. 1363–1370, Nov. 1991, doi: 10.1002/JBM.820251105.
- [101] L. C. Crowley, B. J. Marfell, and N. J. Waterhouse, “Analyzing Cell Death by Nuclear Staining with Hoechst 33342,” *Cold Spring Harb Protoc*, vol. 2016, no. 9, pp. 778–781, Sep. 2016, doi: 10.1101/PDB.PROT087205.
- [102] N. Kumar, Pratibha, A. Trajkovska Petkoska, E. Khojah, R. Sami, and A. A. M. Al-Mushhin, “Chitosan edible films enhanced with pomegranate peel extract: Study on physical, biological, thermal, and barrier properties,” *Materials*, vol. 14, no. 12, Jun. 2021, doi: 10.3390/MA14123305.
- [103] Y. Y. Qin, Z. H. Zhang, L. Li, M. L. Yuan, J. Fan, and T. R. Zhao, “Physio-mechanical properties of an active chitosan film incorporated with montmorillonite and natural antioxidants extracted from pomegranate rind,” *J Food Sci Technol*, vol. 52, no. 3, pp. 1471–1479, Mar. 2015, doi: 10.1007/S13197-013-1137-1/METRICS.
- [104] N. Cao, Y. Fu, and J. He, “Preparation and physical properties of soy protein isolate and gelatin composite films,” *Food Hydrocoll*, vol. 21, no. 7, pp. 1153–1162, Oct. 2007, doi: 10.1016/J.FOODHYD.2006.09.001.
- [105] N. Basavegowda and K. H. Baek, “Combination Strategies of Different Antimicrobials: An Efficient and Alternative Tool for Pathogen Inactivation,” *Biomedicines* 2022, Vol. 10, Page 2219, vol. 10, no. 9, p. 2219, Sep. 2022, doi: 10.3390/BIOMEDICINES10092219.
- [106] G. Albahri *et al.*, “The Therapeutic Wound Healing Bioactivities of Various Medicinal Plants,” *Life* 2023, Vol. 13, Page 317, vol. 13, no. 2, p. 317, Jan. 2023, doi: 10.3390/LIFE13020317.
- [107] S. Sriwidodo, R. Pratama, A. K. Umar, A. Y. Chaerunisa, A. T. Ambarwati, and N. Wathoni, “Preparation of Mangosteen Peel Extract Microcapsules by Fluidized Bed Spray-

- Drying for Tableting: Improving the Solubility and Antioxidant Stability,” *Antioxidants*, vol. 11, no. 7, Jul. 2022, doi: 10.3390/ANTIOX11071331.
- [108] G. Náthia-Neves, A. G. Tarone, M. M. Tosi, M. R. Maróstica Júnior, and M. A. A. Meireles, “Extraction of bioactive compounds from genipap (*Genipa americana* L.) by pressurized ethanol: Iridoids, phenolic content and antioxidant activity,” *Food Research International*, vol. 102, pp. 595–604, Dec. 2017, doi: 10.1016/J.FOODRES.2017.09.041.
- [109] N. Hasona, M. Ahmed, T. Alghassab, M. Alghassab, and A. Alghabban, “Antihyperlipidemic effect of pomegranate peel and Iranian fenugreek extracts on cholesterol-rich diet-induced hypercholesterolemia in guinea pigs,” *Merit Research Journal of Medicine and Medical Sciences*, vol. 4, pp. 196–203, Jan. 2016.
- [110] S. A. El-Sherbeni and W. A. Negm, “The wound healing effect of botanicals and pure natural substances used in in vivo models,” *Inflammopharmacology*, vol. 31, no. 2, pp. 755–772, Apr. 2023, doi: 10.1007/S10787-023-01157-5/METRICS.
- [111] E. P. Tejamukti, W. Setyaningsih, Irnawati, B. Yasir, G. Alam, and A. Rohman, “Application of FTIR Spectroscopy and HPLC Combined with Multivariate Calibration for Analysis of Xanthones in Mangosteen Extracts,” *Scientia Pharmaceutica 2020*, Vol. 88, Page 35, vol. 88, no. 3, p. 35, Aug. 2020, doi: 10.3390/SCIPHARM88030035.
- [112] “Analysis of Curcumin in *Curcuma longa* and *Curcuma xanthorrhiza* Using FTIR Spectroscopy and Chemometrics.” Accessed: Apr. 05, 2024. [Online]. Available: <https://scialert.net/abstract/?doi=rjmp.2015.179.186>
- [113] W. Feng, Z. Hao, M. Li, W. Feng, Z. Hao, and M. Li, “Isolation and Structure Identification of Flavonoids,” *Flavonoids - From Biosynthesis to Human Health*, Aug. 2017, doi: 10.5772/67810.
- [114] L. Yu, M. Zhao, B. Yang, Q. Zhao, and Y. Jiang, “Phenolics from hull of *Garcinia mangostana* fruit and their antioxidant activities,” *Food Chem*, vol. 104, no. 1, pp. 176–181, Jan. 2007, doi: 10.1016/J.FOODCHEM.2006.11.018.
- [115] M. Muchtaridi, N. A. Puteri, T. Milanda, and I. Musfiroh, “Validation Analysis Methods of α -Mangostin, γ -Mangostin and Gartanin Mixture in Mangosteen (*Garcinia mangostana* L.)

- Fruit Rind Extract from West Java with HPLC,” *J Appl Pharm Sci*, vol. 7, no. 10, pp. 125–130, Oct. 2017, doi: 10.7324/JAPS.2017.71018.
- [116] Abdalrahim F. A. Aisha, “Quantification of α -, β - and γ -mangostin in *Garcinia mangostana* fruit rind extracts by a reverse phase high performance liquid chromatography,” *Journal of Medicinal Plants Research*, vol. 6, no. 29, Aug. 2012, doi: 10.5897/JMPR11.1253.
- [117] M. Ahmad, B. M. Yamin, and A. Mat Lazim, “A study on dispersion and characterisation of α -mangostin loaded pH sensitive microgel systems,” *Chem Cent J*, vol. 7, no. 1, pp. 1–6, May 2013, doi: 10.1186/1752-153X-7-85/FIGURES/4.
- [118] F. E. Z. Amrati *et al.*, “Phenolic Composition, Wound Healing, Antinociceptive, and Anticancer Effects of *Caralluma europaea* Extracts,” *Molecules* 2023, Vol. 28, Page 1780, vol. 28, no. 4, p. 1780, Feb. 2023, doi: 10.3390/MOLECULES28041780.
- [119] I. Mssillou *et al.*, “Investigation on wound healing effect of Mediterranean medicinal plants and some related phenolic compounds: A review,” *J Ethnopharmacol*, vol. 298, p. 115663, Nov. 2022, doi: 10.1016/J.JEP.2022.115663.
- [120] F. Kabir, W. W. Tow, Y. Hamauzu, S. Katayama, S. Tanaka, and S. Nakamura, “Antioxidant and cytoprotective activities of extracts prepared from fruit and vegetable wastes and by-products,” *Food Chem*, vol. 167, pp. 358–362, 2015, doi: <https://doi.org/10.1016/j.foodchem.2014.06.099>.
- [121] J. Singh *et al.*, “Pomegranate Peel Phytochemistry, Pharmacological Properties, Methods of Extraction, and Its Application: A Comprehensive Review,” *ACS Omega*, vol. 8, no. 39, pp. 35452–35469, Oct. 2023, doi: 10.1021/ACSOMEGA.3C02586/ASSET/IMAGES/LARGE/AO3C02586_0003.JPEG.
- [122] F. Marra, B. Petrovicova, F. Canino, A. Maffia, C. Mallamaci, and A. Muscolo, “Pomegranate Wastes Are Rich in Bioactive Compounds with Potential Benefit on Human Health,” *Molecules*, vol. 27, no. 17, Sep. 2022, doi: 10.3390/MOLECULES27175555.
- [123] O. D. John, P. Mouatt, S. K. Panchal, and L. Brown, “Rind from Purple Mangosteen (*Garcinia mangostana*) Attenuates Diet-Induced Physiological and Metabolic Changes in Obese Rats,” *Nutrients*, vol. 13, no. 2, pp. 1–19, Feb. 2021, doi: 10.3390/NU13020319.

- [124] Z. Derakhshan *et al.*, “Antioxidant activity and total phenolic content of ethanolic extract of pomegranate peels, juice and seeds,” *Food and Chemical Toxicology*, vol. 114, pp. 108–111, Apr. 2018, doi: 10.1016/J.FCT.2018.02.023.
- [125] K. Udaya Sankar, A. Sulaiman Zarena, and K. Udaya Sankar, “A study of antioxidant properties from *Garcinia mangostana* L. pericarp extract,” *Acta Sci Pol Technol Aliment*, vol. 8, no. 1, pp. 23–34, Mar. 2009, Accessed: Mar. 22, 2024. [Online]. Available: www.food.actapol.net
- [126] Y. Dong and Z. Wang, “ROS-scavenging materials for skin wound healing: advancements and applications,” *Front Bioeng Biotechnol*, vol. 11, p. 1304835, Dec. 2023, doi: 10.3389/FBIOE.2023.1304835/BIBTEX.
- [127] G. Wang, F. Yang, W. Zhou, N. Xiao, M. Luo, and Z. Tang, “The initiation of oxidative stress and therapeutic strategies in wound healing,” *Biomedicine & Pharmacotherapy*, vol. 157, p. 114004, Jan. 2023, doi: 10.1016/J.BIOPHA.2022.114004.
- [128] C. Dunnill *et al.*, “Reactive oxygen species (ROS) and wound healing: the functional role of ROS and emerging ROS-modulating technologies for augmentation of the healing process,” *Int Wound J*, vol. 14, no. 1, pp. 89–96, Feb. 2017, doi: 10.1111/IWJ.12557.
- [129] L. Melguizo-rodríguez, E. de Luna-Bertos, J. Ramos-torrecillas, R. Illescas-montesa, V. J. Costela-ruiz, and O. García-martínez, “Potential Effects of Phenolic Compounds That Can Be Found in Olive Oil on Wound Healing,” *Foods*, vol. 10, no. 7, Jul. 2021, doi: 10.3390/FOODS10071642.
- [130] K. Kaltalioglu, B. Balabanli, and S. Coskun-Cevher, “Phenolic, Antioxidant, Antimicrobial, and In-vivo Wound Healing Properties of *Potentilla erecta* L. Root Extract in Diabetic Rats,” *Iran J Pharm Res*, vol. 19, no. 4, p. 264, Sep. 2020, doi: 10.22037/IJPR.2019.112411.13742.
- [131] I. Guimarães, S. Baptista-Silva, M. Pintado, and A. L. Oliveira, “Polyphenols: A Promising Avenue in Therapeutic Solutions for Wound Care,” *Applied Sciences 2021, Vol. 11, Page 1230*, vol. 11, no. 3, p. 1230, Jan. 2021, doi: 10.3390/APP11031230.

- [132] M. Działo, J. Mierziak, U. Korzun, M. Preisner, J. Szopa, and A. Kulma, “The potential of plant phenolics in prevention and therapy of skin disorders,” *Int J Mol Sci*, vol. 17, no. 2, Feb. 2016, doi: 10.3390/IJMS17020160.
- [133] N. I. M. Fadilah *et al.*, “Antioxidant Biomaterials in Cutaneous Wound Healing and Tissue Regeneration: A Critical Review,” *Antioxidants 2023, Vol. 12, Page 787*, vol. 12, no. 4, p. 787, Mar. 2023, doi: 10.3390/ANTIOX12040787.
- [134] P. Kowalczyk *et al.*, “Mitochondrial Oxidative Stress—A Causative Factor and Therapeutic Target in Many Diseases,” *Int J Mol Sci*, vol. 22, no. 24, p. 22, Dec. 2021, doi: 10.3390/IJMS222413384.
- [135] A. Görlach, “Redox regulation of the coagulation cascade,” *Antioxid Redox Signal*, vol. 7, no. 9–10, pp. 1398–1404, Sep. 2005, doi: 10.1089/ARS.2005.7.1398.
- [136] D. André-Lévigne, A. Modarressi, M. S. Pepper, and B. Pittet-Cuénod, “Reactive Oxygen Species and NOX Enzymes Are Emerging as Key Players in Cutaneous Wound Repair,” *Int J Mol Sci*, vol. 18, no. 10, Oct. 2017, doi: 10.3390/IJMS18102149.
- [137] S. Tjahjani, W. Widowati, K. Khiong, A. Suhendra, and R. Tjokropranoto, “Antioxidant Properties of Garcinia Mangostana L (Mangosteen) Rind,” *Procedia Chem*, vol. 13, pp. 198–203, 2014, doi: 10.1016/J.PROCHE.2014.12.027.
- [138] S. I. Ihsanpuro, S. Gunawan, R. Ibrahim, and H. W. Aparamarta, “Extract with high 1,1-diphenyl-2-picrylhydrazyl (DPPH) inhibitory capability from pericarp and seed of mangosteen (*Garcinia mangostana* L.) using microwave-assisted extraction (MAE) two-phase solvent technique,” *Arabian Journal of Chemistry*, vol. 15, no. 12, p. 104310, Dec. 2022, doi: 10.1016/J.ARABJC.2022.104310.
- [139] S. M. A. El-Hamamsy and H. A. Z. El-khamissi, “Phytochemicals, Antioxidant Activity and Identification of Phenolic Compounds by HPLC of Pomegranate (*Punica granatum* L.) Peel Extracts,” *Journal of Agricultural Chemistry and Biotechnology*, vol. 11, no. 4, pp. 79–84, Apr. 2020, doi: 10.21608/JACB.2020.95837.

- [140] N. I. M. Fadilah *et al.*, “Antioxidant Biomaterials in Cutaneous Wound Healing and Tissue Regeneration: A Critical Review,” *Antioxidants* 2023, Vol. 12, Page 787, vol. 12, no. 4, p. 787, Mar. 2023, doi: 10.3390/ANTIOX12040787.
- [141] D. Yang, H. Chen, H. Wei, A. Liu, D. X. Wei, and J. Chen, “Hydrogel wound dressings containing bioactive compounds originated from traditional Chinese herbs: A review,” *Smart Mater Med*, vol. 5, no. 1, pp. 153–165, Mar. 2024, doi: 10.1016/J.SMAIM.2023.10.004.
- [142] A. Ghani, E. N. Zare, P. Makvandi, and N. Rabiee, “Antioxidant, antibacterial and biodegradable hydrogel films from carboxymethyl tragacanth gum and clove extract: Potential for wound dressings application,” *Carbohydrate Polymer Technologies and Applications*, vol. 7, p. 100428, Jun. 2024, doi: 10.1016/J.CARPTA.2024.100428.
- [143] A. I. Lopes, M. M. Pintado, and F. K. Tavarina, “Plant-Based Films and Hydrogels for Wound Healing,” *Microorganisms* 2024, Vol. 12, Page 438, vol. 12, no. 3, p. 438, Feb. 2024, doi: 10.3390/MICROORGANISMS12030438.
- [144] I. Negut, V. Grumezescu, and A. M. Grumezescu, “Treatment Strategies for Infected Wounds,” *Molecules : A Journal of Synthetic Chemistry and Natural Product Chemistry*, vol. 23, no. 9, Sep. 2018, doi: 10.3390/MOLECULES23092392.
- [145] T. Chaiwarit *et al.*, “Extraction of Tropical Fruit Peels and Development of HPMC Film Containing the Extracts as an Active Antibacterial Packaging Material,” *Molecules*, vol. 26, no. 8, Apr. 2021, doi: 10.3390/MOLECULES26082265.
- [146] A. W. Indrianingsih, V. T. Rosyida, C. Darsih, and W. Apriyana, “Antibacterial activity of *Garcinia mangostana* peel-dyed cotton fabrics using synthetic and natural mordants,” *Sustain Chem Pharm*, vol. 21, p. 100440, Jun. 2021, doi: 10.1016/J.SCP.2021.100440.
- [147] R. H. S. Sitti, P. Sugita, L. Ambarsari, and D. U. C. Rahayu, “Antibacterial Mangosteen (*Garcinia mangostana* Linn.) peel extract encapsulated in Chitosan,” *J Phys Conf Ser*, vol. 1116, no. 4, p. 042037, Dec. 2018, doi: 10.1088/1742-6596/1116/4/042037.

- [148] M. S. Mahmood *et al.*, “Portrayal of *Punica granatum* L. peel extract through High Performance Liquid Chromatography and antimicrobial activity evaluation,” *Brazilian Journal of Biology*, vol. 83, p. e244435, Aug. 2021, doi: 10.1590/1519-6984.244435.
- [149] W. Sajjad *et al.*, “Antibacterial activity of Punica granatum peel extract,” *Mycopath*, vol. 13, pp. 105–111, Dec. 2015.
- [150] T. N. Banu, “Antibacterial Activity of Pomegranate (*Punica granatum*) Fruit Peel Extracts Against Antibiotic Resistant Gram- Negative Pathogenic Bacteria,” *Biosci Biotechnol Res Commun*, vol. 12, no. 4, pp. 1141–1149, Dec. 2019, doi: 10.21786/BBRC/12.4/38.
- [151] U. A. Fischer, R. Carle, and D. R. Kammerer, “Identification and quantification of phenolic compounds from pomegranate (*Punica granatum* L.) peel, mesocarp, aril and differently produced juices by HPLC-DAD-ESI/MS(n),” *Food Chem*, vol. 127, no. 2, pp. 807–821, Jul. 2011, doi: 10.1016/J.FOODCHEM.2010.12.156.
- [152] R. N. BENNETT and R. M. WALLSGROVE, “Secondary metabolites in plant defence mechanisms,” *New Phytol*, vol. 127, no. 4, pp. 617–633, 1994, doi: 10.1111/J.1469-8137.1994.TB02968.X.
- [153] M. Takó *et al.*, “Plant Phenolics and Phenolic-Enriched Extracts as Antimicrobial Agents against Food-Contaminating Microorganisms,” *Antioxidants 2020, Vol. 9, Page 165*, vol. 9, no. 2, p. 165, Feb. 2020, doi: 10.3390/ANTIOX9020165.
- [154] W. Wisuitiprot, S. Wisutthathum, S. Pitiporn, V. Wisuitiprot, P. Kwankhao, and N. Waranuch, “Short Communication Effect of *Garcinia Mangostana* Linn Fruit Peel Ethanolic Extract on Fibroblast Cell Migration,” *J Sci Ind Res (India)*, vol. 19, pp. 14394–14397, Jul. 2019, doi: 10.26717/BJSTR.2019.19.003317.
- [155] M. Siriwattanasatorn, A. Itharat, P. Thongdeeying, and B. Ooraikul, “In Vitro Wound Healing Activities of Three Most Commonly Used Thai Medicinal Plants and Their Three Markers,” *Evid Based Complement Alternat Med*, vol. 2020, 2020, doi: 10.1155/2020/6795383.
- [156] P. A. C. Wulandari *et al.*, “Wound Healing and Antioxidant Evaluations of Alginate from *Sargassum ilicifolium* and Mangosteen Rind Combination Extracts on Diabetic Mice

- Model,” *Applied Sciences* 2021, Vol. 11, Page 4651, vol. 11, no. 10, p. 4651, May 2021, doi: 10.3390/APP11104651.
- [157] N. Tatiya-aphiradee, W. Chatuphonprasert, and K. Jarukamjorn, “Anti-inflammatory effect of *Garcinia mangostana* Linn. pericarp extract in methicillin-resistant *Staphylococcus aureus*-induced superficial skin infection in mice,” *Biomedicine & Pharmacotherapy*, vol. 111, pp. 705–713, Mar. 2019, doi: 10.1016/J.BIOPHA.2018.12.142.
- [158] H. Chen *et al.*, “Enhanced chondrogenic differentiation of human mesenchymal stems cells on citric acid-modified chitosan hydrogel for tracheal cartilage regeneration applications,” *RSC Adv*, vol. 8, no. 30, pp. 16910–16917, May 2018, doi: 10.1039/C8RA00808F.
- [159] S. Lv, J. Liu, Q. Zhou, L. Huang, and T. Sun, “Synthesis of modified chitosan superplasticizer by amidation and sulfonation and its application performance and working mechanism,” *Ind Eng Chem Res*, vol. 53, no. 10, pp. 3908–3916, Mar. 2014, doi: 10.1021/IE403786Q/ASSET/IMAGES/MEDIUM/IE-2013-03786Q_0007.GIF.
- [160] A. P. Serro *et al.*, “Hydrogels in Cutaneous Wound Healing: Insights into Characterization, Properties, Formulation and Therapeutic Potential,” *Gels* 2024, Vol. 10, Page 188, vol. 10, no. 3, p. 188, Mar. 2024, doi: 10.3390/GELS10030188.
- [161] S. Maiti, B. Maji, and H. Yadav, “Progress on green crosslinking of polysaccharide hydrogels for drug delivery and tissue engineering applications,” *Carbohydr Polym*, vol. 326, p. 121584, Feb. 2024, doi: 10.1016/J.CARBPOL.2023.121584.
- [162] Z. Eslami, S. Elkoun, M. Robert, and K. Adjallé, “A Review of the Effect of Plasticizers on the Physical and Mechanical Properties of Alginate-Based Films,” *Molecules* 2023, Vol. 28, Page 6637, vol. 28, no. 18, p. 6637, Sep. 2023, doi: 10.3390/MOLECULES28186637.
- [163] J. Su, J. Li, J. Liang, K. Zhang, and J. Li, “Hydrogel Preparation Methods and Biomaterials for Wound Dressing,” *Life*, vol. 11, no. 10, Oct. 2021, doi: 10.3390/LIFE11101016.
- [164] S. Saghadzadeh *et al.*, “Drug Delivery Systems and Materials for Wound Healing Applications,” *Adv Drug Deliv Rev*, vol. 127, p. 138, Mar. 2018, doi: 10.1016/J.ADDR.2018.04.008.

- [165] Y. Liu *et al.*, “Preparation and characterization of chitosan films with three kinds of molecular weight for food packaging,” *Int J Biol Macromol*, vol. 155, pp. 249–259, Jul. 2020, doi: 10.1016/J.IJBIOMAC.2020.03.217.
- [166] A. Sood, M. S. Granick, and N. L. Tomaselli, “Wound Dressings and Comparative Effectiveness Data,” *Adv Wound Care (New Rochelle)*, vol. 3, no. 8, p. 511, Aug. 2014, doi: 10.1089/WOUND.2012.0401.
- [167] K. C. Broussard and J. G. Powers, “Wound dressings: Selecting the most appropriate type,” *Am J Clin Dermatol*, vol. 14, no. 6, pp. 449–459, Dec. 2013, doi: 10.1007/S40257-013-0046-4.
- [168] M. Bustamante-Torres, D. Romero-Fierro, B. Arcentales-Vera, K. Palomino, H. Magaña, and E. Bucio, “Hydrogels Classification According to the Physical or Chemical Interactions and as Stimuli-Sensitive Materials,” *Gels*, vol. 7, no. 4, Dec. 2021, doi: 10.3390/GELS7040182.
- [169] L. Kaewsichan, D. Riyapan, P. Prommajan, and J. Kaewsrichan, “Effects of sintering temperatures on micro-morphology, mechanical properties, and bioactivity of bone scaffolds containing calcium silicate,” *ScienceAsia*, vol. 37, no. 3, pp. 240–246, 2011, doi: 10.2306/SCIENCEASIA1513-1874.2011.37.240.
- [170] V. T. Hoang *et al.*, “Optical Properties of Buffers and Cell Culture Media for Optofluidic and Sensing Applications,” *Applied Sciences 2019, Vol. 9, Page 1145*, vol. 9, no. 6, p. 1145, Mar. 2019, doi: 10.3390/APP9061145.
- [171] F. Hegaard, R. Biro, K. Ehtiati, and E. Thormann, “Ion-Specific Antipolyelectrolyte Effect on the Swelling Behavior of Polyzwitterionic Layers,” *Langmuir*, vol. 39, no. 4, pp. 1456–1464, Jan. 2023, doi: 10.1021/ACS.LANGMUIR.2C02798/SUPPL_FILE/LA2C02798_SI_001.PDF.
- [172] J. Kim and C. M. Lee, “Wound healing potential of a polyvinyl alcohol-blended pectin hydrogel containing *Hippophae rhamnoides* L. extract in a rat model,” *Int J Biol Macromol*, vol. 99, pp. 586–593, Jun. 2017, doi: 10.1016/J.IJBIOMAC.2017.03.014.

- [173] F. Baino and S. Yamaguchi, “The Use of Simulated Body Fluid (SBF) for Assessing Materials Bioactivity in the Context of Tissue Engineering: Review and Challenges,” *Biomimetics*, vol. 5, no. 4, pp. 1–19, Dec. 2020, doi: 10.3390/BIOMIMETICS5040057.
- [174] L. Su, Y. Jia, L. Fu, K. Guo, and S. Xie, “The emerging progress on wound dressings and their application in clinic wound management,” *Heliyon*, vol. 9, no. 12, p. e22520, Dec. 2023, doi: 10.1016/J.HELIYON.2023.E22520.
- [175] W. Feng and Z. Wang, “Tailoring the Swelling-Shrinkable Behavior of Hydrogels for Biomedical Applications,” *Advanced Science*, vol. 10, no. 28, p. 2303326, Oct. 2023, doi: 10.1002/ADVS.202303326.
- [176] J. Chen, B. L. B. Nichols, A. M. Norris, C. E. Frazier, and K. J. Edgar, “All-Polysaccharide, Self-Healing Injectable Hydrogels Based on Chitosan and Oxidized Hydroxypropyl Polysaccharides,” *Biomacromolecules*, vol. 21, no. 10, pp. 4261–4272, Oct. 2020, doi: 10.1021/ACS.BIOMAC.0C01046.
- [177] M. Xu *et al.*, “Swelling-Induced Information Camouflage and Optical Decryption on a Transparent Recoverable Hydrogel Surface,” *ACS Appl Mater Interfaces*, vol. 14, no. 2, pp. 3591–3600, Jan. 2022, doi: 10.1021/ACSAMI.1C22745/SUPPL_FILE/AM1C22745_SI_007.MP4.
- [178] Y. Liang *et al.*, “Adhesive Hemostatic Conducting Injectable Composite Hydrogels with Sustained Drug Release and Photothermal Antibacterial Activity to Promote Full-Thickness Skin Regeneration During Wound Healing,” *Small*, vol. 15, no. 12, p. 1900046, Mar. 2019, doi: 10.1002/SMLL.201900046.
- [179] S. Yuan, Y. Han, D. Xiang, B. Wang, Y. Chen, and Y. Hao, “An injectable hydroxypropyl- β -cyclodextrin cross-linked gelatin-based hydrogel loaded bone mesenchymal stem cell for osteogenic and in vivo bone regeneration of femoral head necrosis,” *Nanomedicine*, vol. 41, p. 102521, Apr. 2022, doi: 10.1016/J.NANO.2022.102521.
- [180] I. Ali *et al.*, “Reduction-responsive and bioorthogonal carboxymethyl cellulose based soft hydrogels cross-linked via IEDDA click chemistry for cancer therapy application,” *Int J Biol Macromol*, vol. 219, pp. 109–120, Oct. 2022, doi: 10.1016/J.IJBIOMAC.2022.07.229.

- [181] F. Li *et al.*, “Bioinspired nonswellable ultrastrong nanocomposite hydrogels with long-term underwater superoleophobic behavior,” *Chemical Engineering Journal*, vol. 375, p. 122047, Nov. 2019, doi: 10.1016/J.CEJ.2019.122047.
- [182] V. Delplace, P. E. B. Nickerson, A. Ortin-Martinez, A. E. G. Baker, V. A. Wallace, and M. S. Shoichet, “Nonswelling, Ultralow Content Inverse Electron-Demand Diels–Alder Hyaluronan Hydrogels with Tunable Gelation Time: Synthesis and In Vitro Evaluation,” *Adv Funct Mater*, vol. 30, no. 14, p. 1903978, Apr. 2020, doi: 10.1002/ADFM.201903978.
- [183] L. Xu, S. Gao, Q. Guo, C. Wang, Y. Qiao, and D. Qiu, “A Solvent-Exchange Strategy to Regulate Noncovalent Interactions for Strong and Antiswelling Hydrogels,” *Adv Mater*, vol. 32, no. 52, Dec. 2020, doi: 10.1002/ADMA.202004579.
- [184] G. Gao, X. Liu, and Q. Zhang, “Solvent-Resistant and Nonswellable Hydrogel Conductor toward Mechanical Perception in Diverse Liquid Media,” *ACS Nano*, vol. 14, no. 10, pp. 13709–13717, Oct. 2020, doi: 10.1021/ACSNANO.0C05932.
- [185] J. Liu *et al.*, “Ionic Conductive Organohydrogels with Dynamic Pattern Behavior and Multi-Environmental Stability,” *Adv Funct Mater*, vol. 31, no. 24, p. 2101464, Jun. 2021, doi: 10.1002/ADFM.202101464.
- [186] X. Wan, L. Jia, X. Liu, B. Dai, L. Jiang, and S. Wang, “WET-Induced Layered Organohydrogel as Bioinspired ‘Sticky-Slippery Skin’ for Robust Underwater Oil-Repellency,” *Adv Mater*, vol. 34, no. 16, Apr. 2022, doi: 10.1002/ADMA.202110408.
- [187] S. Bian *et al.*, “An Injectable Rapid-Adhesion and Anti-Swelling Adhesive Hydrogel for Hemostasis and Wound Sealing,” *Adv Funct Mater*, vol. 32, no. 46, p. 2207741, Nov. 2022, doi: 10.1002/ADFM.202207741.
- [188] H. M. Nguyen, T. T. Ngoc Le, A. T. Nguyen, H. N. Thien Le, and T. T. Pham, “Biomedical materials for wound dressing: recent advances and applications,” *RSC Adv*, vol. 13, no. 8, p. 5509, Feb. 2023, doi: 10.1039/D2RA07673J.
- [189] S. Guzman-Puyol, J. J. Benítez, and J. A. Heredia-Guerrero, “Transparency of polymeric food packaging materials,” *Food Research International*, vol. 161, p. 111792, Nov. 2022, doi: 10.1016/J.FOODRES.2022.111792.

- [190] Z. Emam-Djomeh, A. Moghaddam, and S. A. Yasini Ardakani, “Antimicrobial Activity of Pomegranate (*Punica granatum* L.) Peel Extract, Physical, Mechanical, Barrier and Antimicrobial Properties of Pomegranate Peel Extract-incorporated Sodium Caseinate Film and Application in Packaging for Ground Beef,” *Packaging Technology and Science*, vol. 28, no. 10, pp. 869–881, Oct. 2015, doi: 10.1002/PTS.2145.
- [191] J. Gómez-Estaca, P. Montero, F. Fernández-Martín, A. Alemán, and M. C. Gómez-Guillén, “Physical and chemical properties of tuna-skin and bovine-hide gelatin films with added aqueous oregano and rosemary extracts,” *Food Hydrocoll*, vol. 23, no. 5, pp. 1334–1341, Jul. 2009, doi: 10.1016/J.FOODHYD.2008.09.013.
- [192] N. Kumar, Pratibha, A. Trajkovska Petkoska, E. Khojah, R. Sami, and A. A. M. Al-Mushhin, “Chitosan Edible Films Enhanced with Pomegranate Peel Extract: Study on Physical, Biological, Thermal, and Barrier Properties,” *Materials*, vol. 14, no. 12, Jun. 2021, doi: 10.3390/MA14123305.
- [193] M. Rawooh *et al.*, “Effect of Tamarind Gum on the Properties of Phase-Separated Poly(vinyl alcohol) Films,” *Polymers 2022, Vol. 14, Page 2793*, vol. 14, no. 14, p. 2793, Jul. 2022, doi: 10.3390/POLYM14142793.
- [194] M. Kuddushi, A. A. Shah, C. Ayranci, and X. Zhang, “Recent advances in novel materials and techniques for developing transparent wound dressings,” *J Mater Chem B*, vol. 11, no. 27, pp. 6201–6224, Jul. 2023, doi: 10.1039/D3TB00639E.
- [195] M. Kuddushi, A. A. Shah, C. Ayranci, and X. Zhang, “Recent advances in novel materials and techniques for developing transparent wound dressings,” *J Mater Chem B*, vol. 11, no. 27, pp. 6201–6224, May 2023, doi: 10.1039/D3TB00639E.
- [196] K. Luo, J. Yin, O. V. Khutoryanskaya, and V. V. Khutoryanskiy, “Mucoadhesive and elastic films based on blends of chitosan and hydroxyethylcellulose,” *Macromol Biosci*, vol. 8, no. 2, pp. 184–192, Feb. 2008, doi: 10.1002/MABI.200700185.
- [197] J. Yin, K. Luo, X. Chen, and V. V. Khutoryanskiy, “Miscibility studies of the blends of chitosan with some cellulose ethers,” *Carbohydr Polym*, vol. 63, no. 2, pp. 238–244, Feb. 2006, doi: 10.1016/J.CARBPOL.2005.08.041.

- [198] M. Kaya *et al.*, “Antioxidative and antimicrobial edible chitosan films blended with stem, leaf and seed extracts of *Pistacia terebinthus* for active food packaging,” *RSC Adv*, vol. 8, no. 8, pp. 3941–3950, Jan. 2018, doi: 10.1039/C7RA12070B.
- [199] J. Zawadzki and H. Kaczmarek, “Thermal treatment of chitosan in various conditions,” *Carbohydr Polym*, vol. 80, no. 2, pp. 394–400, Apr. 2010, doi: 10.1016/J.CARBPOL.2009.11.037.
- [200] M. Kaya *et al.*, “Antioxidative and antimicrobial edible chitosan films blended with stem, leaf and seed extracts of *Pistacia terebinthus* for active food packaging,” *RSC Adv*, vol. 8, no. 8, pp. 3941–3950, Jan. 2018, doi: 10.1039/C7RA12070B.
- [201] J. Zawadzki and H. Kaczmarek, “Thermal treatment of chitosan in various conditions,” *Carbohydr Polym*, vol. 80, no. 2, pp. 394–400, Apr. 2010, doi: 10.1016/J.CARBPOL.2009.11.037.
- [202] P. Kanmani and J. W. Rhim, “Development and characterization of carrageenan/grapefruit seed extract composite films for active packaging,” *Int J Biol Macromol*, vol. 68, pp. 258–266, 2014, doi: 10.1016/J.IJBIOMAC.2014.05.011.
- [203] F. M. Pelissari, M. V. E. Grossmann, F. Yamashita, and E. A. G. Pined, “Antimicrobial, mechanical, and barrier properties of cassava starch-chitosan films incorporated with oregano essential oil,” *J Agric Food Chem*, vol. 57, no. 16, pp. 7499–7504, 2009, doi: 10.1021/JF9002363.
- [204] X. Zhang, J. Liu, H. Yong, Y. Qin, J. Liu, and C. Jin, “Development of antioxidant and antimicrobial packaging films based on chitosan and mangosteen (*Garcinia mangostana* L.) rind powder,” *Int J Biol Macromol*, vol. 145, pp. 1129–1139, Feb. 2020, doi: 10.1016/J.IJBIOMAC.2019.10.038.
- [205] S. Taokaew, N. Chiaoprakobkij, P. Siripong, N. Sanchavanakit, P. Pavasant, and M. Phisalaphong, “Multifunctional cellulosic nanofiber film with enhanced antimicrobial and anticancer properties by incorporation of ethanolic extract of *Garcinia mangostana* peel,” *Materials Science and Engineering: C*, vol. 120, p. 111783, Jan. 2021, doi: 10.1016/J.MSEC.2020.111783.

- [206] N. Charernsriwilaiwat, T. Rojanarata, T. Ngawhirunpat, M. Sukma, and P. Opanasopit, “Electrospun chitosan-based nanofiber mats loaded with *Garcinia mangostana* extracts,” *Int J Pharm*, vol. 452, no. 1–2, pp. 333–343, Aug. 2013, doi: 10.1016/J.IJPHARM.2013.05.012.
- [207] E. Drápalová *et al.*, “Antimicrobial Cost-Effective Transparent Hydrogel Films from Renewable Gum Karaya/Chitosan Polysaccharides for Modern Wound Dressings,” *ACS Appl Polym Mater*, vol. 5, no. 4, pp. 2774–2786, Apr. 2023, doi: 10.1021/ACSAPM.3C00025/ASSET/IMAGES/LARGE/AP3C00025_0011.JPEG.
- [208] N. Kumar, Pratibha, A. Trajkovska Petkoska, E. Khojah, R. Sami, and A. A. M. Al-Mushhin, “Chitosan Edible Films Enhanced with Pomegranate Peel Extract: Study on Physical, Biological, Thermal, and Barrier Properties,” *Materials*, vol. 14, no. 12, Jun. 2021, doi: 10.3390/MA14123305.
- [209] R. Eldib, “Application of Nano-coating and Chitosan Combination Films on Cantaloupe Preservation,” *Pak J Biol Sci*, vol. 23, no. 8, pp. 1037–1043, 2020, doi: 10.3923/PJBS.2020.1037.1043.
- [210] C. Wu *et al.*, “Structural properties of films and rheology of film-forming solutions of chitosan gallate for food packaging,” *Carbohydr Polym*, vol. 146, pp. 10–19, Aug. 2016, doi: 10.1016/J.CARBPOL.2016.03.027.
- [211] R. E. A. Nascimento, J. Monte, M. Cadima, V. D. Alves, and L. A. Neves, “Rendering banana plant residues into a potentially commercial byproduct by doping cellulose films with phenolic compounds,” *Polymers (Basel)*, vol. 13, no. 5, pp. 1–15, Mar. 2021, doi: 10.3390/POLYM13050843.
- [212] H. A. S. Tohamy, M. El-Sakhawy, H. M. El-Masry, I. A. Saleh, and M. M. AbdelMohsen, “Preparation of hydroxyethyl cellulose/ mangiferin edible films and their antimicrobial properties,” *BMC Chem*, vol. 16, no. 1, pp. 1–7, Dec. 2022, doi: 10.1186/S13065-022-00907-W/FIGURES/4.

- [213] H. Levine and L. Slade, “Water as a plasticizer: physico-chemical aspects of low-moisture polymeric systems,” *Water Science Reviews* 3, pp. 79–185, Feb. 2010, doi: 10.1017/CBO9780511552083.002.
- [214] Z. Eslami, S. Elkoun, M. Robert, and K. Adjallé, “A Review of the Effect of Plasticizers on the Physical and Mechanical Properties of Alginate-Based Films,” *Molecules* 2023, Vol. 28, Page 6637, vol. 28, no. 18, p. 6637, Sep. 2023, doi: 10.3390/MOLECULES28186637.
- [215] T. Wu, R. Farnood, K. O’Kelly, and B. Chen, “Mechanical behavior of transparent nanofibrillar cellulose–chitosan nanocomposite films in dry and wet conditions,” *J Mech Behav Biomed Mater*, vol. 32, pp. 279–286, Apr. 2014, doi: 10.1016/J.JMBBM.2014.01.014.
- [216] X. Zhang, J. Liu, H. Yong, Y. Qin, J. Liu, and C. Jin, “Development of antioxidant and antimicrobial packaging films based on chitosan and mangosteen (*Garcinia mangostana* L.) rind powder,” *Int J Biol Macromol*, vol. 145, pp. 1129–1139, Feb. 2020, doi: 10.1016/J.IJBIOMAC.2019.10.038.
- [217] A. Ali *et al.*, “Starch-based antimicrobial films functionalized by pomegranate peel,” *Int J Biol Macromol*, vol. 129, pp. 1120–1126, May 2019, doi: 10.1016/J.IJBIOMAC.2018.09.068.
- [218] Z. A. N. Hanani, F. C. Yee, and M. A. R. Nor-Khaizura, “Effect of pomegranate (*Punica granatum* L.) peel powder on the antioxidant and antimicrobial properties of fish gelatin films as active packaging,” *Food Hydrocoll*, vol. 89, pp. 253–259, Apr. 2019, doi: 10.1016/J.FOODHYD.2018.10.007.
- [219] N. Kumar, Pratibha, A. Trajkovska Petkoska, E. Khojah, R. Sami, and A. A. M. Al-Mushhin, “Chitosan Edible Films Enhanced with Pomegranate Peel Extract: Study on Physical, Biological, Thermal, and Barrier Properties,” *Materials*, vol. 14, no. 12, Jun. 2021, doi: 10.3390/MA14123305.
- [220] S. Taokaew, N. Chiaoprakobkij, P. Siripong, N. Sanchavanakit, P. Pavasant, and M. Phisalaphong, “Multifunctional cellulosic nanofiber film with enhanced antimicrobial and anticancer properties by incorporation of ethanolic extract of *Garcinia mangostana* peel,”

- Materials Science and Engineering: C*, vol. 120, p. 111783, Jan. 2021, doi: 10.1016/J.MSEC.2020.111783.
- [221] G. Sharma, J. George Joy, A. R. Sharma, and J. C. Kim, “Accelerated full-thickness skin wound tissue regeneration by self-crosslinked chitosan hydrogel films reinforced by oxidized CNC-AgNPs stabilized Pickering emulsion for quercetin delivery,” *J Nanobiotechnology*, vol. 22, no. 1, pp. 1–22, Dec. 2024, doi: 10.1186/S12951-024-02596-0/FIGURES/10.
- [222] H. Chopra, S. Bibi, S. Kumar, M. S. Khan, P. Kumar, and I. Singh, “Preparation and Evaluation of Chitosan/PVA Based Hydrogel Films Loaded with Honey for Wound Healing Application,” *Gels*, vol. 8, no. 2, Feb. 2022, doi: 10.3390/GELS8020111.
- [223] J. Zhang, W. Tan, Q. Li, X. Liu, and Z. Guo, “Preparation of Cross-linked Chitosan Quaternary Ammonium Salt Hydrogel Films Loading Drug of Gentamicin Sulfate for Antibacterial Wound Dressing,” *Marine Drugs 2021, Vol. 19, Page 479*, vol. 19, no. 9, p. 479, Aug. 2021, doi: 10.3390/MD19090479.
- [224] A. P. Serro *et al.*, “Hydrogels in Cutaneous Wound Healing: Insights into Characterization, Properties, Formulation and Therapeutic Potential,” *Gels 2024, Vol. 10, Page 188*, vol. 10, no. 3, p. 188, Mar. 2024, doi: 10.3390/GELS10030188.
- [225] A. Uneputty *et al.*, “Strategies applied to modify structured and smooth surfaces: A step closer to reduce bacterial adhesion and biofilm formation,” *Colloid Interface Sci Commun*, vol. 46, p. 100560, Jan. 2022, doi: 10.1016/J.COLCOM.2021.100560.
- [226] P. Zimet *et al.*, “Physico-chemical and antilisterial properties of nisin-incorporated chitosan/carboxymethyl chitosan films,” *Carbohydr Polym*, vol. 219, pp. 334–343, Sep. 2019, doi: 10.1016/j.carbpol.2019.05.013.
- [227] J. R. Pereira *et al.*, “Chitosan Film Containing *Mansoa hirsuta* Fraction for Wound Healing,” *Pharmaceutics 2020, Vol. 12, Page 484*, vol. 12, no. 6, p. 484, May 2020, doi: 10.3390/PHARMACEUTICS12060484.

- [228] O. Nedela, P. Slepicka, and V. Švorčík, “Surface Modification of Polymer Substrates for Biomedical Applications,” *Materials (Basel)*, vol. 10, no. 10, Sep. 2017, doi: 10.3390/MA10101115.
- [229] S. Fahimirad and F. Ajalloueiian, “Naturally-derived electrospun wound dressings for target delivery of bio-active agents,” *Int J Pharm*, vol. 566, pp. 307–328, Jul. 2019, doi: 10.1016/J.IJPHARM.2019.05.053.
- [230] Y. Zhao *et al.*, “Accelerated skin wound healing by soy protein isolate-modified hydroxypropyl chitosan composite films,” *Int J Biol Macromol*, vol. 118, no. Pt A, pp. 1293–1302, Oct. 2018, doi: 10.1016/J.IJBIOMAC.2018.06.195.
- [231] E. A. Grice and J. A. Segre, “The skin microbiome,” *Nat Rev Microbiol*, vol. 9, no. 4, p. 244, Apr. 2011, doi: 10.1038/NRMICRO2537.
- [232] T. R. Johnson *et al.*, “The Cutaneous Microbiome and Wounds: New Molecular Targets to Promote Wound Healing,” *International Journal of Molecular Sciences 2018, Vol. 19, Page 2699*, vol. 19, no. 9, p. 2699, Sep. 2018, doi: 10.3390/IJMS19092699.
- [233] L. S. Miller and J. S. Cho, “Immunity against *Staphylococcus aureus* cutaneous infections,” *Nat Rev Immunol*, vol. 11, no. 8, pp. 505–518, 2011, doi: 10.1038/nri3010.
- [234] K. S. Kaye, L. A. Petty, A. F. Shorr, and M. D. Zilberberg, “Current Epidemiology, Etiology, and Burden of Acute Skin Infections in the United States,” *Clinical Infectious Diseases*, vol. 68, no. Supplement_3, pp. S193–S199, Apr. 2019, doi: 10.1093/CID/CIZ002.
- [235] D. J. Phillips *et al.*, “Evaluation of the Antimicrobial Activity of Cationic Polymers against Mycobacteria: Toward Antitubercular Macromolecules,” *Biomacromolecules*, vol. 18, no. 5, pp. 1592–1599, May 2017, doi: 10.1021/ACS.BIOMAC.7B00210/ASSET/IMAGES/LARGE/BM-2017-002102_0005.JPEG.
- [236] J. Bumrung, C. Chanchao, V. Intasanta, T. Palaga, and S. Wanichwecharungruang, “Water-dispersible unadulterated α -mangostin particles for biomedical applications,” *R Soc Open Sci*, vol. 7, no. 11, Nov. 2020, doi: 10.1098/RSOS.200543.

- [237] J. J. Koh *et al.*, “Rapid bactericidal action of alpha-mangostin against MRSA as an outcome of membrane targeting,” *Biochim Biophys Acta Biomembr*, vol. 1828, no. 2, pp. 834–844, Feb. 2013, doi: 10.1016/J.BBAMEM.2012.09.004.
- [238] S. Y. Park, J. H. Lee, S. Y. Ko, N. Kim, S. Y. Kim, and J. C. Lee, “Antimicrobial activity of α -mangostin against Staphylococcus species from companion animals in vitro and therapeutic potential of α -mangostin in skin diseases caused by *S. pseudintermedius*,” *Front Cell Infect Microbiol*, vol. 13, 2023, doi: 10.3389/FCIMB.2023.1203663/FULL.
- [239] L. O. Felix, B. Mishra, R. Khader, N. Ganesan, and E. Mylonakis, “In Vitro and In Vivo Bactericidal and Antibiofilm Efficacy of Alpha Mangostin Against Staphylococcus aureus Persister Cells,” *Front Cell Infect Microbiol*, vol. 12, Jul. 2022, doi: 10.3389/FCIMB.2022.898794/FULL.
- [240] L. Wang, C. Hu, and L. Shao, “The antimicrobial activity of nanoparticles: present situation and prospects for the future,” *Int J Nanomedicine*, vol. 12, p. 1227, Feb. 2017, doi: 10.2147/IJN.S121956.
- [241] Z. A. N. Hanani, F. C. Yee, and M. A. R. Nor-Khaizura, “Effect of pomegranate (*Punica granatum* L.) peel powder on the antioxidant and antimicrobial properties of fish gelatin films as active packaging,” *Food Hydrocoll*, vol. 89, pp. 253–259, Apr. 2019, doi: 10.1016/J.FOODHYD.2018.10.007.
- [242] S. F. Hamed, Z. Sadek, and A. Edris, “Antioxidant and antimicrobial activities of clove bud essential oil and eugenol nanoparticles in alcohol-free microemulsion,” *J Oleo Sci*, vol. 61, no. 11, pp. 641–648, 2012, doi: 10.5650/JOS.61.641.
- [243] S. Dahham, M. N. Ali, H. Tabassum, and M. Khan, “Studies on Antibacterial and Antifungal Activity of Pomegranate (*Punica granatum* L.),” *American-Eurasian Journal of Agricultural and Environmental Science*, 2010.
- [244] N. N. Costa *et al.*, “Polymeric films containing pomegranate peel extract based on PVA/starch/PAA blends for use as wound dressing: In vitro analysis and physicochemical evaluation,” *Mater Sci Eng C Mater Biol Appl*, vol. 109, Apr. 2020, doi: 10.1016/J.MSEC.2020.110643.

- [245] F. Y. Faris Taufeq, N. H. Habideen, L. N. Rao, P. K. Podder, and H. Katas, "Potential Hemostatic and Wound Healing Effects of Thermoresponsive Wound Dressing Gel Loaded with *Lignosus rhinocerotis* and *Punica granatum* Extracts," *Gels*, vol. 9, no. 1, p. 48, Jan. 2023, doi: 10.3390/GELS9010048/S1.
- [246] T. Chalke, K. Sharma, S. K. Nagare, and S. S. Jirge, "Formulation and Evaluation of Punica Topical Gel for its Content of Gallic Acid and Anti-Microbial Study," *J Drug Deliv*, vol. 6, no. 3, pp. 75–78, Jul. 2016, doi: 10.25258/IJDDT.V6I3.8892.
- [247] I. E. A. Alsaimary, "A Chemotherapeutic Efficacy of Some antibiotics and Punica Grantum L. Extracts against Propionibacterium Acnes Isolated from Acne Vulgaris Case," *Medical Journal of Islamic World Academy of Sciences*, vol. 109, no. 1567, pp. 1–6, 2014, doi: 10.12816/0008185.
- [248] D. Winarni *et al.*, "Topical Administration Effect of Sargassum duplicatum and Garcinia mangostana Extracts Combination on Open Wound Healing Process in Diabetic Mice," *Scientifica (Cairo)*, vol. 2022, 2022, doi: 10.1155/2022/9700794.
- [249] J. J. Wang, Q. H. Shi, W. Zhang, and B. J. S. Sanderson, "Anti-skin cancer properties of phenolic-rich extract from the pericarp of mangosteen (*Garcinia mangostana* Linn.)," *Food and Chemical Toxicology*, vol. 50, no. 9, pp. 3004–3013, Sep. 2012, doi: 10.1016/J.FCT.2012.06.003.
- [250] S. Chivapat, P. Chavalittumrong, P. Wongsinkongman, C. Phisalpong, and A. Rungsipipat, "Chronic Toxicity Study of Garcinia mangostana Linn. pericarp Extract," *The Thai Journal of Veterinary Medicine*, vol. 41, no. 1, pp. 45–54, Mar. 2011, doi: 10.56808/2985-1130.2279.
- [251] F. N. KACI, D. RÜZGAR, A. GÖRMEZ, and D. EFE, "The Evaluation of Cytotoxic and Antibacterial Activity of the Ethanol Extract of Punica granatum L. Peels," *Iğdir Üniversitesi Fen Bilimleri Enstitüsü Dergisi*, vol. 11, no. 3, pp. 2319–2327, Sep. 2021, doi: 10.21597/JIST.875449.

- [252] O. Keta *et al.*, “Pomegranate (*Punica granatum* L.) peel extract: Potential cytotoxic agent against different cancer cell lines,” *Records of Natural Products*, vol. 14, no. 5, pp. 326–339, Sep. 2020, doi: 10.25135/RNP.170.19.11.1477.
- [253] S. B. Jahromi *et al.*, “*Punica granatum* Peel Extract Toxicity in Mice,” *Jundishapur Journal of Natural Pharmaceutical Products 2015 10:4*, vol. 10, no. 4, p. 23770, Nov. 2015, doi: 10.17795/JJNPP-23770.